11-21-2017 11:30 AM

Behaviour of Pre-stressed Concrete Transmission Poles under High Intensity Wind

Ahmed M. Ibrahim, *The University of Western Ontario*

Supervisor: El Damatty, Ashraf, *The University of Western Ontario*
A thesis submitted in partial fulfillment of the requirements for the Doctor of Philosophy degree in Civil and Environmental Engineering
© Ahmed M. Ibrahim 2017

ABSTRACT

Among different types of electrical transmission line structures, pre-stressed concrete transmission poles have the advantages of low installation and maintenance costs, appropriate delivery time, and high corrosion resistivity. Typically, these poles are designed to resist synoptic wind loading. Current design codes do not consider the effect of high intensity wind (HIW) events in the form of downbursts and tornadoes on pre-stressed concrete poles despite the fact that those weather events are the main cause of failure of transmission line structures. The first comprehensive study conducted to assess the behaviour of pre-stressed concrete transmission poles under HIW is presented in this thesis. A numerical model is developed and validated incorporating the following: (1) three-dimensional downburst and tornado wind fields previously developed and validated using computational fluid dynamics simulations; (2) an analytical technique previously developed and validated to predict the non-linear behaviour of the transmission line conductors under non-uniform loads resulting HIW events (3) a non-linear finite element model developed in this thesis to simulate the structural behaviour of pre-stressed concrete poles. This numerical model can predict the response of pre-stressed concrete transmission pole structures under downbursts and tornadoes as well as under synoptic wind. The model is then expanded to include the dynamic effects and then used to assess the dynamic response of pre-stressed concrete transmission pole structures to turbulent synoptic wind. The results are used to assess the magnification in straining actions associated with dynamic behaviour as well as the adequacy of the provisions for synoptic wind incorporated in the American Society of Civil Engineers guidelines. Knowing that the turbulence is less significant in HIW compared to synoptic wind, the results of this part of the study provide an upper bound for the dynamic effects associated with downbursts and tornadoes. This upper bound value provides justification for analyzing pre-stressed concrete transmission pole systems under downbursts and tornadoes in a quasi-static manner.

Extensive parametric studies are then conducted using the developed numerical model to determine the critical downburst and tornado configurations leading to peak straining actions for a number of guyed pre-stressed concrete pole systems, which are initially designed to remain un-cracked under synoptic wind load. Failure studies are then conducted to assess the downburst and tornado velocities that lead to a full collapse of the poles. The adequacy of load cases recently developed by researchers at the University of Western Ontario to simulate the critical effects of downbursts and tornadoes on lattice steel transmission towers is then assessed for application to pre-stressed concrete pole structures.

Keywords

Pre-stressed Concrete Poles, High Intensity Wind, Downburst, Tornado, Transmission Line Structures, Dynamic Response, Guyed Poles.

CO-AUTHORSHIP

This thesis has been prepared in accordance with the regulations for an Integrated Article format thesis stipulated by the School of Graduate and Postdoctoral Studies at Western University. Statements of the co-authorship of individual chapters are as follows

Chapter 2: Finite Element Modelling of pre-stressed concrete poles under downbursts and tornadoes

All the numerical work was conducted by A. Ibrahim under close supervision of Dr. A. A. El Damatty, and Dr. A. Elansary. Drafts of Chapter 2 were written by A. Ibrahim and modifications were done under supervision of Dr. A. A. El Damatty and Dr. A.M. El Ansary. A paper co-authored by A. Ibrahim, A. A. El Damatty and A.M. EL Ansary has been published in the *Journal of Engineering Structures.*

Chapter 3: Dynamic behaviour of pre-stressed concrete transmission poles under synoptic wind loading

All the numerical work was conducted by A. Ibrahim under close supervision of Dr. A. A. El Damatty and Dr. H. Aboshosha. Drafts of Chapter 3 were written by A. Ibrahim and modifications were done under supervision of Dr. A. A. El Damatty. A paper co-authored by A. Ibrahim, A. A. El Damatty, and H. Aboshosha will be submitted to the *Journal of Wind Engineering and Industrial Aerodynamics.*

Chapter 4: Behaviour, design and non-linear failure analysis of guyed pre-stressed concrete poles under downbursts

All the numerical work was conducted by A. Ibrahim under close supervision of Dr. A. A. El Damatty. Drafts of Chapter 4 were written by A. Ibrahim and modifications were done

under supervision of Dr. A. A. El Damatty. A paper co-authored by A. Ibrahim and A. A. El Damatty will be submitted to the *Journal of Engineering Structures.*

Chapter 5: Behaviour, design and non-linear failure analysis of guyed pre-stressed concrete poles under tornadoes

All the numerical work was conducted by A. Ibrahim under close supervision of Dr. A. A. El Damatty. Drafts of Chapter 5 were written by A. Ibrahim and modifications were done under supervision of Dr. A. A. El Damatty. A paper co-authored by A. Ibrahim and A. A. El Damatty will be submitted to the *Journal of Engineering Structures.*

To the soul of my grandfather *Mohamed ElEngawi*

To my beloved grandmother *Hanifa Mohamed*

To my parents *Mansour Sadek* and *Howida ElEngawi*

To my sisters *Omnia and Israa* and my brother *Mohamed*

To my uncles *Ashraf, Adel, Hassan* and *Alaa*

For patience, caring, support, encouragement, and sharing these years of hard work

To my supervisor, *Dr. Ashraf A. El Damatty*

For his support and guidance as well as sharing his experience during these years

ACKNOWLEDGMENTS

I would like to express my utmost gratitude to the people who helped me along the journey of my PhD.

My deepest thanks and extreme gratitude are due to my supervisor Dr. Ashraf El Damatty for his continuous encouragement, support, guidance and advice.

I am deeply grateful to my colleagues Ahmed Alaa Elansary, Ahmed Musa, Ahmed Suleiman, Amal Elawady, Ahmed Elshaer, Moustafa Aboutabikh, Ahmed Shehata, Fouad El Ezaby, Ibrahim Ibrahim, Mohamed Hamada, Nayyera ELGharably and Carolina Santos for helping me throughout the various stages of my research.

Last but not least, my greatest thanks go to my beloved family. I cannot help but feel immense gratitude towards my parents, my brother and my sisters for encouraging and supporting me in all means possible throughout the course of my life.

TABLE OF CONTENTS

LIST OF TABLES

LIST OF FIGURES

CHAPTER 1

INTRODUCTION

1.1 <u>General</u>

Electricity is essential for running most of –if not all- the businesses around the globe. The continuous support of electricity is a vital concern for all governments worldwide. Transmission line structures (TLs) are responsible for electrical energy transmission. Any deficiency in such structures can seriously threaten people`s lives and activities. High intensity wind (HIW) events in the form of downbursts and tornadoes are the main reason for 80% of TLs weather-related failures as stated by Dempsey and White (1996). In China, in 2005, 18 transmission towers carrying 500 kV lines and another 60 towers carrying 110 kV lines collapsed due to strong wind events such as downbursts, tornadoes and typhoons (Zhang 2006). In Canada, many transmission line structures have failed in the past twenty years as a result of downbursts such as those reported by Manitoba Hydro (Mccarthy and Melsness, 1996) and (Hydro One, Ontario, 2006). In 2015, Hydro One reported a large power outage for more than 47,000 consumers in Teviotdale, Ontario, Canada, due to an F2 tornado. In 2016, 23 transmission towers failed during a series of downburst events in Australia (Australian Wind Alliance, 2016). As reported by Ishac and White (1994), South Western Ontario exhibits the highest rates of tornadoes among all the populated areas in Canada. Those tornadoes were the reason of most of transmission line failures in this area. Five out of six weather related failures of transmission towers that belong to Ontario Hydro Company were due to tornadoes as reported by Behncke and White (2006). CIGRE (2006) stated that 65 % of weather related events on transmission line structures were due to tornadoes.

The safety of transmission line structures is not only threatened by HIW events, the dynamic excitations of TLs caused by synoptic wind loads were considered the cause of the TLs failures as reported by Li (2000), Savory et al. (2001) and Li and Bai (2006). As such, the protection of transmission line structures against downbursts, tornadoes and synoptic wind loads is necessary for the continuous support of electricity.

The main components of TLs are conductors, insulator strings, ground wires and the supporting tower. Transmission lines' structural supporting systems can be self-supported or guyed. The towers can be in the form of pole-type structures or lattice steel towers. Pole-type structures are classified into wooden, steel and pre-stressed concrete poles. Due to their low installation and maintenance costs, appropriate delivery time and corrosion resistivity, pre-stressed concrete transmission poles are widely spread more than wooden or steel poles. The current thesis focuses on the behavior of self-supported and guyed pre-stressed concrete poles under downbursts, tornadoes.
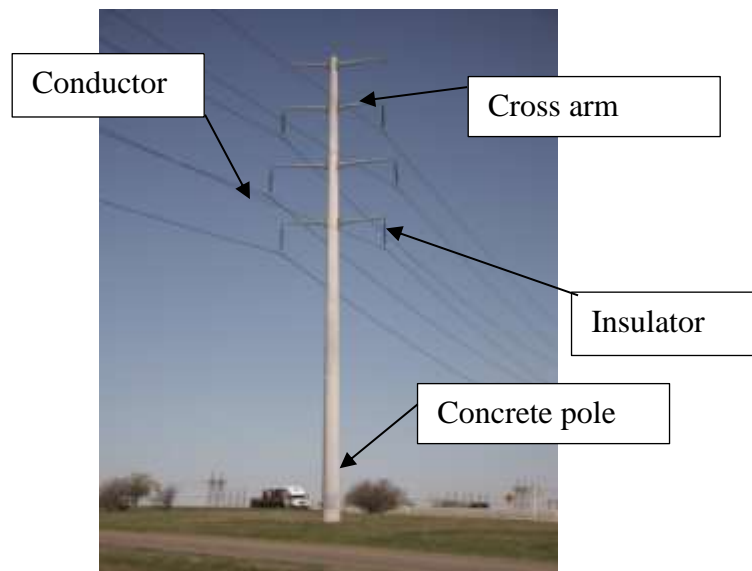
Fig. 1-1 Concrete Pole.

1.2 **Literature**

1.2.1 **Historical background on pre-stressed concrete poles**

Fouad et al. (1992) reported that the first concrete pole was constructed in Germany in 1856 to support telegraph lines. This type of poles was not widely used at the early years because of its high cost and the heavy weight. In 1907, Otto Schlosser produced the first spun cast concrete pole. The spinning process allowed the manufacturing of hollow sections and hence the poles became lighter. Moving forward from 1907 to 1932, about 250, 000 concrete poles were produced in Europe (Fouad et al. 1992). Introducing the spinning technique in addition to the low maintenance cost of these poles compared to the steel ones were the two main reasons for the rapid increase of the spun concrete poles construction. In 1930, Eugene Freyssinet produced the first pre-stressed concrete pole. The first spun cast pre-stressed concrete pole was used in the 1950's in Europe. The spun cast poles tapered section made these type of poles better in serviceability, erection and weight. In North America, the first concrete pole was used in the 1930's and the first pre-stressed concrete pole was produced at the 1950's. Nowadays, spun tapered pre-stressed concrete poles, as single or H-frame sections, are widely used in the southeastern region of the United States in distribution, lightening and transmission purposes.

By comparing pre-stressed concrete poles to the steel and wooden ones, the steel poles are more expensive and require more maintenance and delivery times, while the wooden poles are becoming less attractive because of the increased cost of heavy forest cutting and the concerns about fire and other environmental issues such as insects' attacks. Fouad et al. (1992) reported that 4 to 6 million wooden poles become defective each year mainly due to rot and attack by insects and woodpeckers. The pre-stressed concrete poles can provide elastic behavior under normal wind

speeds, corrosion resistance and low maintenance cost. Pre-stressed concrete poles are initially more expensive, but on life cycle basis they can be more economic than wooden poles.

1.2.2   Failures of pre-stressed concrete poles

Kuebler (2008) reported that sudden forces on electrical lines due to wind can cause crack and spall to the inner cement paste, then the pre-stressing strands can break into the hollow middle section of the pole causing the loss of flexural resistance and stability of the pole. Improper embedment and vehicle impacts can cause poles' failure in shear. Dilger et al. (1996) stated that failure of pre-stressed concrete poles can be linked to the differential shrinkage between the inside and the outside layer of the pole resulting in longitudinal cracks that can develop in the weaker cement paste layer. Segregation of concrete and poor concrete mixtures can also be a cause of many durability problems for the poles. Some pole failures can be attributed to water infiltration that causes rusting of the reinforcement leading to excessive cracks. The following figures show some failure modes of various pre-stressed concrete poles:

Fig. 1-2 shear failure of the pole due to a vehicle impact (Kuebler 2008)

Fig. 1-3 Longitudinal cracking, corrosion and spalling caused by differential shrinkage and

segregation of concrete mix (Kuebler 2008)

Typically, pre-stressed concrete poles are designed based on the loads specified in the ASCE-74 (2010) and the design criteria described in the ASCE-123 (2012). These guidelines recommend that the pre-stressed concrete poles remain un-cracked under synoptic wind loads. The current study aims to assess the effect of localized high intensity wind events on the poles designed following the ASCE 74 (2010) and ASCE 123 (2012) provisions.

1.2.3   High intensity wind (HIW)

Downbursts and Tornadoes are a category of weather storms that are referred to as high intensity wind (HIW) events. Those events are characterized by high wind speeds that affect a relatively narrow area. They are different than large scale events, such as hurricanes, because of their different profiles and their localized size and effect.

1.2.3.1   Downburst wind field

A downburst is defined as a violent downdraft of moist and cold air that suddenly impinges into the ground and spreads horizontally as per Fujita (1985). Wolfson et al. (1985), Holmes et al. (1997), Fujita (1990), Gast and Schroeder (2003) and Choi (2004) have made a few attempts to obtain downburst field measurements. However, gathering full-scale data for such localized events is extremely hard. As such, numerical simulation of downbursts is considered as an alternative to estimate the downburst wind velocity field.

A number of numerical approaches were used to simulate the downburst wind field such as the ring vortex model, the cooling source model and the impinging jet model. The ring vortex models adopted by Zhu and Etkin (1985), Ivan (1986) and Vicroy (1992) were found to be inaccurate in predicting the downburst wind field near the ground as reported by Savory et al. (2001). The impinging jet model was suggested by Fujita (1985) and was then used by Hangan et al. (2003), Kim and Hangan (2007), Sengupta and Sarkar (2008) and Aboshosha et al. (2015). Vermeire et al. (2011) modelled the downburst wind field using the cooling source model with large eddy simulations (LES). The results of the cooling source method did not agree well with the impinging jet model results. Among various modeling techniques, the impinging jet model is believed to be the most practical from engineering point of view since the wind field is characterized using a physical parameter which is the downward jet velocity that can be easily linked to the measured values of horizontal velocity. In the current study, the numerical model developed by Hangan et al. (2003) is used as the basis of the downburst wind field adopted in this study. Hangan et al. (2003) numerical model was validated later by Kim and Hangan (2007) based on full-scale data reported in Wood et al. (2001). Hangan et al. (2003) model simulated the spatial and time variations of the wind field associated with downbursts. The downburst outflow in this model

consists of two velocity components: radial (horizontal) component (V_{RD}) and axial (vertical) component (V_{VL}). The values of the two velocity components at a specific point in space are functions of its height relative to the ground and its location relative to the center of the downburst. The downburst velocity acting on a pole depends on the jet velocity V_j, the jet diameter D_j, and the geometric parameters R and θ shown in **Fig. 1-4**.
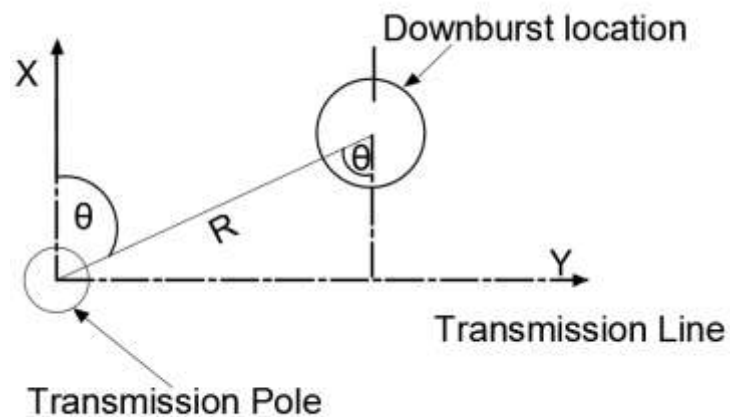
Fig. 1-4 Downburst Parameters

1.2.3.2   Tornado wind field

Tornadoes are defined by Fujita (1981) as rotating wind vortices with high wind speeds affecting relatively narrow paths. Fujita and Pearson (1973) classified tornadoes according to their intensity and size. Sizes are defined by path length and width, while intensities are defined by gust wind speed. The scale ranges from F0 to F5. The major specific characteristic of tornadoes is its local high intensity wind speed. The small size of tornadoes prints compared to the extended length of a transmission line system makes the prediction of the response of transmission line towers to such events quite challenging. Similar to downbursts, the major complexity comes from the fact that the forces acting on the conductors, ground wires and the supporting tower vary according to the

relative location of the tornado event with respect to the tower. Field measurements of tornados are even harder to obtain since the intensity and scale of tornadoes cannot be measured by traditional recording stations in the field. Therefore, the simulation of tornado events relies mainly on numerical modeling.

A number of attempts were made by Harlow and Stein (1974), Rotunno (1977), Lewellen et al. (1997), Lewellen et al. (2000) and Hangan and Kim (2008) to numerically simulate the tornado wind field. The model that was developed and validated by Hangan and Kim (2008) is incorporated in this thesis. Hangan and Kim (2008) conducted a three dimensional computational fluid dynamics (CFD) simulation for the wind field associated with tornadoes. The simulation was conducted at a steady state manner and, consequently, the velocity profile does not varying with time. Hangan and kim (2008) validated their CFD model by comparing the velocity field results with Baker (1981), Wurman (1998) and Sarkar et al. (2005). Tornado wind field consists mainly of two velocity components in the horizontal plan, which are the radial V_{mr} and tangential V_{mt} components and one vertical component which is the axial V_{ma} component. The location of the tornado wind field with respect to the transmission pole is defined by the two polar parameters (R) and (θ) as shown in **Fig. 1-5**.
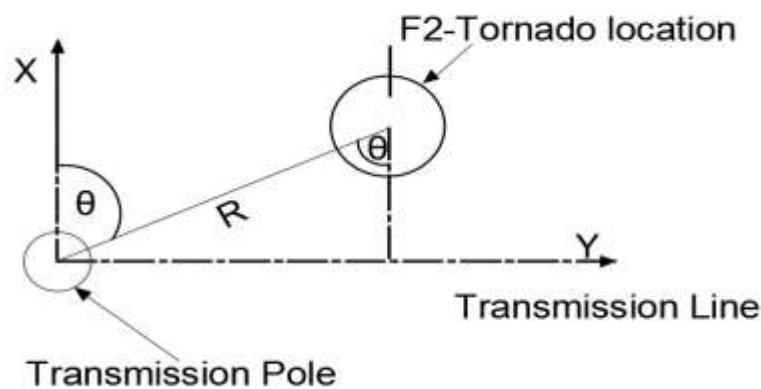
Fig. 1-5 Tornado Parameters

1.2.3.3   Response of transmission line structures to HIW

The previously mentioned failures of transmission line structures under tornadoes and downbursts and the lack of guidelines considering downburst and tornado wind loads in the design motivated a group of researchers at the University of Western Ontario, Canada, to investigate the behavior of transmission line structures under HIW. Savory et al. (2001) investigated the failure of self-supported transmission line structures under tornadoes. Shehata et al. (2005) developed and validated the first finite element model to simulate the behaviour of transmission line systems under downburst loadings. Shehata and El Damatty (2007) investigated the effect of varying the downburst parameters on a guyed transmission line structure. Shehata et al. (2008) developed a coupled finite element- optimization technique to determine the critical downburst parameters on transmission towers' members. Darwish et al. (2010) studied the dynamic characteristics of transmission lines under turbulent downburst loading. Ladubec et al. (2012) extended the linear analysis conducted by Shehata and El Damatty (2008) by including the P-Δ effect in the analysis of a guyed transmission line system under downbursts. An increase of 20 % of the peak forces in the tower's main legs and chord members were obtained in this study in comparison with Shehata and El Damatty (2008) results. Elawady (2016) performed a number of numerical and experimental studies on the effect of downburst forces on transmission lattice steel towers. Shehata et al. (2005) model was extended by Hamada et al. (2010) to be capable of investigating the behavior of transmission line structures under tornadoes. The response of guyed lattice tower systems to tornadoes was investigated by Hamada and El Damatty (2011). The variations of F2 and F4 tornado locations with respect to the transmission lines were considered in this study. Hamada and El Damatty (2015) conducted a non-linear failure analysis of guyed tranmssion lines

under F2 tornadoes. Altalmas et. al (2012) studied the progressive failure of transmission line structures under tornadoes.

The numerical investigations conducted in all the above studies require conducting a large number of non-linear analyses by considering the potential values of the size and location of the high intensity wind event; resulting in significant computation time requirement. A major part of the computational efforts result from the prediction of the behaviour of the conductors as they are highly nonlinear and can be subjected to non-uniform transient loading during HIW events. As such, Aboshosha (2014) focused on the behaviour of the conductors under HIW events in general and under downbursts in particular. Aboshosha and El Damatty (2014) developed a numerical technique to investigate the behavior of transmission line conductors under downburst and tornado loadings taking into account the non-linear behavior of the conductors including sagging, pre-tensioning forces and insulator's stiffness. Aboshosha and El Damatty (2015) developed a closed form solution to estimate the conductor's reactions under downbursts. In addition to that, Aboshosha (2014) derived an expression for the conductors' aerodynamic damping which is utilized in assessing the dynamic response of transmission line conductors under downburst loading.

A major outcome of the research conducted at UWO was the development for the first time of a set of load cases that can be used in analyzing and designing transmission line structures to resist downburst and tornadoes. A major challenge in this development was to identify load cases that provide an envelope for all possible downburst and tornado configurations given the variability in location and size of those events. El Damatty and Elawady (2015) proposed three load cases simulated the critical effects of downbursts on transmission towers. The load cases were provided in the form of velocity profiles acting along the height of the tower as well as along the spans of

the adjacent conductors. One of the those load cases required the evaluation of the longitudinal forces in the conductors under non-uniformly distributed load, which is a difficult task to be performed in day-to-day design by practicing engineers. As such, Elawady and El Damatty (2016) developed a number of charts and a linear interpolation technique that can be used to predict such longitudinal forces. Similar efforts were done to develop critical load cases for tornadoes. El Damatty and Hamada (2016) proposed 12 load cases simulating the critical effects of tornadoes on transmission towers. Those load cases were then simplified by Hamada and El Damatty (2016) to eight load cases. It should be mentioned that both the downburst and tornado load cases have been considered by the ASCE-74 committee during its update of its guidelines for transmission line loading to represent the first guidelines including downburst and tornado load provisions worldwide. Also, it should be noted that all the above developed load cases focused on steel lattice transmission line structures.

1.2.4 Synoptic wind loading and dynamic effects

The synoptic wind field consists of a mean component which is static and a fluctuating component (turbulent), which varies with time. The turbulent component can trigger a dynamic response of the structure, which can lead to a failure from the gust effect. Most of the previous studies which investigated the dynamic behaviour of transmission line systems under wind loads focused on conductors and on lattice steel towers as the main supporting system (Momomura et al. 1997) and (Horr et al. 2004). Loredo-Souza and Davenport (1998) concluded that the aerodynamic damping of the conductors has a major effect on the dynamic behaviour of transmission line structures. The contribution of dynamic component to the response of self-supported and guyed transmission lattice structures was found relatively low in the study conducted by Aboshosha et al. (2016). That

was attributed to the difference between the loading and the tower frequencies and the decoupling of the mode shapes of both the lattice steel transmission towers and the conductors.

Regarding pole structures, few studies were performed to assess their vulnerability to dynamic loads. Chen et al. (2006), Lantrip (1995) and Polyzois et al. (1998) conducted a number of studies to identify the free-vibration modes of transmission poles. Dai and Chen (2008) studied the effect of the pre-stress level on the modal behavior of pre-stressed concrete poles. Chen and Dai (2010) concluded that strong coupling exist between the poles and the conductors vibrations. The reduced redundancy of pole-type structures makes them more vulnerable to dynamic excitations (Chen and Dai, 2010). The complexity of performing dynamic analysis of transmission line structures arises from the fact that the stiffness properties of those structures are frequency-dependent. This might lead to coupling between the response of conductors and the supporting towers (Simiu and Scanlan 1996), (Madugula 2002), (IEC 2003) and (Chen and Dai 2010).

1.3 Research gaps

In view of the above literature, it is obvious that no studies have been conducted in the literature to assess the behaviour of pre-stressed concrete transmission poles under high intensity wind. To do so, a numerical model that includes the specifics of pre-stressed concrete poles together with conductor modeling and high intensity wind field has to be developed. The dynamic behaviour of pre-stressed concrete poles under turbulent wind needs to be quantified. This would require extending the above-mentioned numerical model to include the dynamic effects. By quantifying the dynamic effects, decision can be made whether or not it is possible to carry-on the analyses under high intensity wind in a quasi-static manner. Detailed studies are needed to describe the behaviour of pre-stressed concrete poles under downbursts and tornadoes, to assess if poles designed to remain un-cracked under synoptic wind loads can survive without failure downbursts

and tornadoes and up to which magnitude. In addition, studies are needed to assess whether the downburst and tornado load cases developed recently for lattice towers can be valid for pre-stressed concrete transmission pole structures.

1.4 Thesis objectives

The main objectives of the thesis are summarized as follows:

1- Develop and validate a numerical tool capable of predicting the non-linear behavior of pre-stressed concrete transmission pole structures to various type of wind loading resulting from either synoptic or HIW events.

2- Extend the above model to include the dynamic effect and use the model to assess the contribution of the dynamic component in the response of pre-stressed concrete transmission poles under both mean and turbulent synoptic wind components.

3- Perform extensive studies on guyed pre-stressed concrete pole structures under downbursts and tornadoes to understand the behaviour and determine how vulnerable they are to those events.

4- Assess the applicability of the downburst and tornado load cases recently developed for steel lattice towers to pre-stressed concrete pole structures.

1.5 Thesis organization

The thesis has been prepared in "Integrated-Article" format. In chapter 1, a review of the literature related to the response of transmission line structures to downbursts, tornadoes and synoptic wind is presented. This is followed by addressing the gaps in literature and outlining the objectives of the thesis.   In Chapter 2, a general numerical model is developed and validated to predict the quasi-static response of pre-stressed concrete transmission pole structures to wind loading. The

model is general to handle synoptic, downburst and tornado wind. This model is extended in Chapter 3 to include the dynamic effect and assess the contribution of the resonant component on the response of pre-stressed concrete transmission poles under synoptic wind. The reason this chapter focused on synoptic wind is that it was shown in previous studies that the turbulent component is more significant in synoptic wind compared to high intensity wind. Studies related to the third and fourth objectives of the Thesis are conducted in Chapters 4 and 5 focusing on downbursts and tornadoes, respectively. Chapter 6 presents the conclusions drawn from the current study and the recommendations for future work.

1.5.1   Finite element modelling of pre-stressed concrete poles under downbursts and tornadoes

In this chapter, a built in-house numerical model is developed incorporating the following: (1) a three-dimensional downburst and tornado wind field previously developed and validated using computational fluid dynamics simulations; (2) A computationally efficient analytical technique previously developed and validated to predict the non-linear behaviour of the conductors under non-uniform loads resulting from those events (3) a non-linear finite element model developed in this chapter to simulate the structural behaviour of pre-stressed concrete poles considering a number of parameters such as: concrete nonlinearity, pre-stressing strands behaviour, shrinkage, creep, relaxation and tension stiffening.

The non-linear finite element model is validated using experimental data available in the literature. Extensive parametric studies are conducted using the numerical model to determine the critical downburst and tornado configurations leading to peak overturning moment acting on a pole which is designed to remain un-cracked under synoptic wind load. Failure studies are then conducted to assess the downburst and tornado velocities that would lead to a full collapse of the pole.

1.5.2 Dynamic behaviour of pre-stressed concrete poles under synoptic wind loading

In chapter 3, the numerical model that is developed in chapter 2 is extended to be capable of predicting the dynamic response of pre-stressed concrete transmission poles under both the mean and fluctuating components of synoptic wind loads. A full non-linear dynamic analysis is conducted under a time history variation of wind velocity. The peak total responses, such as conductors' reactions and pole's base moment are determined from this analysis. The same analysis is repeated in quasi-static manner. Dynamic amplification factors (DAF), defined as the ratio between the maximum response based on a non-linear dynamic analysis and the corresponding value based on a quasi-static analysis, are calculated for the pole and the conductors to quantify the dynamic impact of synoptic wind loads. This factor is used to assess the importance of including the resonant component while estimating the response of the transmission pole. In addition to that, gust response factors (GRF) defined as the ratio between the peak and mean responses are evaluated and compared to GRF recommended by ASCE-74 (2010). A parametric study is conducted on three pre-stressed concrete transmission line systems. The mean value of the incoming wind speed is the main variable included in the parametric study. Knowing that the turbulence of synoptic wind is higher that the corresponding one of HIW, the DAF and GRF obtained from this study provides the upper bound of the dynamic effect of HIW on Pre-stressed concrete poles.

1.5.3 Behaviour, design and non-linear failure analysis of guyed pre-stressed concrete poles under downbursts

In chapter 4, the numerical model that is developed in chapter 2 and the results obtained from chapter 3 are utilized to investigate the behavior of guyed pre-stressed concrete poles under downburst loads. A parametric study is conducted by varying the downbursts locations relative to

three different spans of guyed pole systems. The results of this parametric study is utilized to identify critical downburst configurations leading to peak straining actions on the pole and the guys. This is followed by comparing the obtained critical load cases to the load cases recommended by El Damatty et al. (2013). A failure non-linear analysis is then conducted for the three considered guyed pre-stressed concrete transmission line system to determine the downburst jet velocity at which the guyed pole systems fail.

1.5.4 Behaviour, design and non-linear failure analysis of guyed pre-stressed concrete poles under tornadoes

In this chapter, the behavior of guyed pre-stressed concrete poles under tornado loads is investigated using the model that is developed in chapter 2 and the results obtained from chapter 3. A parametric study is conducted by varying the tornadoes locations relative to three different spans of guyed pole systems. The results of this parametric study is utilized to identify critical tornado configurations leading to peak forces on the pole and the guys. This is followed by a comparison between the parametric study results and tornado load cases proposed by Hamada and El Damatty (2016).

1.6 <u>References</u>

Aboshosha H., (2014), "Response of Transmission Line Conductors under Downburst Wind", PhD thesis, Western University, Canada

Aboshosha, H., and El Damatty, A.A., (2014), "Effective technique for the reactions of transmission line conductors under high intensity winds", Wind and Structures. 18(3), 235-252.

Aboshosha, H., and El Damatty, A., (2015), "Engineering method for estimating the reactions of transmission line conductors under downburst winds", Engineering Structures 99, 272-284.

Aboshosha, H., Bitsuamlak, G., El Damatty A., (2015), "Turbulence characterization of downbursts using LES", Journal of Wind Engineering and Industrial Aerodynamics. 136, 44–61.

Aboshosha, H., Ibrahim, A.M., El Damatty, A.A. and Hamada,A., (2016), "Dynamic Behaviour of Transmission Line Structures under Synoptic Wind Loads". Proceeding of CIGRE-IEC colloquim, Montreal, QC, Canada.

Altalmas, A., El Damatty, A. A., and Hamada, A. (2012). "Progressive failure of transmission towers under tornado loading". Annual Conference of the Canadian Society 21 for Civil Engineering 2012: Leadership in Sustainable Infrastructure, CSCE 2012, June 6, 2012 - June 9, Canadian Society for Civil Engineering, Edmonton, AB, Canada, 2220- 2229.

American Society of Civil Engineers (ASCE), (2010) "Guidelines for electrical transmission line structural loading", ASCE manuals and reports on engineering practice, No. 74, New York, NY, USA.

American Society of Civil Engineers (ASCE), (2012) "Prestressed Concrete Transmission Pole Structures", ASCE manuals and reports on engineering practice, No. 123, Reston, VA, USA.

Australian Wind Alliance, (2016): http://www.windalliance.org.au/

Baker, D. E. (1981). "Boundary layers in laminar vortex flows". Ph.D. thesis. Purdue University, USA.

Behncke, R.H., and White, H. B. (2006). "Applying Gust Loadings to Your Lines" Proceedings of the 9th International Conference on Overhead Lines, American Society of Civil Engineers (ASCE), Fort Collins, Colorado.

Chen, S.E., Ong C. K. and Antonsson K., (2006), "Modal Behaviors of Spun-Cast Pre-Stressed Concrete Pole Structures", Proceeding of IMAC – XXIV.

Chen S.E., and Dai K., (2010), "Modal Characteristics of Two Operating Power Transmission Poles," Shock and Vibration, vol. 17, no. 4-5, 551-561.

Choi E.C.C., (2004), "Field measurement and experimental study of wind speed profile during thunderstorms", J. Wind Eng. Ind. Aerodyn., 92, 275-290.

CIGRÉ (Conseil International des Grands Réseaux Électriques/ International Council on Large Electrical Systems) SC-22 WG22-06 (2006). "Review of IEC 826: Loading and Strength of Overhead Lines. Part 3: Analysis of Recent Transmission Line Failures". Scientific Committee B2 on Overhead Lines.

Dai,K. and Chen, S.E. (2008), "Vibration of spun-cast prestressed concrete poles", Proceedings IMAC – XXV, Orlando, Florida, USA.

Darwish, M., El Damatty A.A., and Hangan, H., (2010), "Dynamic characteristics of transmission line conductors and behaviour under turbulent downburst loading", Wind and Structures 13(4), 327-346.

Dempsey, D. and White, H., (1996) "Winds wreak havoc on lines", Transm Distrib World 48(6), 32-37.

Dilger, W.H., Ghali, A., and Rao, S.V.K.M. (1996). "Improving the Durability and Performance of Spun-Cast Concrete Poles". PCI Journal, Vol. 41, No. 2, March-April 1996, 68-90.

Elawady A., (2016), " Development of design loads for transmission line structures subjected to downbursts using aero-elastic testing and numerical modeling", PhD thesis, Western University, Canada.

Elawady, A. and El Damatty, A., (2016), "Longitudinal Force on Transmission Towers Due to Non-Symmetric Downburst Conductor Loads" Engineering Structures 127:206-226.

El Damatty, A. and Elawady, A., (2015), "Critical Load Cases for Lattice Transmission Line Structures under Downbursts" The 14th International Conference on Wind Engineering, ICW14, June 21-26, Brazil.

El Damatty A. and Hamada A. (2016). "F2 tornado velocity profiles critical for transmission line structures." Engineering Structures, Vol. 106, 436- 449.

El Damatty, A.A., Hamada, A., Elawady, A. (2013), "Development of Critical Load Cases Simulating the Effect of Downbursts and Tornados on Transmission Line Structures", proceedings of the Eighth Asia-Pacific Conference on Wind Engineering, Chennai, India.

Failure Investigation Report, HYDRO ONE NETWORKS INC, (2006), "Failure of towers 610 and 611, circuit X503E – 500 kV guyed towers near the Township of Waubaushene, Ontario, August 2, 2006". Line Engineering.

Fouad, F.H., Sherman, D., and Werner, R.J. (1992). "Spun prestressed concrete poles – past, present, and future". Concrete International, 14(11): 25–29.

Fujita, T., (1981). "Tornadoes and downbursts in the context of generalized planetary scales." J.Atmos.Sci., 38(8), 1511-34.

Fujita, T., (1985), "The downburst: microburst and macroburst", SMRP Research Paper 210, University of Chicago, USA.

Fujita, T., (1990), "Downbursts: meteorological features and wind field characteristics", Journal of Wind Engineering and Industrial Aerodynamics 36, 75–86.

Fujita, T., and Pearson, A. D. (1973). "Results of FPP classification of 1971 and 1972 tornadoes." 8th Conference on Severe Local Storms (abstracts only), USA, 609.

Gast, K.D., Schroeder, J.L., (2003). "Supercell rear-flank downdraft as sampled in the 2002 thunderstorm outflow experiment", Proceedings of the 11th International Conference on Wind Engineering. ICWEIA, 2233–2240.

Hamada, A., Damatty, A.A.E., Hangan, H., and Shehata, A.Y. (2010). "Finite element modelling of transmission line structures under tornado wind loading". Wind and Structures, 13(5): 451-469.

Hamada, A., and El Damatty, A. A. (2011). "Behaviour of guyed transmission line structures under tornado wind loading". Computers and Structures, 89(11-12), 986-1003.

Hamada, A., and El Damatty, A. A. (2015). "Failure analysis of guyed tranmssion lines under F2 tornado event ". Engineering Structures, 85, 11-25.

Hamada M. and El Damatty A. (2016). "Load cases simulating tornadoes- Economic implications for transmission line structures design". Proceedings of CIGRE-IEC colloquim, Montreal, QC, Canada.

Hangan, H., Roberts, D., Xu, Z., and Kim, J., (2003), "Downburst simulation. Experimental and numerical challenges", Proceedings of the 11th International Conference on Wind Engineering, Lubbock, TX, USA.

Hangan, H. and Kim, J. (2008). "Swirl ratio effects on tornado vortices in relation to the Fujita scale". Wind and Structures, An International Journal, 11(4), 291-302.

Harlow, F. H., and Stein, L. R. (1974). "Structural analysis of tornado-like vortices", J.Atmos.Sci., 31(8), 2081-98.

Holmes, J. D., Banks, R. W., & Paevere, P., (1997), "Measurements of topographic multipliers and flow separation from a steep escarpment. Part 1. Full scale measurements." Journal of Wind Engineering and Industrial Aerodynamics, 67-71, 885-892.

Horr, A.M., Yibulayin, A., and Disney, P., (2004), "Nonlinear spectral dynamic analysis of guyed towers. Part II: Manitoba towers case study". Canada Journal of Civil Engineering, 31(6): 1061-1076.

http://www.valmont.com/valmont/markets/ utilities/transmission-poles.

International Electrotechnical Commission (IEC), (2003), "Design Criteria of Overhead Transmission Lines", International Standard IEC-60826" Geneva, Switzerland.

Ishac, M.F. and White, H.B. (1994). "Effect of tornado loads on transmission lines". In Proceedings of the 1994 IEEE Power Engineering Society Transmission and Distribution Conference, April 10, 1994 - April 15, 1994. Publ by IEEE, Chicago, IL, USA, 521- 527.

Ivan, M., (1986), "A ring-vortex downburst model for flight simulations", Journal of Aircraft 23, 232-236.

Kim, J. and Hangan, H., (2007), "Numerical simulations of impinging jets with application to downbursts", Journal of Wind Engineering and Industrial Aerodynamics 95(4), 279-298.

Kuebler,M., (2008), "Torsion in Helically Reinforced Prestressed Concrete Poles", M.Sc. thesis, University of Waterloo, Waterloo, Ontario, Canada.

Ladubec, C., El Damatty, A., and El Ansary, A., (2012), "Effect of geometric nonlinear behaviour of a guyed transmission tower under downburst loading", Proceedings of the International Conference on Vibration, Structural Engineering and Measurement, Shanghai, China, Trans. Tech. Publications, 1240-1249.

Lantrip, T.B., (1995), "Identification of Structural Characteristics of Spun Prestressed Concrete Poles Using Modal Testing Methods", M.Sc. Thesis, Dept. of Civil and Environmental Engineering, University of Alabama at Birmingham.

Lewellen, D. C., Lewellen, W. S., and Xia, J. (2000). "The influence of a local swirl ratio on tornado intensification near the surface", J.Atmos.Sci., 57(4), 527-44.

Lewellen, W. S., Lewellen, D. C., and Sykes, R. I. (1997). "Large-eddy simulation of a tornado's interaction with the surface", J.Atmos.Sci., 54(5), 581-605.

Li, C.Q. (2000). "Stochastic model of severe thunderstorms for transmission line design". Probabilistic Engineering Mechanics, 15(4): 359-364.

Li, H. and Bai, H. (2006). "High-voltage transmission tower-line system subjected to disaster loads". Progress in Natural Science, vol. 16, no. 9, 899–911.

Loredo-Souza, A. and Davenport, A.G. (1998), "The effects of high winds on transmission lines". J. Wind Eng. Ind. Aerodyn., 74-76, 987-994.

Madugula, M. K. S., (2002), "Dynamic Response of Lattice Towers and Guyed Masts". American Society of Civil Engineers (ASCE), New York, NY, USA.

McCarthy, P., and Melsness, M., (1996), "Severe weather elements associated with September 5, 1996 hydro tower failures near Grosse".

Momomura, Y., Marukawa, H., Okamura, T., Hongo, E. and Ohkuma, T., (1997). "Full-scale measurements of wind induced vibration of a transmission line system in a mountainous area". Journal of Wind Engineering and Industrial Aerodynamics, 72, 241-252.

Polyzois, D., Raftoyiannis, I.G. and Ibrahim, S., (1998), "Finite elements method for the dynamic analysis of tapered composite poles", Composite structures (43) 25-34.

Rotunno, R. (1977). "Numerical simulation of a laboratory vortex tornado theory", J.Atmos.Sci., 34(12), 1942-56.

Sarkar, P., Haan, F., Gallus, Jr., W., Le, K. and Wurman, J. (2005). "Velocity measurements in a laboratory tornado simulator and their comparison with numerical and full-scale data." 37th Joint Meeting Panel on Wind and Seismic Effects.

Savory, E., Parke, G. A. R., Zeinoddini, M., Toy, N., and Disney, P. (2001). "Modelling of tornado and microburst-induced wind loading and failure of a lattice transmission tower". Eng.Struct., 23(4), 365-375.

Sengupta, A. and Sarkar, P., (2008) "Experimental measurement and numerical simulation of an impinging jet with application to thunderstorm microburst winds", Journal of Wind Engineering and Industrial Aerodynamics 96, 345–365.

Shehata, A. Y., and El Damatty, A. A. (2007). "Behaviour of guyed transmission line structures under downburst wind loading." Wind and Structures, an International Journal, 10(3), 249-268.

Shehata, A. Y., and El Damatty, A. A. (2008). "Failure analysis of a transmission tower during a microburst." Wind and Structures, 11(3), 193-208.

Shehata, A., El Damatty, A.A., and Savory, E., (2005). "Finite element modeling of transmission line under downburst wind loading". Finite Elements in Analysis and Design 42(1), 71-89.

Shehata, A., Nassef, A., and El Damatty, A., (2008), "A coupled finite element-optimization technique to determine critical microburst parameters for transmission towers", Finite Elements in Analysis and Design 45(1), 1-12.

Simiu, E. and Scanlan, R. (1996). "Wind Effects on Structures", Third Edition, John Wiley and Sons.

Vermeire, B., Orf, L. and Savory, E., (2011), "Improved modelling of downburst outflows for wind engineering applications using a cooling source approach", Journal of Wind Engineering and Industrial Aerodynamics 99, 801–814.

Vicroy, D., (1992), "Assessment of microburst models for downdraft estimation", Journal of Aircraft 29, 1043-1048.

Wolfson, M., DiStefano, J., Fujita, T., (1985), "Low-altitude wind shear characteristics in the Memphis, TN area", Proceedings of the 14th conference on severe local storms, American Meteorological Society, Indianapolis, IN, USA., 322–7.

Wood, G., Kwok, K., Motteram, N., and Fletcher, D., (2001), "Physical and numerical modelling of thunderstorm downbursts", Journal of Wind Engineering and Industrial Aerodynamics 89, 535-552.

Wurman, J. (1998). "Preliminary results from the ROTATE-98 tornado study", Preprints, 19th Conf. On severe local storms, Minneapolis, MN, 14-18 September.

Zhang, Y., (2006), "Status quo of wind hazard prevention for transmission lines and countermeasures", East China Electric Power 34(3), 28-31.

Zhu, S., and Etkin, B., (1985), "Model of the wind field in a downburst", Journal of Aircraft 22, 595-601.

CHAPTER 2

FINITE ELEMENT MODELLING OF PRE-STRESSED CONCRETE POLES UNDER DOWNBURSTS AND TORNADOES

2.1. <u>Introduction</u>

Downbursts and Tornadoes are a category of weather storms that are referred to as high intensity wind (HIW) events. Those events are characterized by high wind speeds that affect a relatively narrow area. They are different than large scale events, such as hurricanes, because of their localized size and effect. Transmission lines are among the structures that are very sensitive to HIW. This is because of their length that typically extends for many kilometers making the probability of localized wind events, such as downbursts and tornadoes, to affect one of the towers of the line very high. As a result, many failure incidents of transmission line structures have been reported around the world. Dempsey and White (2006) stated that 80% of weather- related transmission line failures around the world were caused by HIW events. Howes and Dempsey (1993) stated that more than 90 % of 94 structural failure events in Australia were induced by severe thunderstorms, including downbursts. Zhang (2006) reported the failure of 18 transmission towers carrying 500 kV lines and 60 towers carrying 110 kV lines in 2005 because of various wind events including downbursts, tornadoes and typhoons. In Canada, many of transmission line failures occurred in the past twenty years as a result of downbursts and tornadoes such as those reported by McCarthy and Melsness (1996) and a failure investigation report by HYDRO ONE NETWORKS INC. (2006).

The above failures led to the initiation of an extensive research program at the University of Western Ontario, Canada, to study various aspects related to this problem. The research included development and validation of the HIW wind fields based on numerical simulations. Shehata et al. (2005) developed a comprehensive structural analysis numerical model that incorporated the downburst wind fields and simulated various components of a transmission line system including the towers, insulators and conductors. Hamada et al. (2010) developed a similar model that incorporated the tornado wind fields. Because of the localized nature of HIW events, the simulations conducted by these numerical models involved a large number of analyses involving varying the size and the location of the downbursts and tornadoes. The purpose was to determine the configurations leading to peak internal forces in transmission line members. As a result, the computational time needed to quantify the peak internal forces in all members of a tower is significantly large mainly because of the nonlinear analyses required to predict the conductors' responses. In order to solve this issue, Aboshosha and El Damatty (2014) developed a semi-analytical solution to predict the response of conductors to the non-uniform loading associated with tornadoes and downbursts. All of the above studies focused on steel transmission line systems consisting of lattice steel towers. Another type of structures commonly used in transmission line systems is the pre-stressed concrete poles. Typically, this types of poles are self-supported, guyed or H-framed. **Fig. 2-1** (a,b) shows photos of different types of poles.

(a) Cantilever concrete pole   (b) H-Frame concrete pole

Fig. 2-1. Concrete Pole systems

The advantages of the pre-stressed concrete poles are the low installation and maintenance costs, short construction time and corrosion resistivity. Reviewing the literature, it is found that no previous studies have been conducted to investigate the behavior of pre-stressed concrete poles to HIW events. In 2007, in Kitchener, Canada, a number of pre-stressed concrete poles failed during a high wind storm (Kuebler, 2008). The failure was attributed to the excessive forces acting on the conductors. The main objective of the current study is to develop a numerical model capable of predicting the behavior of pre-stressed concrete poles to HIW events, taking into account the variation in the location of those events. In terms of numerical simulation, the main difference between pre-stressed concrete poles and steel towers is the modelling of the material behaviour.

Since tornadoes and downbursts are extreme events, it would be reasonable to accept cracking to happen in a pre-stressed concrete pole once subjected to those events as long as no collapse occurs.

As such, the material model should be able to predict the post cracking behavior of the poles under HIW loading.

The numerical model developed in this study incorporates:

(1) The three-dimensional downburst and tornado wind fields previously developed and validated by Hangan et al. (2003) and Hangan and Kim (2008), respectively.

(2) The computationally efficient semi-analytical technique developed and validated by Aboshosha and El Damatty (2014) to predict the non-linear behavior of the conductors under HIW while accounting for the effects of the conductors' pretension forces, sagging and insulator's stiffness.

(3) A non-linear finite element model developed in the current study to simulate the structural behavior of the pre-stressed concrete poles considering the material non-linearity and the pre-tensioning losses.

The study starts by providing a brief description of the downburst and tornado wind fields used. The first two components of the model (wind field and conductors modelling) were previously validated. As such, a validation is conducted in the current study for the developed non-linear finite element model by comparing its prediction to the results of tests conducted on pre-stressed concrete poles and reported in the literature. The developed and validated numerical model is then used to simulate a pre-stressed pole as a case study. The pole is designed under the loads specified by the ASCE-74 (2010) guidelines. Those guidelines do not consider HIW loads. The design follows the specifications described in the ASCE-123 (2012) guidelines which focus on pre-

stressed concrete transmission line poles. The poles are designed to sustain normal wind loads up to a certain speed such that it remains un-cracked.

Parametric studies are then conducted to determine the most critical downburst and tornado configurations for this pole. Non-linear analyses are also conducted to determine the downburst and tornado velocities that this pole is able to sustain before full collapse. A comparison between the effect of the downburst and tornado critical load cases is made.

2.2.   **Downburst wind field**

Fujita (1985) defined a downburst as a mass of cold and moist air that drops suddenly from a thunderstorm cloud base and impinges the ground surface and then transfers horizontally. As mentioned earlier, the localized nature of the downbursts makes field measurements hard to obtain. Limited full-scale measurements were reported in literature by Wolfson et al. (1985), Holmes et al. (1997), Fujita (1990), Gast and Schroeder (2003) and Choi (2004). As such, numerical simulation of such events is considered a useful mean to estimate wind field velocities. A Computational Fluid Dynamics (CFD) model was developed by Hangan et al. (2003). This model simulated the spatial and time variations of the wind field associated with downbursts. The downburst outflow in this model consists of two velocity components: radial (horizontal) component (V_{RD}) and axial (vertical) component (V_{VL}). The values of the two velocity components at a specific point in space are functions of its height relative to the ground and its location relative to the center of the downburst. Kim and Hangan (2007) validated this model based on full scale data reported by Wood et al. (2001). The radial and vertical velocity components associated with the downbursts events are evaluated in this study along the pre-stressed concrete transmission pole

and along the length of the attached conductors. The wind field associated with the downburst is mainly affected by the parameters V_j, D_j, R and θ as shown in **Fig. 2-2**.
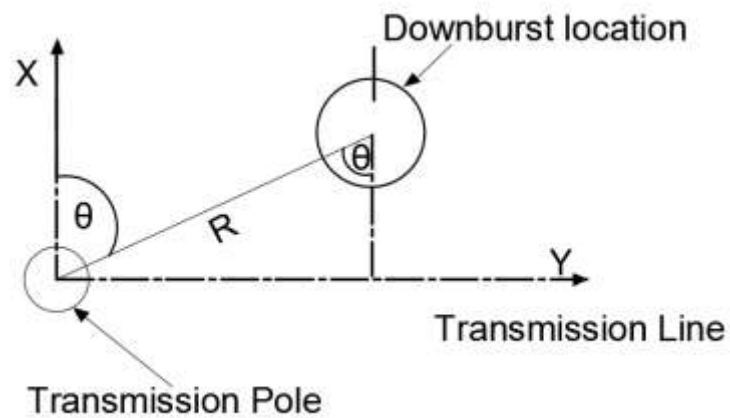
Fig. 2-2. Downburst Parameters

As shown in **Fig. 2-2**, the location of the center of the downburst with respect to the pole center is determined by the polar coordinates (distance (R) and the angle (θ)). The downburst is defined by its jet diameter (Dj) and its jet velocity (Vj). To assess how the location of the downburst affects the magnitude and the distribution of the wind loads, the radial and vertical velocities acting along the height and the span of a transmission line system are presented.

The considered pole has a height of 25.5 m and the conductor has a span of 100m and is attached at an elevation of 23m. **Fig. 2-3** shows the distribution of both the transverse (along the X-direction) and vertical velocities along 3 spans from each side of the pole. This number of spans was recommended by Shehata et al. (2005) to be considered for the analysis of an intermediate tower.

The velocities are normalized by the jet velocities Vj. The plots show the cases of R/Dj=1.2, $\theta=0^0$ and R/Dj=0.6, $\theta=30^0$. The downburst size Dj is equal to 500m in both cases. The distributions along the height of the poles of the radial and vertical velocities for the two downburst configurations are shown in **Fig. 2-4**. The distributions are plotted at the instant that gives the peak value at the pole centre.
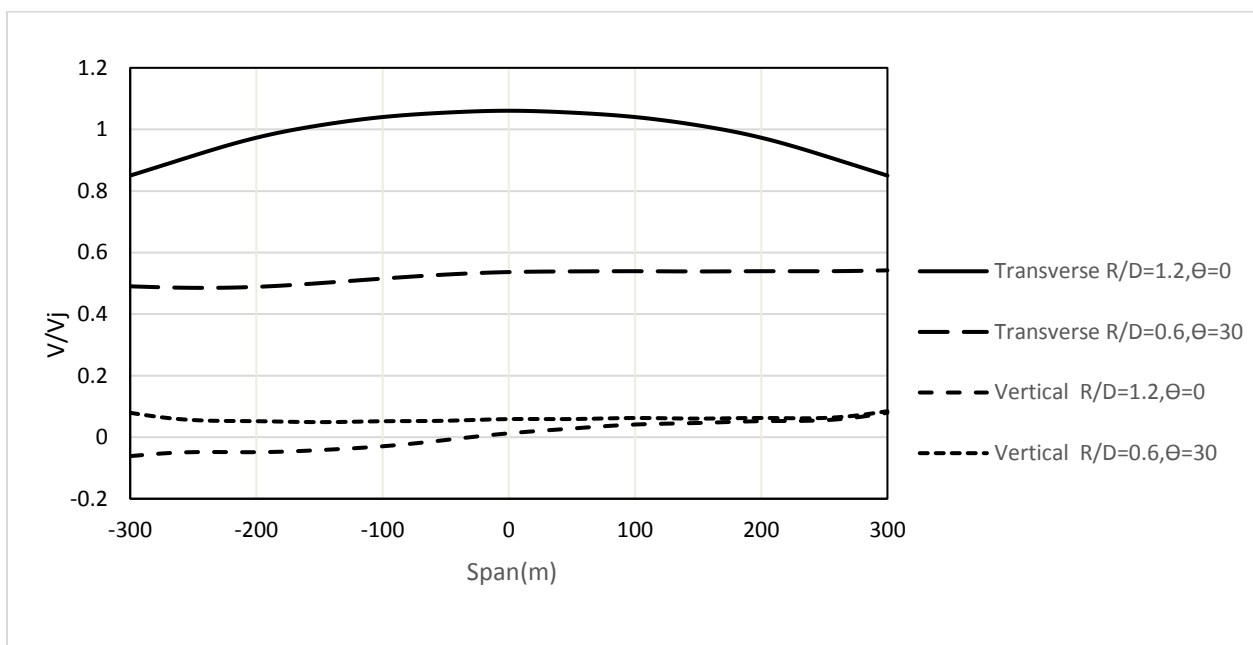
Fig. 2-3. Transverse and vertical velocity distributions along six conductor spans
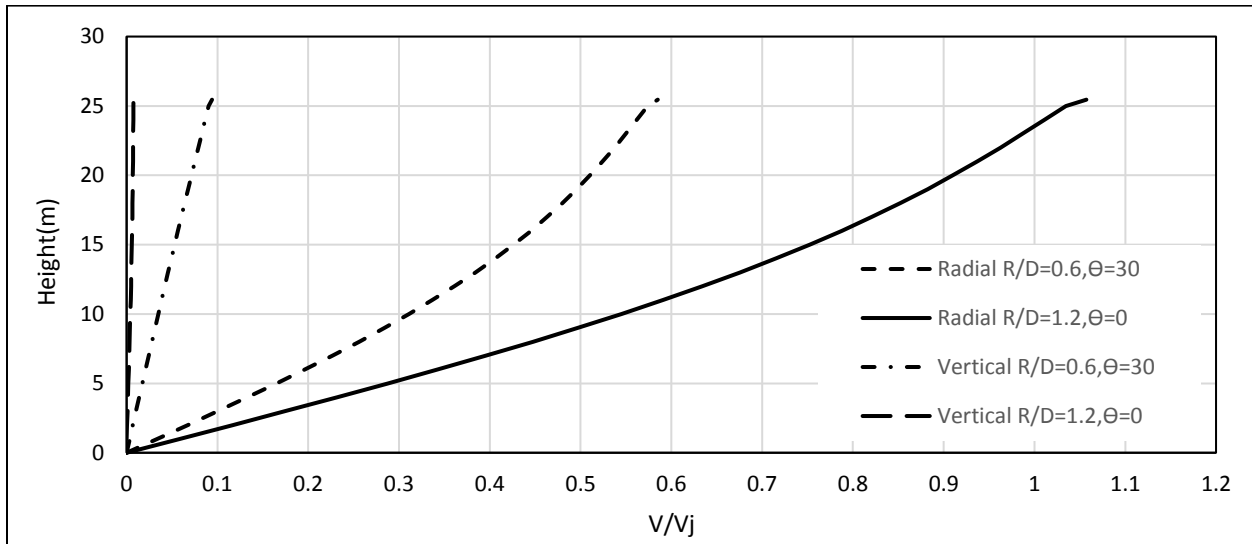
Fig. 2-4. Radial and vertical velocity distribution along the pole height

The plots show the significant variation in the velocity values depending on the location of the downburst. They indicate that the first configuration of R/Dj=1.2, $\theta=0^0$ leads to higher velocity values. They also show that the radial velocities are significantly higher than the vertical velocity values.

2.3.   Tornado wind field

Tornadoes are defined by Fujita (1981) as rotating wind vortices with high wind speeds affecting relatively narrow paths. A tornado wind field consists of three mean velocity components, radial V_r, vertical V_v and tangential V_t velocities. The intensity and scale of tornadoes cannot be measured by traditional recording stations in the field. Therefore, the simulation of tornado events relies mainly on numerical modeling. Fujita and Pearson (1973) classified tornadoes according to their intensity and size. Intensity is defined by the gust wind speed, while the size is defined by the path length and width.

Hangan and Kim (2008) conducted a three dimensional computational fluid dynamics (CFD) simulation for the wind field associated with tornadoes. The simulation was conducted at a steady-state manner. Therefore, the velocity profile does not vary with time. Hangan and kim (2008) validated their CFD model by comparing the obtained velocity field with the results of the tests conducted by Baker (1981), Wurman (1998) and Sarkar et al. (2005). Hangan and Kim (2008) CFD model is used in the current study to evaluate the F2 tornado velocity components acting on pre-stressed concrete transmission lines.

The location of the tornado wind field with respect to the transmission pole is defined by the two polar parameters (R) and (θ) as shown in **Fig. 2-5**.
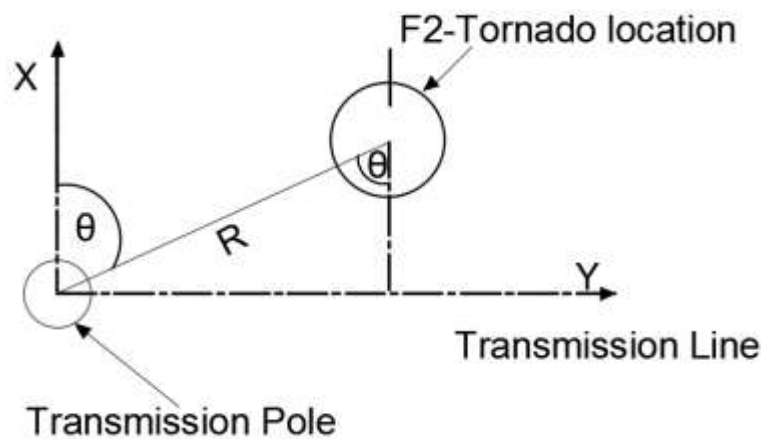
Fig. 2-5. Tornado Parameters

The reasons behind limiting the study to the F2 tornado scale is that the vast majority of observed tornadoes are F2 or less and that it is not practically possible to design for tornado intensity beyond that of F2.

The distribution of the F2- tornado velocity profile along the transmission line system considered in the previous section is presented here. For the conductors, the radial and tangential velocities are resolved to obtain the velocity component in the direction transverse to the conductor (along the X-direction). The distributions are provided for two different tornado configurations (R=100m, $\theta =0^0$ and R=300m, $\theta =30^0$). For each configuration, the transverse and the vertical distributions are provided along six conductor spans.

For the pole, the horizontal resultant of both tangential and radial components is calculated and plotted along the height of the pole together with the axial (vertical) component. All the velocities are normalized by the maximum F2 tornado speed of 72 m/sec (V_{f2max}) specified by the Fujita scale.
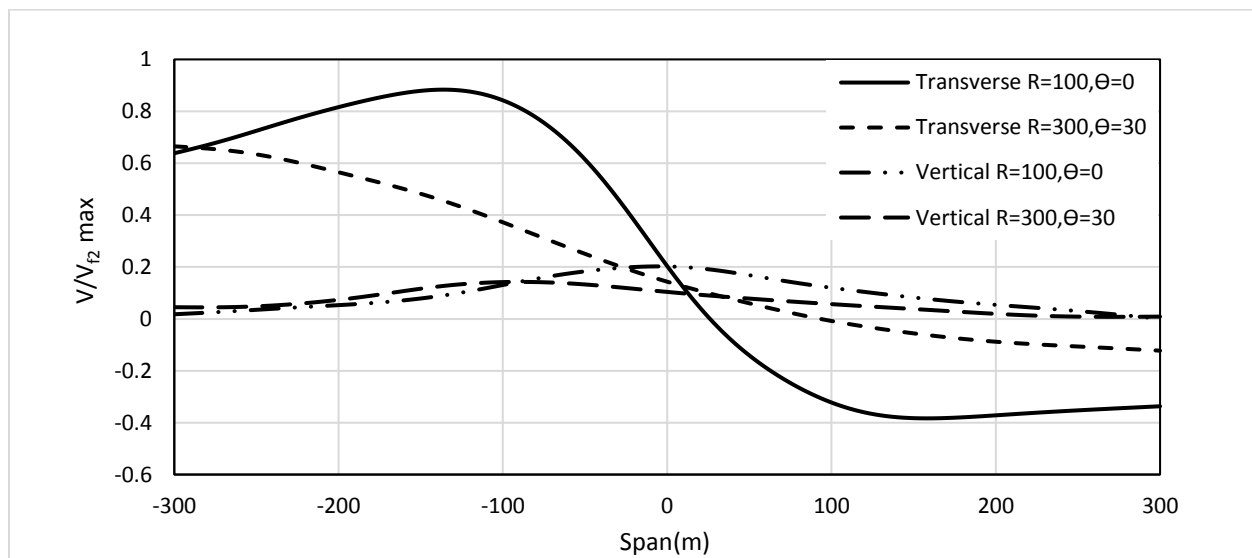
Fig. 2-6. Vertical, radial and tangential velocity distribution along six conductor spans
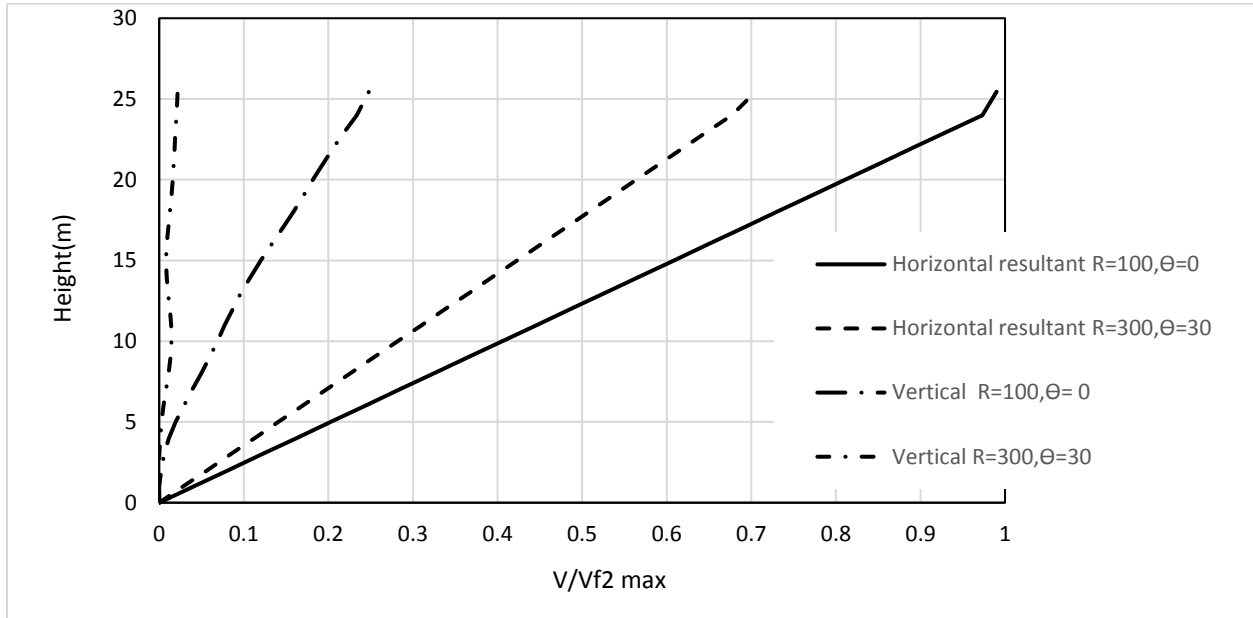
Fig. 2-7. Vertical and horizontal resultant velocity distribution along the pole height

2.4.   Numerical model

As mentioned earlier, the numerical model consists of three components. The loads are obtained

from the wind fields described above. This velocity wind field is transformed into forces using the

procedure provided by ASCE-74 (2010) based on the following equation:

$$F_{wi} = \frac{1}{2}\rho_a\, G C_f\, A(Z_v\, V_i\,)^2 \qquad (2\text{-}1)$$

Where F_{wi} is the force developing in the i direction, ρ_a is the density of air = 1.225 (Kg/m^3), G is

the gust factor , C_f is the drag force coefficient, A is the nodal projected area perpendicular to i

direction, Z_v is the terrain factor and V_i is the downburst/tornado velocity in the i direction (units

m/sec). For conductors and circular concrete poles, the value of the drag coefficient is taken equal

to 1.0 according to ASCE-74 (2010) guidelines, and the same value is recommended for gust and terrain factors.

Conductors' reactions are predicted using the analytical technique developed by Aboshosha and El Damatty (2014). This technique accounts for the variation of the loads along the conductor spans, insulators flexibility and the non-linear behaviour of the conductors including sagging and pre-tensioning forces. The technique is based on applying compatibility of displacements and equilibrium of forces using a semi-closed form solution that calculates the displacement and reactions of the conductor under HIW events. Aboshosha and El Damatty (2014) has proven that this semi-closed form numerical technique is more efficient compared to the finite element method in terms of computational time.

2.4.1 Development of finite element model of pre-stressed concrete poles

Frame elements are used to model the pre-stressed concrete poles which are subjected to axial forces and bending moments. The complexity of capturing the non-linear behavior of pre-stressed concrete poles arises from the cracking and non-linear behavior of concrete, in addition to the long term effects such as creep, shrinkage and relaxation. The flowchart below shows the various steps involved in the non-linear finite element analysis developed in the current study.
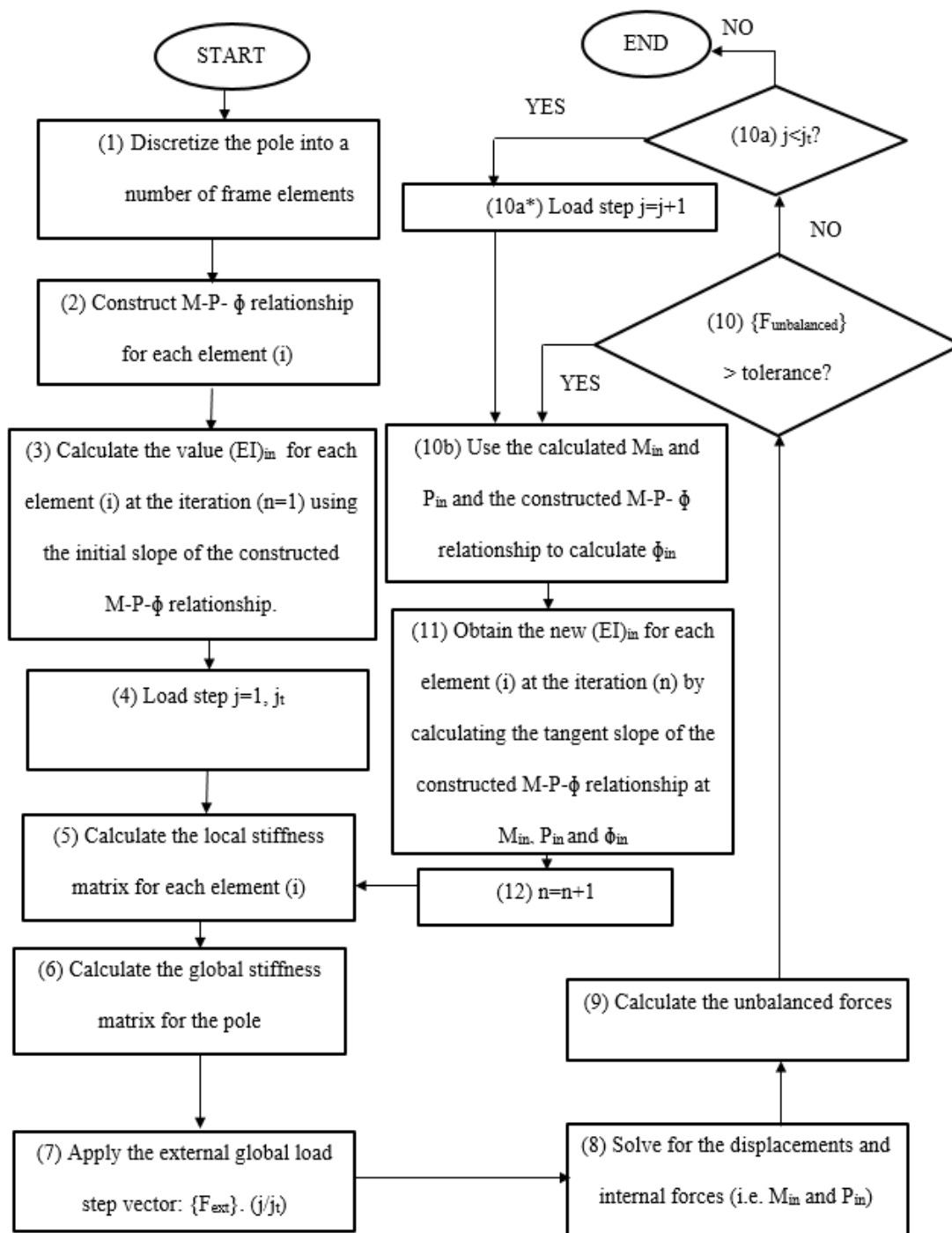
Fig. 2-8. Non-linear finite element analysis flowchart

A description of each block of the above flow chart is provided below:

1- The pre-stressed concrete pole is discretized into a number of frame elements along its height.

2- The M-P-ϕ relationship for each element (i) along the pole height is constructed using Gutierrez and Ochoa (2001). This relationship captures the behaviour of the pre-stressed concrete cross section before and after cracking until failure occurs. The failure can be due to concrete crushing or strands rupture. A brief about the procedures and the assumptions of Gutierrez and Ochoa (2001) is presented later by the end of this subsection.

3- Each element (i) is assumed to be un-cracked as a first iteration i.e. (n=1). The value $(EI)_{in}$ is obtained using the initial slope of the constructed M-P-ϕ relationship. E represents the modulus of elasticity of the element (i), while I represents the moment of inertia of the element (i).

4- The external load is discretized into a number of load steps j_t.

5- The local stiffness matrix for each frame element i is calculated.

6- The local stiffness matrices are assembled and the boundary conditions are applied to obtain the global stiffness matrix.

7- The load step vector is applied on the concrete pole structure. This load vector includes the gravity loads in addition to a factor of both the HIW loads acting on the pole and conductors' reactions due to HIW events. This factor is the ratio between the load step j and the total number of load steps j_t.

$$\{F_{ext}\}_j = \{F_{HIW}\}.\left(\frac{j}{j_t}\right) + \{F_{Gravity}\} \qquad (2\text{-}2)$$

Where:

$\{F_{ext}\}_j$: The load step vector applied on the structure.

$\{F_{HIW}\}$: The high intensity wind loads applied on the structure.

$\{F_{Gravity}\}$: The gravity loads applied on the structure.

$\{F_{ext}\}$: The total external load vector.

8- The displacement vector is determined and the internal forces developed in each element
of the pole are calculated.

$$\{D\}_n = \left[K_{global}\right]_n^{-1}.\{F_{ext}\}_j \qquad (2\text{-}3)$$

$$\{f_{int}\}_{in} = [K_{local}]_{in}.[r]_i.\{d\}_{in} \qquad (2\text{-}4)$$

Where:

n: Iteration number

$\{D\}_n$: The global displacement vector calculated in iteration n.

$[K_{global}]_n$: The global assembled stiffness matrix for the structure after applying the
boundary conditions.

$\{F_{int}\}_{in}$: The local internal forces vector of the element "i" computed in iteration "n".

$[K_{local}]_{in}$: The local stiffness matrix for the element "i" computed in iteration "n".

[r]$_i$: The local transformation matrix for the element "i" .

{d}$_{in}$: The local displacement vector for the element "i" computed in iteration "n".

9- The unbalanced forces vector is evaluated.

$$\{F_{unbalanced}\}_n = \{F_{ext}\}_j - [R]^T.\{F_{intglobal}\}_n \qquad (2\text{-}5)$$

{F$_{unbalanced}$}$_n$: The unbalanced forces vector of the structure computed in iteration "n".

[R]: The global transformation matrix of the structure.

{F$_{intglobal}$}$_n$: The internal global forces vector of the structure computed in iteration "n".

10- The unbalanced forces are compared to the specified tolerance.

(a) If the unbalanced forces vector is less than this tolerance, the displacements and internal forces computed in this iteration can be considered as the response of the structure under the applied load step.

(b) If the unbalanced forces exceed this tolerance, the internal forces calculated in step 8 (which includes M$_{in}$ and P$_{in}$) are used to determine the corresponding curvature (ϕ_{in}) using the constructed M-P-ϕ diagrams.

11- Based on the values obtained from step 10(b), new values for (EI)$_{in}$ are calculated using equation (2-6). The updated (EI)$_{in}$ are used to calculate an updated stiffness matrix. It should be noted that the updated matrix can be whether cracked or un-cracked depending on the value of the internal forces developed in each element.

$$(EI)_{in} = \frac{M_{in}}{\phi_{in}} \qquad (2\text{-}6)$$

For each iteration n, $(EI)_{in}$ represents the product of the modulus of elasticity and the sectional moment of inertia of the element i, M_{in} is the bending moment acting on the element i and ϕ_{in} is the curvature of the element i.

12- A new iteration (n) is evaluated.

$$n = n + 1 \qquad (2\text{-}7)$$

Steps from 5 to 12 are repeated until tolerance is achieved.

If the load step (j) is equal to the total number of load steps (j_t), the numerical model terminates and the displacements and internal forces computed in the last iteration (n) are considered as the response of the structure under the total applied load. While, if the load step (j) is less than the total number of load steps (j_t), a new load step is applied to the structure as per equation (2-8):

$$j = j + 1 \qquad (2\text{-}8)$$

It is worth to mention that at any load step j, iteration n and element i, if the internal moment (M_{in}) is found to be greater than the maximum moment in the constructed M-P-ϕ relationship (bending moment capacity), the numerical model terminates due to bending failure.

It should be noted that the nonlinear finite element model developed is highly dependent on the analytical model developed by Gutierrez and Ochoa (2001). This model is capable of considering concrete and strands nonlinearities as well as constructing M-P-ϕ diagrams for pre-stressed concrete cross sections under biaxial bending and axial loads. The model accounts for post-

cracking behaviour of the pre-stressed concrete poles including tension stiffening, creep and relaxation of strands.

To be able to construct M- ϕ relationship under a specific axial load P, a set of strains and neutral axes positions are assumed for the pre-stressed concrete cross section. The cross section is discretized into a finite number of areas. Each area has its own strain as well as each pre-stressing stand. The strain values at the areas and pre-stressing strands depend on their location with respect to the neutral axis of the cross section. As such, the forces developed in the concrete areas and the pre-stressing strands are evaluated based on the stress-strain relationships used by Gutierrez and Ochoa (2001). A series of equations are then solved iteratively to obtain the bending moment (M) which corresponds to a certain curvature value (ϕ) under an axial load (P). M-P- ϕ relationships are then constructed for pre-stressed concrete cross sections.

The main assumptions of Gutierrez and Ochoa (2001) model can be summarized as follows:

1- Strain distribution across the cross section is linear.

2- The concrete stress-strain relationship in compression is a combination of an ascending second degree parabola and a descending straight line as expressed by the following equations:

For $\varepsilon / \varepsilon_0 < 1$

$$f_c = \left(2 - \frac{y}{c}\frac{\varepsilon}{\varepsilon_0}\right)\frac{y}{c}\frac{\varepsilon}{\varepsilon_0}f_c'' \qquad (2\text{-}9)$$

For $\varepsilon / \varepsilon_0 > 1$

$$f_c = \left(1 - \beta\left(\frac{y}{c}\frac{\varepsilon}{\varepsilon_0} - 1\right)\right)f_c'' \qquad (2\text{-}10)$$

Where, f_c is the compressive stress, ε is the concrete strain, ε_0 is the concrete strain at maximum concrete stress, β is the confinement factor, y is the height of the compression portion measured from the cross section center, c is the height of the cross section subjected to compression measured from the center and f''_c is the concrete maximum allowable strength.

3- Ramberg-Osgood function, as recommended by Mattock (1979), is utilized for the pre-stressed steel stress-strain relationship.

4- The concrete tensile behavior before and after cracking including tension stiffening is considered using Vecchio and Collins (1986) equations.

As a demonstrative example, **Fig. 2-9** presents the M-ϕ relationship under a compression load (P) equal to 350 kN for a hollow circular pre-stressed concrete cross section with an outside diameter of 700 mm, inside diameter of 400 mm, f''_c of 30 MPa and a number of 8 low relaxation strands having a total area of 140 mm^2.
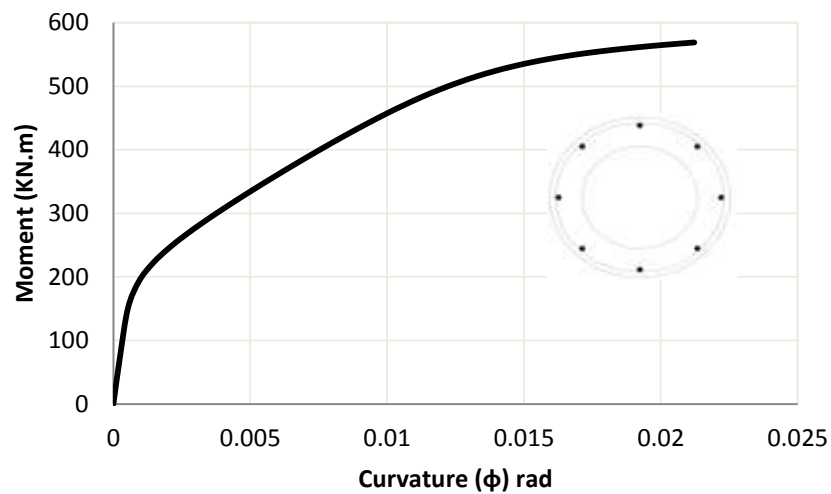
Fig. 2-9. M-ϕ diagram at P = -350 kN

2.4.2   Validation of the developed finite element model

In order to validate the developed numerical model, three pre-stressed hollow circular poles that were previously tested under an applied point load are modelled using the in-house developed numerical model where frame elements are used to model the tested poles. The numerical results are compared to those obtained from the tests. The following table shows the properties of the three poles used in the validation:

Table 2-1. Poles' properties

Pole (No.)	Height (m)	Outer Top Diameter (mm)	Thickness at Top(mm)	Outer Tapering slope (m/m)	Inner Tapering slope (m/m)	Number of Strands	f_c'' (N/mm^2)
1	13.7	391	70	0.009	0.008	28	75.8
2	22.3	335	64	0.009	0.008	24	65.5
3	21.3	197	51	0.0075	0.006	8	73.1

It should be mentioned that the strands used in the three tested poles were low relaxation strands of an area equal to 99 mm^2. Poles 1, 2 and 3 were tested by Fouad et al. (2000), Fouad et al. (1994) and Fouad and Simpson (1999), respectively.
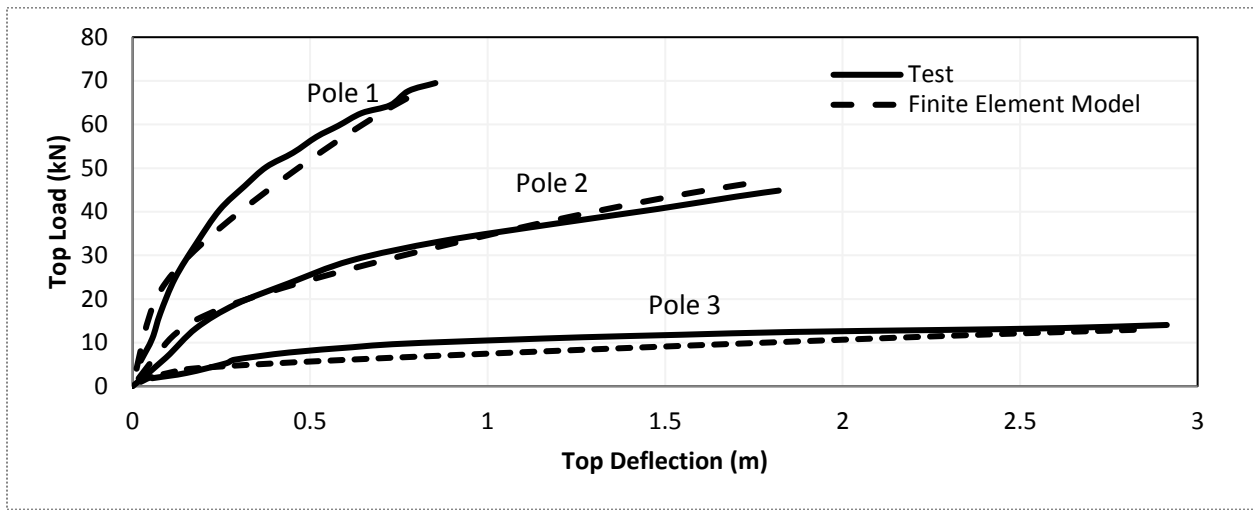
Fig. 2-10. Load versus top deflection obtained from the numerical model and the test

The relationship between the applied load and the top deflection of the pole obtained from both the experiments and the numerical analyses are shown in **Fig. 2-10**. The figure shows a very close agreement between the experimental and the numerical results with a maximum difference of 4% and 3% in peak load and maximum deflection, respectively. The bending failure mode is found to be the governing mode predicted from the test and the numerical model. This provides a validation for the accuracy of the developed numerical model and its ability to predict the behavior and failure of pre-stressed concrete pole structures.

2.5. <u>Case study</u>

Having developed and validated the numerical model, the study proceeds by using this numerical model to study the performance of a self-supported pre-stressed concrete pole under downbursts and tornadoes. The following steps are conducted in this study:

1- Design a pre-stressed concrete pole to remain un-cracked under a certain magnitude of normal wind load.

2- Perform parametric study by changing the downburst size and location in order to determine the critical downburst configuration leading to maximum effect on the pole under a specific downburst jet velocity.

3- Conduct a non-linear analysis for the pole using this critical downburst configuration that considers post cracking behavior in order to determine the downburst jet velocity that would lead to a full collapse of the pole.

4- Perform a parametric study by changing the F2-tornado location in order to determine the critical F2-tornado configuration that would lead to the maximum effect on the pole.

5- Conduct a non-linear analysis for the pole using this critical tornado configuration that considers post cracking behavior in order to determine the F2 tornado velocity that would lead to a full collapse of the pole.

A pre-stressed concrete pole similar to the one analyzed by Dai and Chen (2008) is considered. The pole height is 30m with a length of 25.45m above the ground. The outer diameters at the tip and the bottom are 281 and 802 mm, respectively, while the inside diameter of the pole varies between 141 mm at the top to 621 mm at the bottom. The concrete strength is 75.8 MPa and a number of 20 low relaxation strands having a total area of 93 mm^2 are used for pre-stressing.

Two conductors are used in this study. The conductors are located on both sides of the pole and their properties are shown in the following table:

Table 2-2. Conductor properties

Elevation (m)	Diameter (mm)	Weight (N/m)	Modulus of Elasticity (N/m^2)	Sag (m)	Span (m)	Cross arm (inch)section	Cross arm length (m)
23	34.69	30	$1.89*10^{11}$	2	100	10x10x3/8	2.44

The analysis of the tower included synoptic wind, ice, broken conductor, construction and maintenance loads. Different load combinations specified in the ASCE-74 (2010) are considered. The design synoptic wind load is chosen to be 40 m/sec which is the recommended design speed for almost 90 percent of the USA. It is found that the design of the pole is governed by the wind load case. The pre-stressed concrete pole with the conductor properties presented in the previous table is considered to be designed to remain un-cracked under the effect of synoptic wind speed of 40 m/sec

The distribution of the bending moment arising from the synoptic wind load of reference speed 40 m/sec (M_a) normalized by the cracking bending resistance of the pole along its height (M_{cr}) is shown in **Fig. 2-11**. The cracking bending resistance of the pole is determined using the M-P-ϕ diagrams previously developed and validated in section 4.
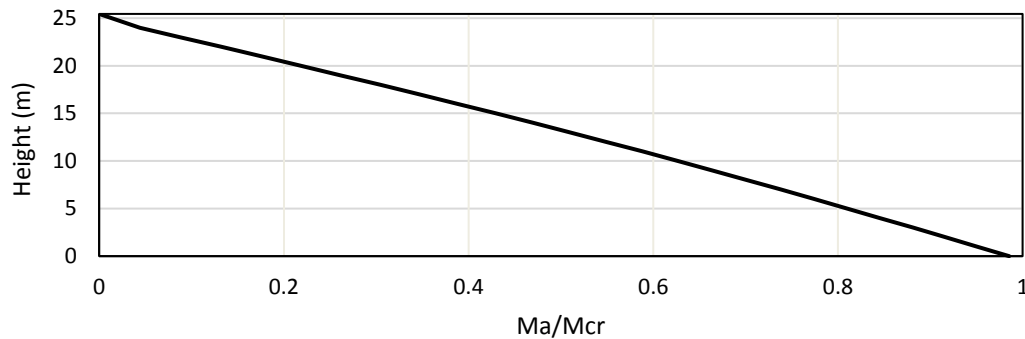
Fig. 2-11. Ratio between M_a and M_{cr} along the pole height

The maximum ratio between the applied moment due to synoptic wind loading and the cracking moment is found at the base of the pole and its value is 0.985. This pole will be assessed in the following two sections under the effect of downburst and tornado loadings to check if this design is adequate to sustain HIW loadings without collapsing.

2.6. <u>Downburst study</u>

The pole designed to remain un-cracked under normal wind loads corresponding to reference wind speed of 40 m/sec is considered for downburst analysis. The objective is to find the downburst velocity that the pole can sustain without suffering from full collapse. The first step required in the downburst analysis is the determination of the critical downburst configuration which leads to maximum straining actions.

2.6.1 Critical downburst configuration

A total number of 924 downburst configurations are considered as different load cases acting on the pole system. The objective is to determine the configuration that leads to maximum bending

moment on the pole. The parametric study is conducted for a fixed value for the jet velocity V_j= 50m/sec. The downburst configuration is defined by the jet diameter D_j and the geometric parameters (R and θ) shown in **Fig. 2-2**.

 In the parametric study, the downburst jet diameter is assumed to be varying from 500 m to 1500 m with an increment of 100 m. The ratio R/D_j is assumed to be varying from 0 to 2 with an increment of 0.1 while the angle (θ) is varied between 0^0 and 90^0 with an increment of 30^0. The overturning moment (M_a) normalized by the pole ultimate capacity (M_r) at the pole base is determined for each configuration.

The results of the parametric study are presented in **Fig. 2-12**(a-d). Each figure corresponds to a specific value of "θ" and shows the variation of the ratio (M_a/M_r) with D_j and (R/D_j).
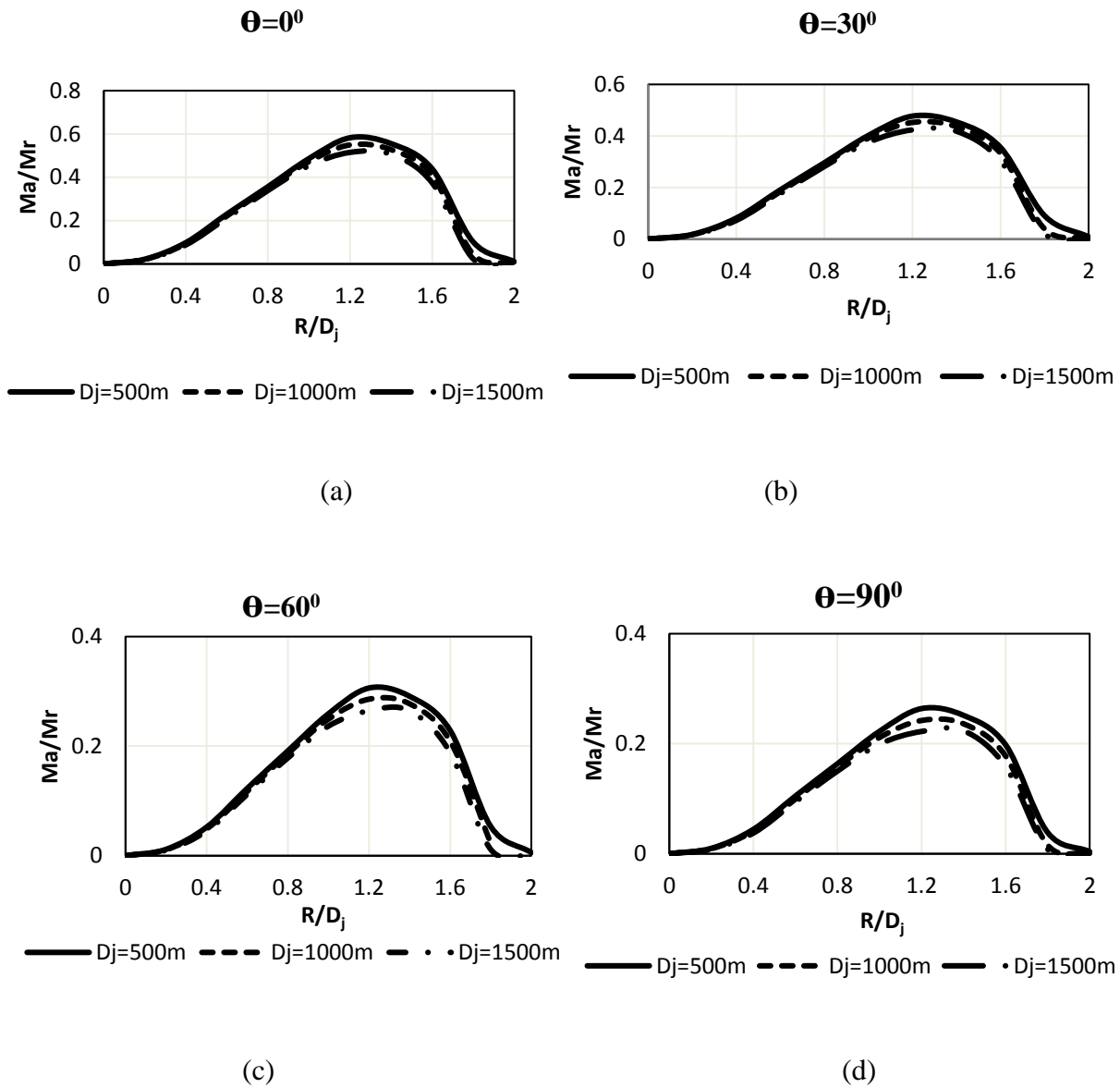
Fig. 2-12. (a-d) Variation of (M_a/M_r) with R/D_j

The figures indicate that the maximum (M_a/M_r) ratio occurs consistently at $R/D_j=1.2$. As such, the processing of the results is then focused on this ratio. **Fig. 2-13** shows the variation of (M_a/M_r) with θ for $R/D_j=1.2$ and $D_j=500m$ while **Fig. 2-14** shows the variation of the same ratio with D_j for $R/D_j=1.2$ and $\theta=0^0$.
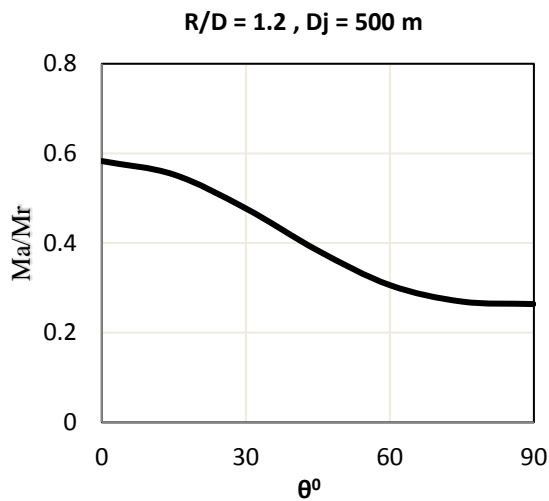
Fig. 2-13. Variation of (M_a/M_r) with θ **Fig. 2-14.** Variation of (M_a/M_r) with D_j
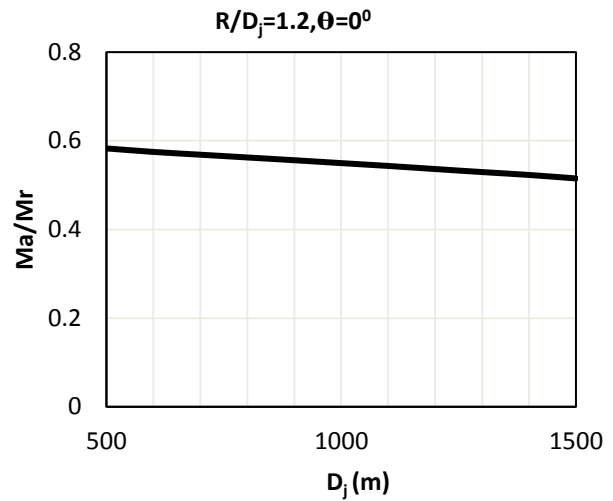
Based on the previous figures, the critical downburst configuration is when $\theta=0^0$, $D_j=500$m and $R/D_j=1.2$.

2.6.2 Failure analysis under critical downburst configuration

After determining the critical downburst configuration, a failure analysis is performed on the considered transmission pre-stressed pole to identify the downburst jet velocity at which the pole collapses.

The ratio (M_a/M_r) under downburst jet velocities varying between 50 and 70 (m/sec) with an increment of 5 (m/sec) are calculated and plotted in **Fig. 2-15**. It is found that the pole fails when the downburst jet velocity V_j exceeds 65 (m/sec).
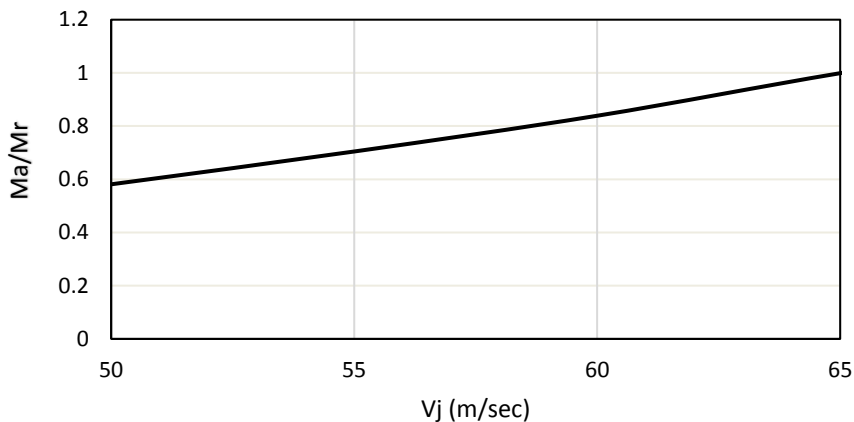
Fig. 2-15. Variation of (M_a/M_r) with V_j

With the increase of the jet velocity, excessive cracks start to propagate throughout the length of the pole. Once the acting moment due to the critical downburst case exceeds the moment of resistance of the pole, total collapse occurs. The failure mode of the pole is a bending failure and is attributed to the crushing of concrete. **Fig. 2-16** shows the crack propagation in almost 70% of the pole height under the downburst critical case with a jet velocity of 65m/sec.

Fig. 2-16. Variation of (M_a/M_{cr}) with the pole height

In conclusion, based on the studied pole system, the pole which is designed to be un-cracked under synoptic wind speed of 40 m/sec can sustain a jet velocity of 65 m/sec with excessive cracks and without failure. However, any increase in the jet velocity beyond this value will cause concrete crushing failure of the pole.

2.7.   **Tornado Study**

Similar to the downburst study, a parametric study is performed on the same pre-stressed concrete pole where the transmission line system is subjected to 312 different F2 tornado load cases. The main objective of the tornado parametric study is to determine the critical F2-tornado configuration which leads to the maximum bending moments on the pole and to assess if the pole will sustain this critical F2- tornado configuration without a full collapse. The tornado wind field used in the parametric study is scaled such that the value of the wind speed is 50 m/sec which is the lower limit for the F2-torando velocity (V_{f2}) as specified by Fujita (1981). The tornado configuration is defined by the geometric parameters (R and θ) shown in **Fig. 2-5**.

2.7.1   Critical tornado configuration

In the parametric study, the radial distance R is assumed to be varying from 12 m to 288 m with an increment of 12 m, while the angle (θ) is varied between 0^0 and 180^0 with an increment of 15^0. The ratio between the overturning moment (M_a) normalized and the pole ultimate capacity (M_r) is determined for each configuration. The results of the tornado parametric study are presented in

Fig. 2-17 (a-c). The figures show the variation of the ratio (M_a/M_r) with the distance parameter (R) for different ranges of the angle (θ).

(a)

(b)

(c)
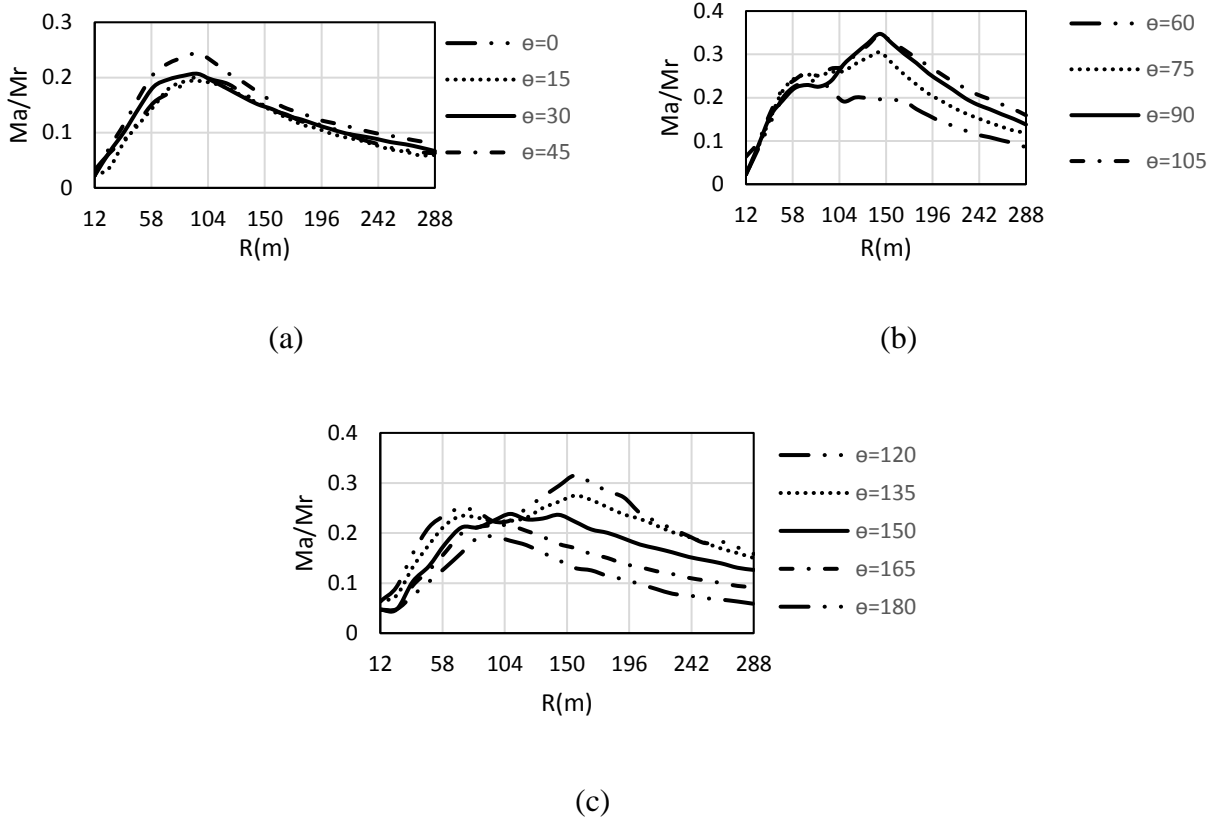
Fig. 2-17. (a-c) Variation of (M_a/M_r) with (R)

All the plots show a similar trend involving an increase of (M_a/M_r) with (R) up to a certain critical

value and then a decrease beyond this value. The critical value of (R) varies between 100 m and

150 m depending on the angle (θ). The results indicate that the absolute maximum value for the

ratio (M_a/M_r) occurs at R=144m. As such, the variation of (M_a/M_r) with (θ) is plotted in **Fig. 2-18**,

which indicates that the maximum value occurs at $\theta=105^0$.
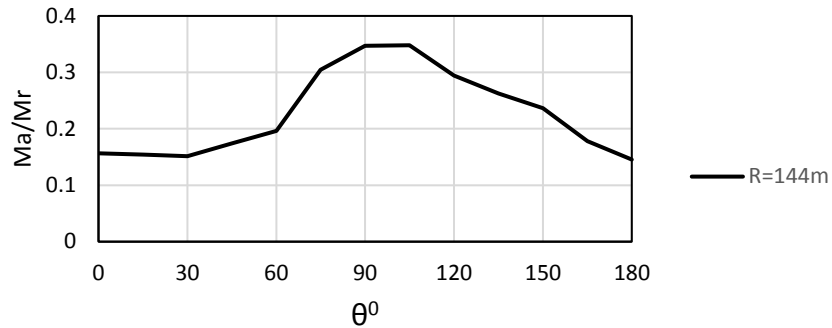
Fig. 2-18. Variation of (M_a/M_r) with (θ) at R =144m

The conductors' transverse reaction under F2-tornado cases play a major role in determining the critical tornado configuration. The variation of the conductors' transverse reaction (along the X-direction) (R_x) normalized by the maximum resultant horizontal conductor reaction (R_{hmax}) with θ at R=144m is shown in **Fig. 2-19.**
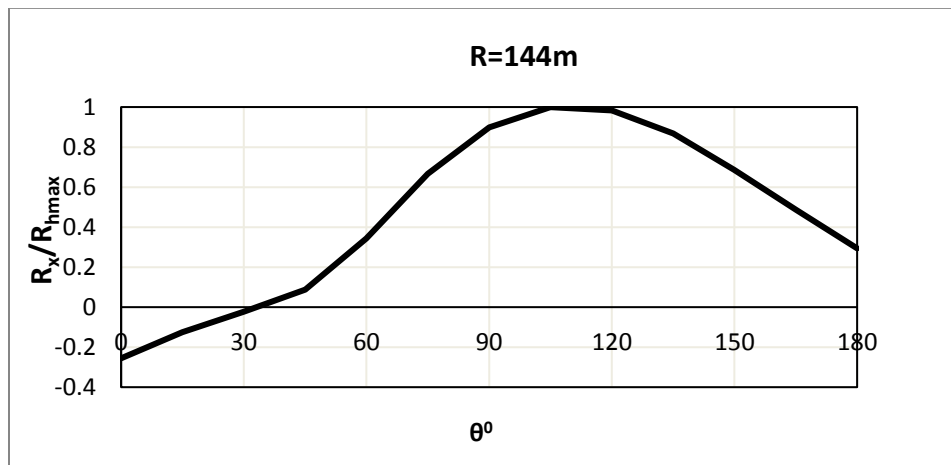
Fig. 2-19. Variation of conductor reactions with θ

It is found from the figure that the maximum resultant horizontal conductor reaction occurs when $\theta=105^0$. This explains the critical (M_a/M_r) value at $\theta=105^0$.

2.7.2 Non-linear analysis under critical tornado configuration

An incremental non-linear analysis is conducted at this critical configuration (R=144m,Θ=105^0)

by varying F2-tornado wind speed (V_{f2}) from 50 to 72 m/sec. The variation of the ratio (M_a/M_r)

with (V_{f2}) for the critical tornado configuration is shown in **Fig. 2-20**.
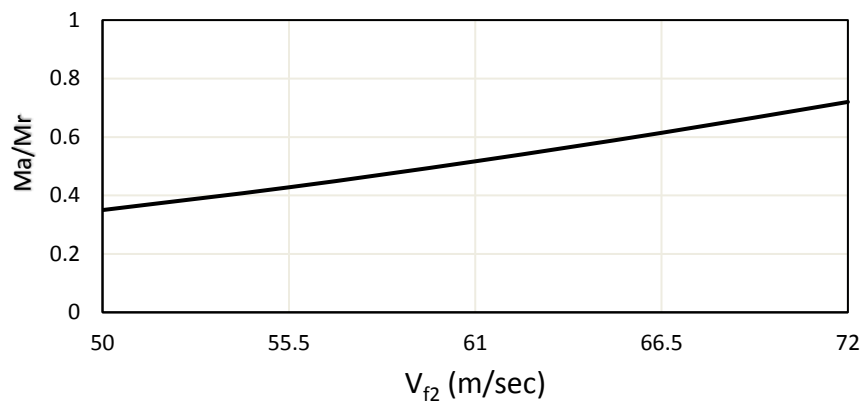
Fig. 2-20. Variation of (M_a/M_r) with V_{f2}

The results indicate that the ratio (M_a/M_r) does not reach a value of 1.0 at the maximum F2- tornado

speed (V_{f2max}) of 72m/sec. This means that this pole designed under synoptic wind speed of

40m/sec is not expected to collapse if subjected to an F2-tornado. **Fig. 2-21** indicates that the crack

propagation under the F2-tornado critical load case and a tornado velocity of 72 m/sec reaches 43

percent of the pole height.
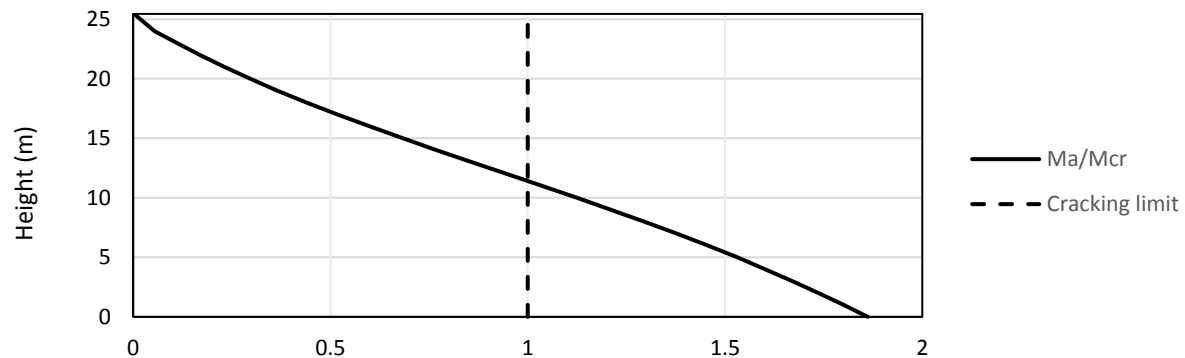
Fig. 2-21. Variation of (M_a/M_{cr}) with the pole height

2.8.   Comparison between downburst and tornado critical load cases

The conducted failure analyses predict that the pole can collapse at a downburst jet velocity (V_j) of 65 m/sec, while, it can survive an F2 tornado having a maximum wind speed of 72 m/sec. It should be noted that the maximum velocity in the downburst wind field is equal to approximately 1.1 V_j. This means that the downburst with jet velocity V_j = 65 m/sec has almost the maximum wind speed as the maximum value of the F2-tornado.

An attempt is made in this section to explain why the downburst turns to be more critical than the tornado for the pole. **Fig. 2-22** shows the downburst configuration leading to the maximum effect on the pole.
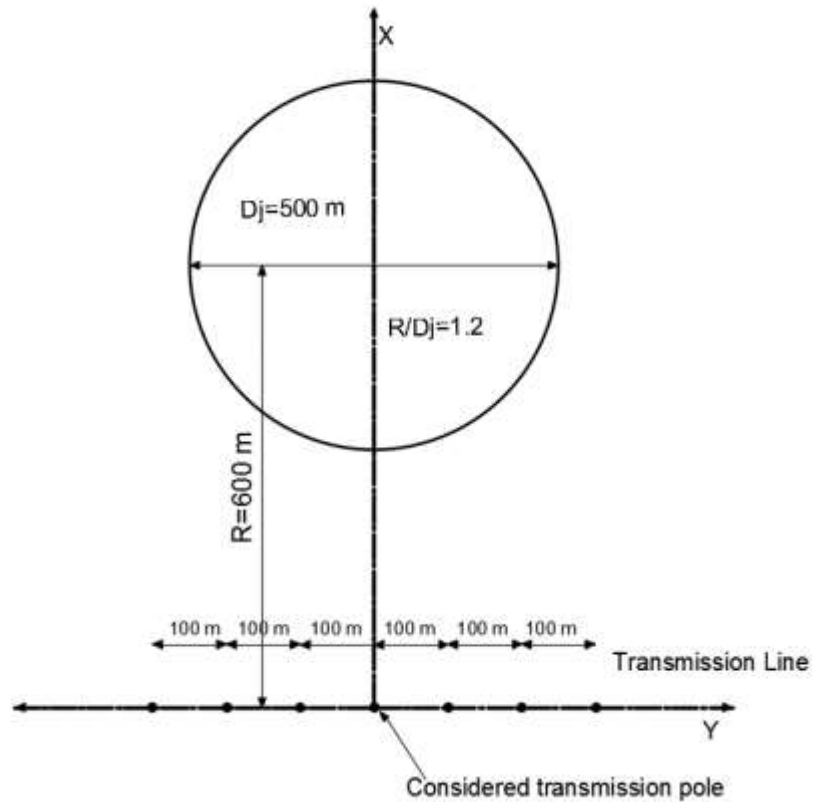
Fig. 2-22. Critical downburst configuration

This configuration leads to the maximum value of transverse velocity acting on the conductors. Also, at this location, the forces acting on the conductors and the pole act along the same direction. The distribution of transverse velocities on the conductors and the pole along the X-direction (V_x) due to this configuration are shown in **Figs. 2-23 and 2-24**, respectively.
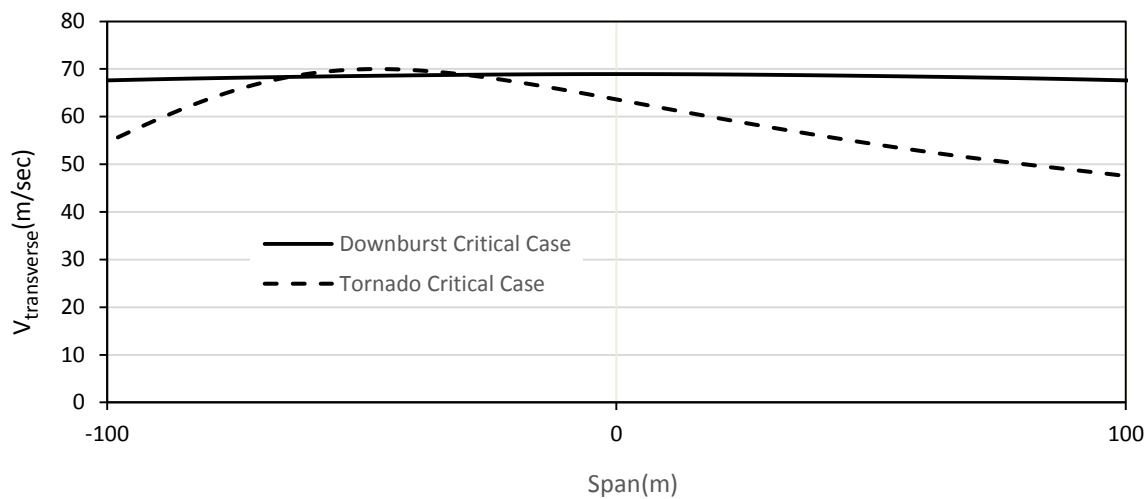
Fig. 2-23. Variation of V_x along the conductor span
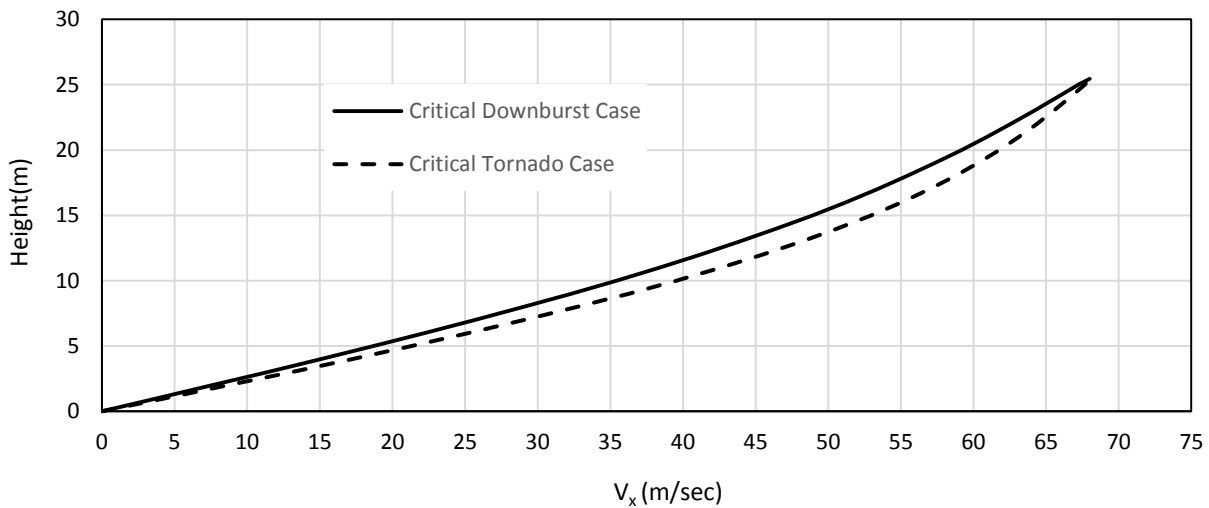
Fig. 2-24. Variation of V_x along the pole height

Fig. 2-25 shows the location of the tornado leading to maximum effect on the pole. It should be noted that the tangential velocity is the dominant component in the case of tornado.
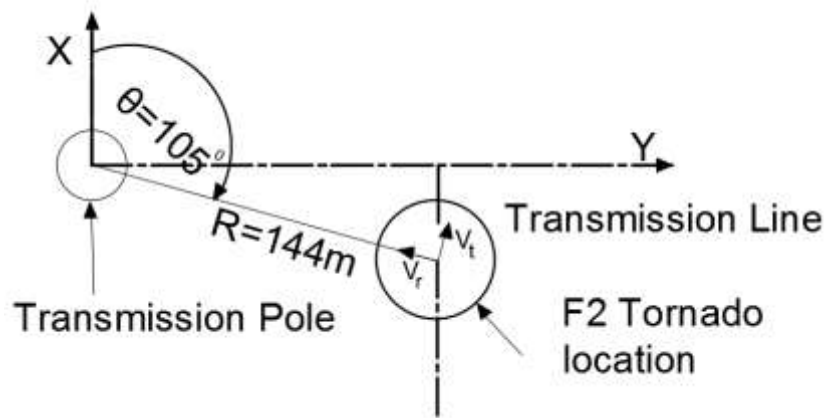
Fig. 2-25. Critical F2-Tornado configuration

The distribution of the transverse velocity (V_x) acting on the conductors due to this configuration is shown in **Fig. 2-23**. The distribution of the tangential and radial velocity components along the height of the pole due to this configuration is shown in **Fig. 2-26**. Those components are resolved to obtain the distribution of the velocities along X-direction (transverse to the conductor) as shown in **Fig. 2-24**. The reason that this configuration turns to be critical among all the F2-tornado cases is because it leads to large velocity values acting on both the conductors and the pole along the same direction (transverse to the conductors).
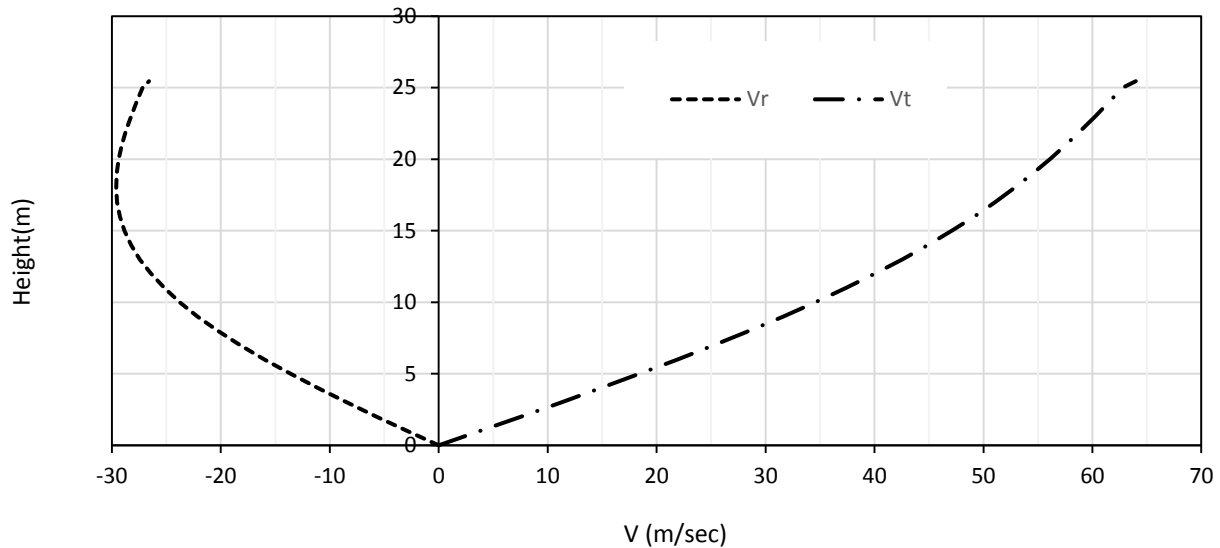
Fig. 2-26. Variation of V_r and V_t along the pole height

By examining **Figs. 2-23** and **2-24**, it can be seen that for both the critical downburst and tornado configurations (which have almost the same maximum wind speed), the pole is subjected to almost same velocity distribution, while the conductors are subjected to significant larger velocities for the downburst case. This explains why the downburst turns to be more critical.

2.9.   **Conclusions**

In the current study, a numerical technique is developed combining the following: 1) CFD models to simulate downbursts and tornadoes wind fields. 2) A semi-closed form solution that is capable of determining the conductor reactions under such localized high intensity wind events. 3) A non-linear finite element model for pre-stressed concrete pole structures that can predict the internal forces and deformations of such types of poles under HIW. The numerical model is validated using experimental results available in the literature. The numerical model is then used to study the

behavior of a pre-stressed concrete pole supporting a 100 m span conductor. The pole is designed to remain un-cracked under a synoptic wind speed of 40 m/sec.

Extensive parametric studies are conducted for the considered pole under 924 downburst cases and 312 F2-tornado cases. For downbursts, the parametric study involves varying the location and diameter of the downburst. For tornadoes, only the location is varied. The critical downburst and tornado configurations are obtained from those parametric studies.

Incremental non-linear failure analyses are then conducted for the pole using the determined downburst and tornado critical configurations. The following conclusions can be drawn from the study:

1- Maximum downburst effect occurs when $\theta=0^0$, $D_j=500m$ and $R/D_j=1.2$.

2- A full collapse for the pole associated with concrete crushing occurs at a downburst jet velocity higher than 65 m/sec. The absolute maximum wind speed corresponding to this jet velocity is about 72 m/sec.

3- Maximum F2 tornado effect occurs for a tornado configuration of R=144m and $\theta=105^0$.

4- The pole is able to sustain the maximum F2-tornado wind speed of 72 m/sec without experiencing full collapse.

5- For the same maximum wind speed, the critical downburst and tornado cases produce almost the same values for the velocities acting on the pole. In the meanwhile, higher velocity distribution is shown to occur for the downburst case. This is the main reason than downbursts turns to be more critical than tornadoes for the pre-stressed concrete transmission pole system.

2.10. <u>References</u>

Aboshosha, H., and El Damatty, A.A., (2014), "Effective technique for the reactions of transmission line conductors under high intensity winds", Wind and Structures. 18(3), 235-252.

American Society of Civil Engineers (ASCE), (2010) "Guidelines for electrical transmission line structural loading", ASCE manuals and reports on engineering practice, No. 74, New York, NY, USA.

American Society of Civil Engineers (ASCE), (2012) "Prestressed Concrete Transmission Pole Structures", ASCE manuals and reports on engineering practice, No. 123, Reston, VA, USA.

Baker, D. E. (1981). "Boundary layers in laminar vortex flows". Ph.D. thesis. Purdue University, USA.

Choi E.C.C., (2004), "Field measurement and experimental study of wind speed profile during thunderstorms", J. Wind Eng. Ind. Aerodyn., 92, 275-290.

Dai,K.S. and Chen,S.E., (2008), "Vibration of Spun-cast Prestressed Concrete Poles", Proceedings of IMAC XXV, Orlando, FL,USA.

Dempsey, D. and White, H., (1996) "Winds wreak havoc on lines", Transm Distrib World 48(6), 32-37.

Failure Investigation Report, HYDRO ONE NETWORKS INC, (2006), "Failure of towers 610 and 611, circuit X503E – 500 kV guyed towers near the Township of Waubaushene, Ontario, August 2, 2006". Line Engineering.

Fouad, F. H., and Simpson, A. M., (1999), "Enhanced spun concrete pole design using newly developed high-strength prestressing strand". Dept, of Civil and Envir. Engrg., University of Alabama at Birmingham, Birmingham, Ala., USA.

Fouad, F. H., Durden, H., and Calvert, E. A. (2000). "Analysis of substation dead-end concrete structures". Proc, 2000 ASCE Structures Congress, ASCE.

Fouad, F.H., Scott,L.N., and Calvert, E. (1994), "Performance of Spun Prestressed Concrete Poles During Hurricane Andrew", PCI J.,102-110.

Fujita, T., (1990), "Downbursts: meteorological features and wind field characteristics", Journal of Wind Engineering and Industrial Aerodynamics 36, 75–86.

Fujita, T. T., and Pearson, A. D. (1973). "Results of FPP classification of 1971 and 1972 tornadoes." 8th Conference on Severe Local Storms (abstracts only), USA, 609.

Fujita, T., (1985), "The downburst: microburst and macroburst", SMRP Research Paper 210, University of Chicago, USA.

Fujita, T. T. (1981). "Tornadoes and downbursts in the context of generalized planetary scales." J.Atmos.Sci., 38(8), 1511-34.

Gast, K.D., Schroeder, J.L., (2003). "Supercell rear-flank downdraft as sampled in the 2002 thunderstorm outflow experiment", Proceedings of the 11th International Conference on Wind Engineering. ICWEIA, 2233–2240.

Hamada, A., Damatty, A.A.E., Hangan, H., and Shehata, A.Y. 2010. Finite element modelling of transmission line structures under tornado wind loading. Wind and Structures, 13(5): 451-469.

Http://www.valmont.com/valmont/markets/ utilities/transmission-poles

Https://www.flickr.com/photos/81578389@N00/4283617188

Kim, J. and Hangan, H., (2007), "Numerical simulations of impinging jets with application to downbursts", Journal of Wind Engineering and Industrial Aerodynamics 95(4), 279-298.

Hangan, H. and Kim, J. (2008), "Swirl ratio effects on tornado vortices in relation to the Fujita scale", Wind and Structures, An International Journal, 11(4), 291-302.

Hangan, H., Roberts, D., Xu, Z., and Kim, J., (2003), "Downburst simulation. Experimental and numerical challenges", Proceedings of the 11th International Conference on Wind Engineering, Lubbock, TX, USA.

Hawes, H., Dempsey, D., (1993), "Review of recent Australian transmission line failures due to high intensity winds". Proceedings of the Task Force of High Intensity Winds on Transmission Lines, Buenos Aires.

Holmes, J. D., Banks, R. W., & Paevere, P., (1997), "Measurements of topographic multipliers and flow separation from a steep escarpment. Part 1. Full scale measurements." Journal of Wind Engineering and Industrial Aerodynamics, 67-71, 885-892.

Kuebler,M., (2008), "Torsion in Helically Reinforced Prestressed Concrete Poles", M.Sc. thesis, University of Waterloo, Waterloo, Ontario, Canada.

Mattock, A. H., (1979), "Flexural Strength of Prestressed Concrete Sections by Programmable Calculator", PCI J, 24(1):32-54.

McCarthy, P., and Melsness, M., (1996), "Severe weather elements associated with September 5, 1996 hydro tower failures near Grosse".

Rodriguez-Gutierrez, J. A., and Aristizabal-Ochoa, J. D., (2001), "M-P-ø Diagrams for reinforced, partially, and fully prestressed concrete sections under biaxial bending and axial load", J. Struct. Engrg.,; 127(7): 763-773.

Sarkar, P., Haan, F., Gallus, Jr., W., Le, K. and Wurman, J. (2005). "Velocity measurements in a laboratory tornado simulator and their comparison with numerical and full-scale data." 37th Joint Meeting Panel on Wind and Seismic Effects.

Shehata, A., El Damatty, A.A., and Savory, E., (2005), "Finite element modeling of transmission line under downburst wind loading", Finite Elements in Analysis and Design 42(1), 71-89.

Vecchio, F. J., and Collins, M. P., (1986), "The modified compression field theory for reinforced concrete elements subjected to shear", ACI J.; 83(2), 219–231.

Wolfson, M., DiStefano, J., Fujita, T., (1985), "Low-altitude wind shear characteristics in the Memphis, TN area", Proceedings of the 14th conference on severe local storms, American Meteorological Society, Indianapolis, IN, USA., 322–7.

Wood, G., Kwok, K., Motteram, N., and Fletcher, D., (2001), "Physical and numerical modelling of thunderstorm downbursts", Journal of Wind Engineering and Industrial Aerodynamics 89, 535-552.

Wurman, J. (1998). "Preliminary results from the ROTATE-98 tornado study", Preprints, 19th Conf. On severe local storms, Minneapolis, MN, 14-18 September.

Zhang, Y., (2006), "Status quo of wind hazard prevention for transmission lines and countermeasures", East China Electric Power 34(3), 28-31.

CHAPTER 3

DYNAMIC BEHAVIOUR OF PRE-STRESSED CONCRETE TRANSMISSION POLES UNDER SYNOPTIC WIND LOADING

3.1. Introduction

Transmission line structures are critical elements of the modern infrastructure system as they carry electricity from the generation stations to the distribution systems. Those structures should be designed to resist different types of environmental loads including wind effects. The velocity wind field consists of a mean component which is static and a fluctuating component (turbulent), which varies with time. The turbulent component can trigger a dynamic response of the structure, which can lead to a failure from the gust effect. Many literature have reported failures of transmission line structures under dynamic wind loads such as the studies conducted by Li (2000), Savory et al. (2001) and Li and Bai (2006).

The main components of a transmission line system are the conductors, insulators, ground wires and the supporting towers. The supporting towers can be in the form of lattice steel towers or pole-type structures. Most of the previous studies which investigated the dynamic behaviour of transmission line systems under wind loads focused on conductors and on lattice steel towers as the main supporting system (Momomura et al. 1997) and (Horr et al. 2004). Loredo-Souza and Davenport (1998) concluded that the aerodynamic damping of the conductors has a major effect on the dynamic behaviour of transmission line structures. The contribution of the resonant component of the response of self-supported and guyed transmission lattice structures was found relatively low in the study conducted by Aboshosha et al. (2016). That was attributed to the

difference between the loading and the tower frequencies and the decoupling of the mode shapes of both the lattice steel transmission towers and the conductors.

Regarding pole structures, few studies were performed to assess their vulnerability to dynamic loads. Chen et al. (2006), Lantrip (1995) and Polyzois et al. (1998) conducted a number of studies to identify the free-vibration modes of transmission poles. Dai and Chen (2008) studied the effect of the pre-stress level on the modal behavior of pre-stressed concrete poles. Chen and Dai (2010) concluded that strong coupling exist between the poles and the conductors' vibrations. The reduced redundancy of pole-type structures makes them more vulnerable to dynamic excitations (Chen and Dai 2010).

The studies conducted on the pole-type structures were mainly focusing on the free-vibration dynamic properties of the poles. However, there is a lack in the literature in studying the forced vibrations of pole-type structures. Dai (2009) performed a time history analysis to assess transmission pole structures' response under blast loading. To the best of the authors' knowledge, the current study is the first study to assess the dynamic performance of transmission poles under both mean and fluctuating synoptic wind loads. Among different types of pole transmission line structures, pre-stressed concrete poles are wide spread compared to other types such as wooden and steel poles. This is due to their low installation and maintenance costs in addition to the corrosion resistivity. Hence, Pre-stressed concrete pole systems are considered in this study.

The complexity of performing dynamic analysis of transmission line structures arises from the fact that the stiffness properties of those structures are frequency-dependent. This might lead to coupling between the response of conductors and the supporting towers (Simiu and Scanlan 1996), (Madugula 2002), (IEC 2003) and (Chen and Dai 2010).

The main objectives of the current study are to:

1- Develop and validate a numerical tool which can predict the non-linear dynamic response of pre-stressed concrete transmission pole structures under mean and turbulent synoptic wind components.

2- Use the developed tool to identify the range of velocities at which the resonant component contributes significantly to the total response of a number of pre-stressed concrete transmission pole systems having different conductors' spans.

3- Evaluate the gust response factors of the pole systems and compare them to the gust response factors obtained using the expressions incorporated in the ASCE74 (2010).

The study is divided into six sections. In section 3.1, introduction and objectives of the study are provided. In section 3.2, a description of the numerical model developed and validated is outlined. Section 3.3 provides details about the three different pre-stressed concrete transmission pole systems considered in the study. A sample of the results of the dynamic and quasi-static analyses of the three different systems is presented in section 3.4. The variation of dynamic amplification factors and gust response factors with mean wind speeds are obtained from the analyses. The gust response factors are then compared to the ones evaluated using ASCE74 (2010) provisions in section 3.5. The findings and conclusions obtained from the study are presented in section 3.6.

3.2. <u>Numerical model</u>

Aboshosha and El Damatty (2015) conducted nonlinear dynamic analysis of multi-spanned conductors using an in-house numerical model. This model was extended to be capable of performing both quasi-static and dynamic analyses for steel lattice transmission line structures under turbulent wind loading by Aboshosha et al. (2016). This model was validated using the

results of a multi-span guyed transmission line aero-elastic wind tunnel test conducted at the Boundary Layer Wind Tunnel Laboratory (BLWTL) at Western University by Hamada et al. (2017). A comparison between the numerical model and the test results showed a very good agreement as reported by Aboshosha et al. (2016). In the current study, Aboshosha et al. (2016) model is extended further to account for the dynamic behaviour of pre-stressed concrete poles under turbulent wind loading. This is done by incorporating the following together: (1) a procedure to generate turbulent wind field developed by Chen and Letchford (2004 a,b) and Chay *et al.* (2006), (2) the non-linear model for the conductors previously developed and validated by Aboshosha and El Damatty (2015) and (3) a non-linear finite element model for pre-stressed concrete poles previously developed and validated by Ibrahim et al. (2017).

The incorporation of the three developed and validated tools together form a unique package capable of predicting the dynamic and quasi-static responses of pre-stressed concrete transmission pole structures under the mean and fluctuating components of a wind field.

A brief description of the procedure used to generate the turbulence is provided in the next subsection. This is followed by a description of the various steps involved in the dynamic analysis. In each step description, the related numerical details are explained so the reader can gain an understanding about the features and capabilities of the entire numerical model.

3.2.1 **Turbulent wind field generation**

Synoptic winds are decomposed into mean and fluctuating velocity components. Chen and Letchford (2004 a,b) and Chay *et al.* (2006) developed a numerical technique to generate the fluctuating wind velocities. In this technique, the Power Spectrum Density (PSD), which describes the energy of the wind fluctuations in the frequency domain, developed by Von Karman (1948), was used to evaluate turbulent velocities. This technique is adopted in the current study. The length

scale is considered equal to 67 m according to the ASCE 74 (2010) assuming an open terrain exposure. A sample of the variation of the produced velocity with time at a height of 20 m for a mean wind speed of 15 m/sec is shown in **Fig. 3-1**.
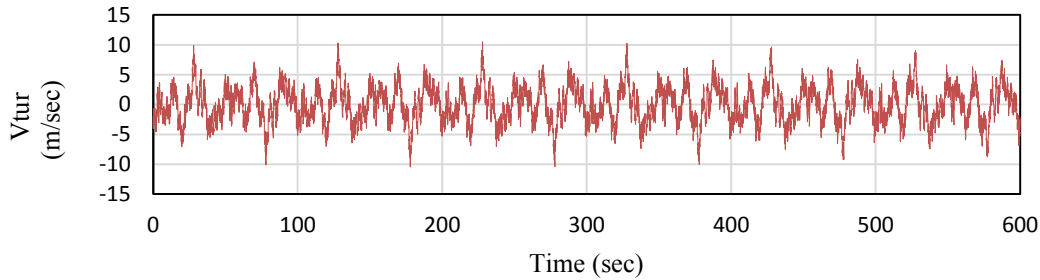
Fig. 3-1. generated turbulent velocity for open terrain exposure at 20 m height

3.2.2 Steps for performing dynamic and quasi-static analyses

The response of pre-stressed concrete transmission poles under mean and fluctuating synoptic wind is highly non-linear. This is attributed to the non-linearity of the conductors due to sagging, pre-tensioning and insulators' stiffness. In addition to that the pre-stressed concrete poles' behaviour is non-linear due to stress-strain non-linear relationship of concrete and pre-stressing strands, cracking and long term effects such as creep, shrinkage and strands' relaxation.

The dynamic behavior of transmission line structures subjected to fluctuating synoptic wind can be evaluated using full non-linear dynamic analysis under the instantaneous value of the wind velocity which includes both the mean and the fluctuating components. This method is very time consuming and hence not practical. Sparling and Wegner (2007) developed a technique which significantly reduces the computational time without compromising the accuracy of the solution.

Sparling and Wegner (2007) technique was followed by Aboshosha and El Damatty (2015) in analyzing various transmission line conductors subjected to synoptic and non-synoptic wind. A very good matching was obtained for the conductor responses with the corresponding values

obtained from fully non-linear dynamic analyses. As such, Sparling and Wegner (2007) technique is incorporated in the current study, the steps and the details of the technique are explained below:

3.2.2.1   Step 1: Non-linear static analysis under the mean loads

Non-linear static analysis is conducted to obtain the transmission pole systems' response under the mean wind component (M). The non-linear behavior of a pre-stressed concrete pole system is evaluated using two separate analyses for the conductors and the pre-stressed concrete poles which are outlined below:

3.2.2.1.1 Modeling of conductors

Non-linear static analysis of the conductors is conducted under the synoptic wind mean component using the semi-analytical method developed by Aboshosha and El Damatty (2014, 2015). This technique accounts for conductors' sagging, pre-tensioning forces and insulator's stiffness. The conductors' reactions and displacements are calculated using this technique.

3.2.2.1.2 Modeling of pre-stressed concrete poles

The non-linear static behaviour of the poles is investigated using the non-linear finite element model developed and validated by Ibrahim et al. (2017). Frame elements are used to model the pre-stressed concrete poles which are subjected to axial forces and bending moments. In this technique, the effects of non-linear stress-strain relationship of concrete and pre-stressing strands as well as creep, shrinkage and relaxation of strands are taken into consideration. The concrete poles are analyzed under mean wind component in addition to the conductor reactions previously calculated in 3.2.2.1.1.

3.2.2.2 Step 2: linear dynamic analysis under the fluctuating loads

Linear dynamic analysis of the system is conducted under the fluctuating wind component to obtain the fluctuating response (F). The pole system properties used in the linear dynamic analysis such as stiffness (K), aerodynamic and structural damping (C) are calculated based on the non-linear analysis conducted in step 1. The fluctuating response (F) obtained in this step is equal to the summation of the resonant (R) and the background (B) responses.

The Linear dynamic analysis of a pre-stressed concrete pole system is conducted using step by step Newmark's integration method (Bathe, 1996). The equation of motion of the transmission pole system is expressed by Equation (3-1).

$$[M]\{\ddot{u}\} + [C]\{\dot{u}\} + [K]\{u\} = \{F_w(t)\} \tag{3-1}$$

Where $[M]$ is the mass matrix, $[C]$ is the damping matrix, $[K]$ is the stiffness matrix, $\{F_w(t)\}$ is the fluctuating dynamic wind load vector at time t, $\{u\}$, $\{\dot{u}\}$ and $\{\ddot{u}\}$ are the displacement, velocity and acceleration responses of the system, respectively.

The stiffness matrix of a transmission pole system [K] is formed by combining the stiffness matrices of the pole and the conductors' elements. Pole elements are modeled using 2-nodded frame elements with 6 degrees of freedom per node (i.e. 3 displacements and 3 rotations), while each conductor span is modeled using 10 two nodded-cable elements.

The damping matrix $[C]$ results from the aerodynamic damping as well as the structural damping of the transmission pole systems. Bachmann et al. (1995) stated that the structural damping of the conductors can be ignored compared to the aerodynamic damping. As such, the damping matrix $[C]$ can be expressed by Equation (3-2).

$$[C] = \begin{bmatrix} C_{ca} & 0 \\ 0 & C_{pa}+C_{ps} \end{bmatrix} \tag{3-2}$$

Where C_{ca} and C_{pa} are the aerodynamic damping matrices for the conductors and the poles and C_{ps} is the structural damping of the pole.

The aerodynamic damping matrices of the conductors and the transmission poles, C_{ca} and, C_{pa} are diagonal matrices that have damping coefficients, C_{ai}, at locations of the degrees of freedom corresponding to the wind direction. The damping coefficients at the poles and the conductors' nodes are expressed by Equation (3-3).

$$C_{ai} = \rho C_{di} A_i V_i \tag{3-3}$$

Where ρ is the air density which is taken equal to 1.25 kg/m³, C_{di} is the drag coefficient at node i , A_i is the projected area of the conductor or the pole elements around node i and V_i is the applied mean wind speed.

 The structural damping of the transmission poles C_{ps} is modeled using Raleigh damping as shown in Equation (3-4).

$$[C_{ps}] = \alpha[M_p] + \beta[K_p] \tag{3-4}$$

Where M_p and K_p are the mass and stiffness matrices of the pole, α and β are constants controlling the structural damping. In this study α and β are chosen to obtain an un-cracked pole damping that is equal to 2% and a cracked pole damping of 5 % for the first two pole vibration modes according to Loredo-Souza and Davenport (2003) and Newmark and Hall (1982).

It should be mentioned that the pre-stressed concrete pole systems considered in this study are designed to remain un-cracked under a synoptic wind speed of 40 m/sec according to ASCE 123

(2012) and ASCE 74 (2010). Hence, the damping ratio used for the poles under wind speeds less than or equal to the cracking wind speed (i.e.40 m/sec) is assumed to be 2 %. While, the damping ratio is assumed to be 5 % under higher wind speeds.

By conducting linear dynamic analysis on the transmission pole system, the fluctuating response of the system (F) can be obtained. This response includes the background component (B) and the resonant component (R).

3.2.2.3 Step 3: linear quasi-static analysis under the fluctuating loads

A quasi-static analysis of the transmission pole system under the fluctuating wind component is conducted. Similar to step 2, the stiffness used in the quasi-static analysis is calculated based on the non-linear analysis performed in step 1. The main purpose of conducting the quasi-static analysis is to obtain the background response of the system (B). The background response is obtained throughout solving Equation (3-5).

$$[K]\{u\} = \{F_w(t)\} \qquad\qquad (3-5)$$

3.2.2.4 Step 4: Obtaining R, T and QS

The background response (B) obtained from step 3 is subtracted from the fluctuating response (F) obtained from step 2 so that the resonant response (R) can be evaluated. As such, the total dynamic response (T) (i.e. including the dynamic effect) can be determined by adding the mean (M), background (B) and resonant (R) responses. While, the quasi-static response (QS) (i.e. neglecting the dynamic effect) is obtained by adding the mean (M) response to the background one (B). The steps are summarized and illustrated in the following flowchart:
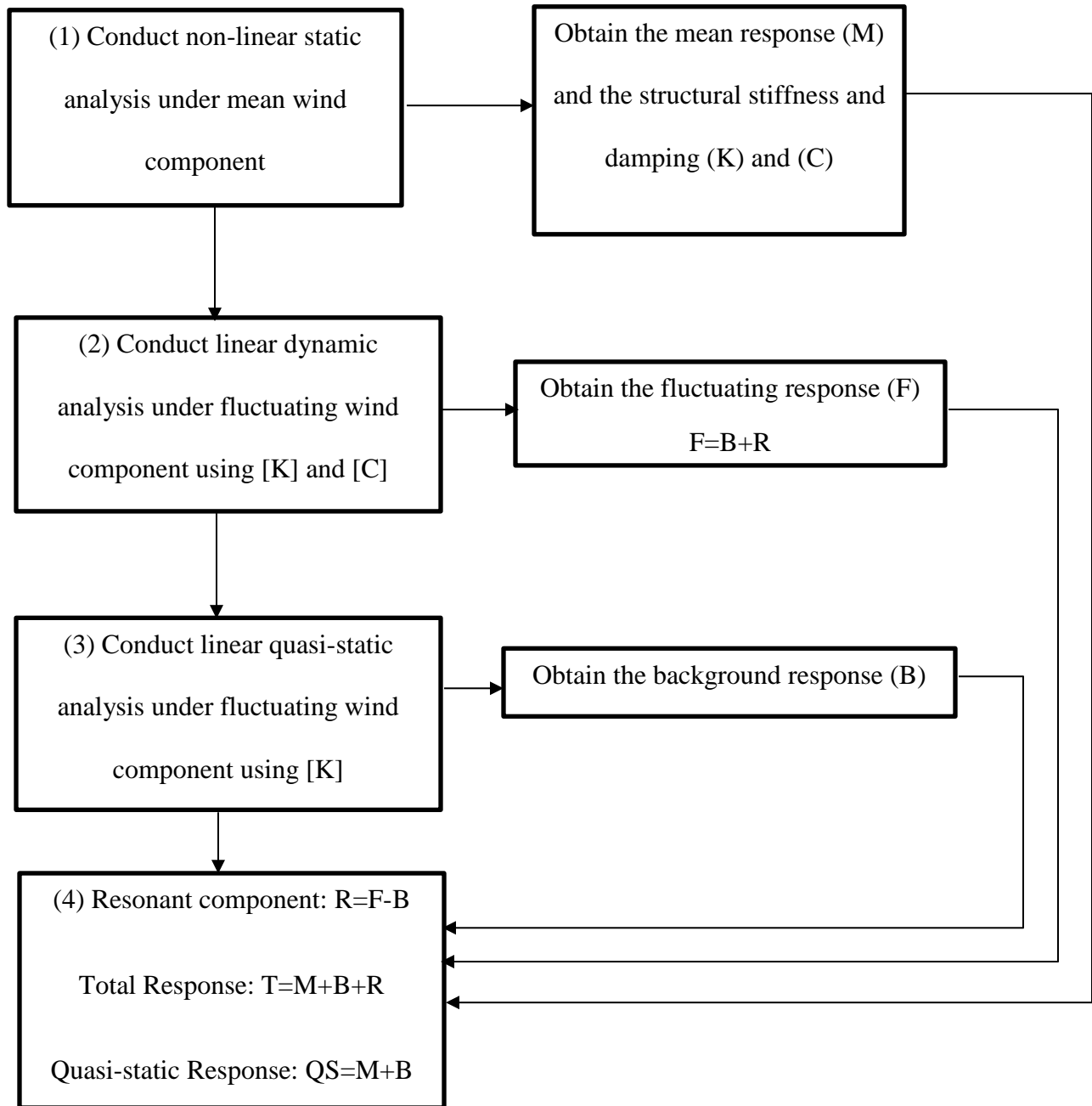
Fig. 3-2. Flow chart for the dynamic analysis of pre-stressed concrete poles systems

3.3. <u>Description of the considered pre-stressed concrete pole systems</u>

The numerical model is employed to evaluate the dynamic behavior of three different pre-stressed concrete poles. The total dynamic responses are computed as well as the quasi-static responses so that the resonant component effect can be assessed. Dynamic amplification factor (DAF) and gust response factors (GRF) are then evaluated for various wind speeds. The DAF is defined as the ratio between the total dynamic and the quasi-static responses while the GRF is defined as the ratio between the dynamic and the mean response. The calculated GRFs are compared to the corresponding values evaluated using Davenport's expressions incorporated in the ASCE74 (2010).

Three transmission pole systems are considered in this study. The three systems have the following common geometric and material properties:

- Unsupported height of poles of 25.5 m.

- Cross arms' length of 2.4 m supporting two conductors.

- Conductors having a projected area of 0.04 m^2, weight per unit length of 30 N/m and insulator length of 2.1 m and sag value of 2% relative to the span.

- Concrete with compressive strength of 75.8 MPa and reinforced with M10 low relaxation pre-stressing strands.

The three systems differ in terms of conductor spans, number of strands and the dimensions of the bottom and top cross sections of the poles. The specific properties of the three systems are given in **Table 3-1**, where, D_{outtop}, $D_{outbottom}$, D_{intop} and $D_{inbottom}$ are the outside top diameter, outside bottom diameter, inside top diameter and inside bottom diameter of the concrete poles,

respectively. $N_{strands}$ are the number of low relaxation pre-stressing strands assumed in the poles. The cross section properties of the poles are selected such that the poles of the three systems remain un-cracked under a synoptic wind speed of 40 m/sec based on the ASCE 123 (2012) and ASCE 74 (2010) guidelines.

Table 3-1 Properties of the considered pole systems

Conductors		Pre-stressed Concrete pole				
Span(m)	Sag(m)	D_{outtop} (mm)	D_{intop} (mm)	$D_{outbottom}$ (mm)	$D_{inbottom}$ (mm)	$N_{strands}$
100	2	280	140	740	547	20
200	4	596	196	1034	586	20
300	6	1096	396	1558	807	24

3.4. <u>Results of analyses of the considered TL systems under turbulent wind</u>

A parametric study is conducted on three pre-stressed concrete pole systems by varying the mean applied wind speed from 10 to 60 m/sec with an increment of 5 m/sec. As mentioned before, the stiffness of a transmission pole system is frequency dependent. By changing the value of the mean wind load applied on the pole system, the frequency of the whole system changes leading to a different response. The numerical model described earlier is employed to analyze the three transmission pre-stressed concrete pole systems.

Samples of the results of the parametric study are provided in this section. Firstly, the numerical model is employed to quantify the variation of mean, background, resonant, total dynamic and quasi-static responses with time for a sample mean wind speed of 40 m/sec applied to the 100 m pole system. In subsection 3.4.2, the power spectral density (PSD) responses of the conductors' reactions and the pole base moments are evaluated for the 200 m pole system under two mean

wind speeds of 15 and 50 m/sec, respectively. As such, the frequencies of the transmission pole system under those two different mean wind speeds can be identified. In subsection 3.4.3, the variation of two different peak responses (conductor reaction and base moment) with the mean applied wind speed is presented for the 300 m pole system.

3.4.1 Variation of the mean, resonant and background responses of the 100 m pole system with time

According to NRC (2005) and AIJ (2004), the turbulence statistics are typically stable over the range of 600-3600 sec. As such, the duration time used in the dynamic analysis is taken equal to 600 sec. **Fig. 3-3** (a) and (b) show a sample of the predicted conductor and pole base moment responses, respectively. The shown responses are for a transmission pole system with a conductor span of 100 m subjected to a mean wind speed of 40 m/s. As shown in the figure, mean, background and resonant responses are obtained. By summing all of those responses the total response which includes the dynamic effect is evaluated. Summation of the mean and background responses leads to obtaining the quasi-static response (i.e neglecting the dynamic effect) of the pole system.
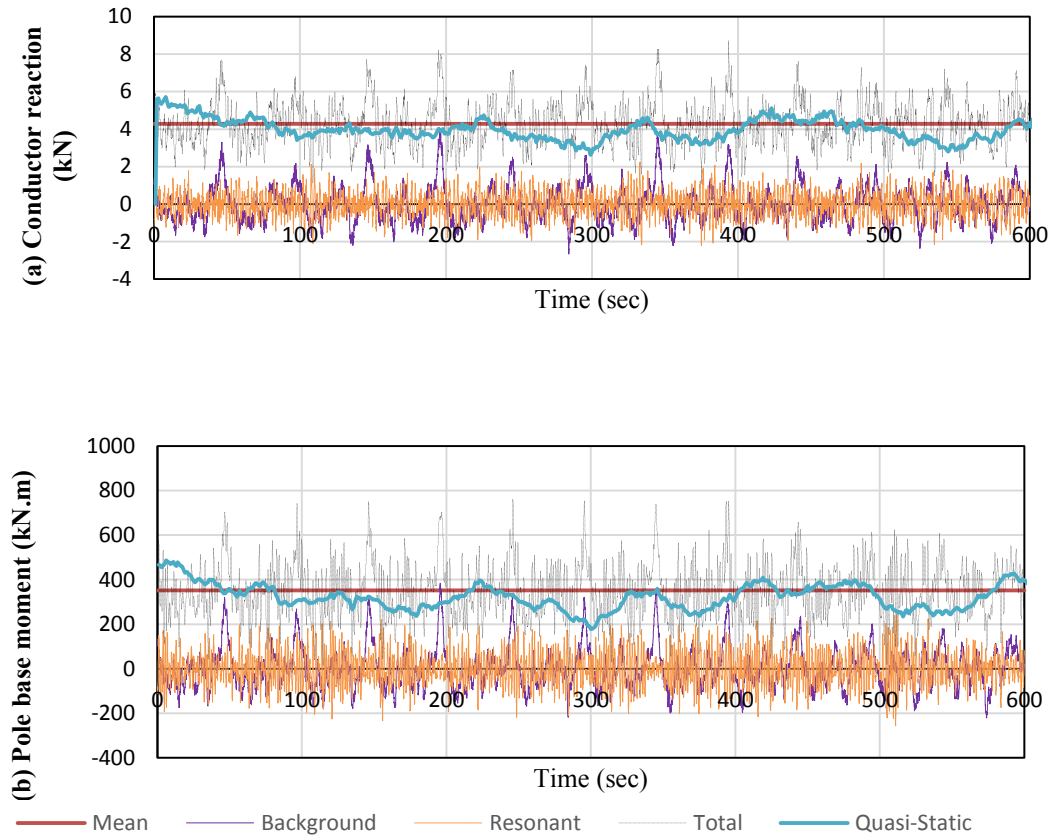
Fig. 3-3. (a,b) Conductor reaction and base moment for the 100m pole system under $V_{mean}=40$

m/s

It should be noted that the total dynamic response is higher that the quasi-static response due to

the inclusion of the dynamic effect. The DAF for the conductor reaction and the pole base moment

are found to be equal to 1.07 and 1.14, respectively. This indicates that the resonant component is

more significant in the pole's base moment than that in the conductor's reaction under a mean

wind speed of 40 m/sec.

3.4.2 Identifying the 200 m pole system frequencies

As mentioned earlier, the transmission pole systems' frequencies (f) are dependent on the value of

the mean wind load. In this subsection, the frequencies of the 200 m pole system are identified

under two different wind speeds (i.e. 15 and 50 m/sec). The transmission pole system frequency and the conductor frequency are evaluated using the power spectral density (PSD) analysis. PSD curves are obtained for both the fluctuating and background pole base moment and the conductor reaction responses.

Figs. 3-4 and 3-5 show PSD curves of the above quantities for wind speeds of 15 m/sec and 50 m/sec, respectively.
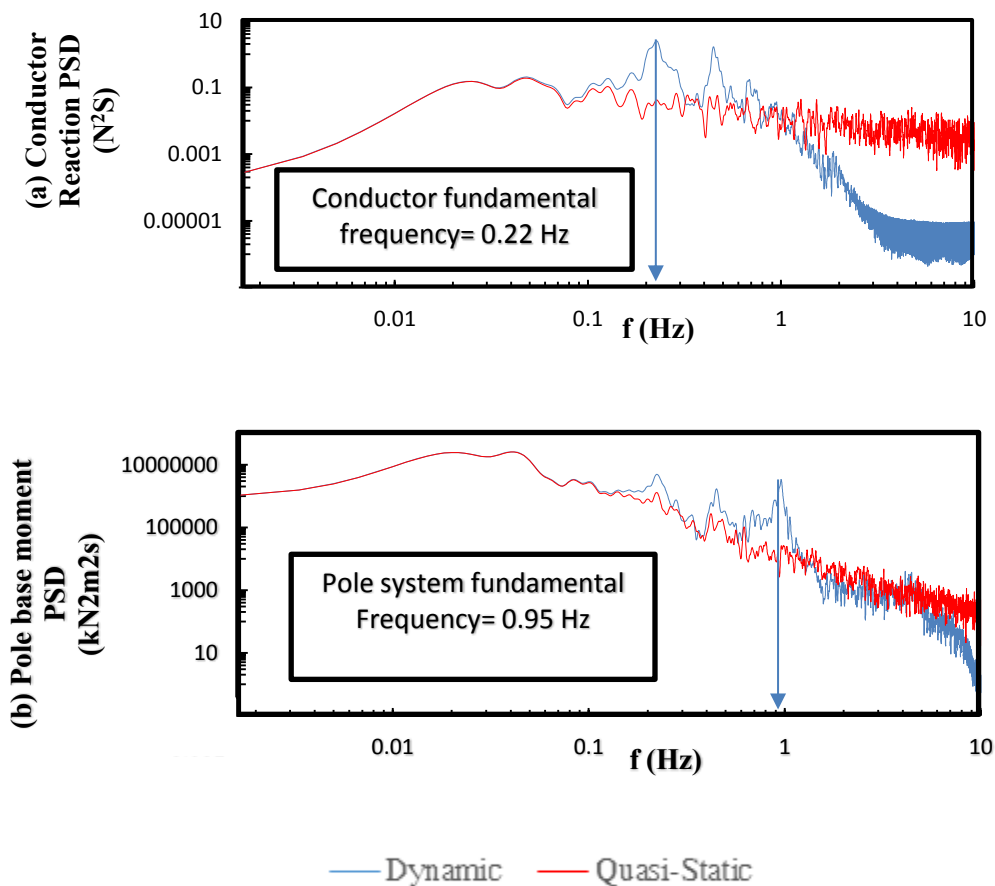
Fig. 3-4. (a, b) PSD curves for the 200 m pre-stressed concrete pole under V_{mean}=15 m/s
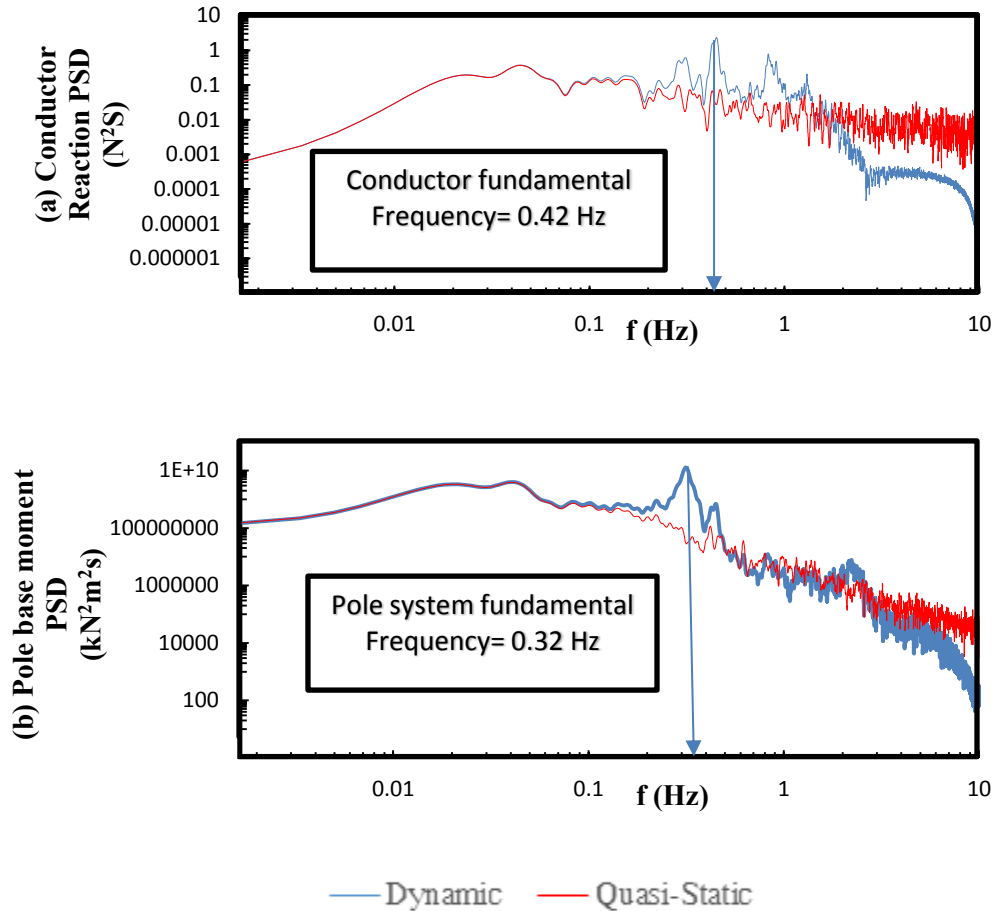
Fig. 3-5. (a,b) PSD curves for the 200 m pre-stressed concrete pole under V_{mean}=50 m/s

It should be mentioned that the frequencies of the conductors and transmission pole systems can be identified at the values corresponding to the peaks of the PSD curves. As such, the conductor's and the pole system frequencies under a mean wind speed of 15 m/sec are 0.22 Hz and 0.95 Hz, respectively. While the conductors and the transmission pole system frequencies under a mean wind speed of 50 m/sec are 0.42 Hz and 0.32 Hz, respectively.

By analyzing the PSD curve peaks under the mean wind speed of 15 m/sec, the dynamic effect is found to be not significant due to the large difference between the conductor and pole system frequencies (i.e 0.22 Hz and 0.95 Hz).

It should be noted that a clear reduction in the pole frequency occurs by increasing the mean wind speed (i.e. from 0.95 under 15 m/sec to 0.32 Hz under 50 m/sec). This is attributed to the fact that the considered pre-stressed concrete poles are designed to remain un-cracked under a mean wind speed of 40 m/sec. As such, any increase beyond the applied mean wind speed will lead to the cracking of the pole and consequently the pole system frequency will decrease. As such, the pole system frequency become close to the conductor's frequency (i.e. 0.32 Hz and 0.42 Hz). A coupled pole- conductor mode is found to occur in the 200 m pole system under a mean wind speed of 50 m/sec. This coupled mode magnifies the resonant component. Hence, the pole structure becomes more vulnerable to wind excitations.

3.4.3   Variation of the peak responses with wind speed for the 300 m pole

Peak total and quasi-static responses are evaluated for the 300 m pole system. **Fig. 3-6** shows the variation of the peak responses with the change in the mean velocity. Two responses are selected for comparison purpose which represents: (i) conductor reaction and (ii) pole base moment. **Fig. 3-6** indicates that the peak values of the responses increase with the increase of the velocity. The figure also indicates that the pole generally exhibit larger differences between the peak total and quasi-static responses than the conductors for wind speeds greater than 40 m/sec. This is due to the cracking of the pole under mean wind speeds higher than 40 m/sec. The cracking of the pole decreases its frequency to be closer to the conductors' frequencies. As such, coupled pole-conductor mode develops and the system becomes more vulnerable to dynamic excitations.
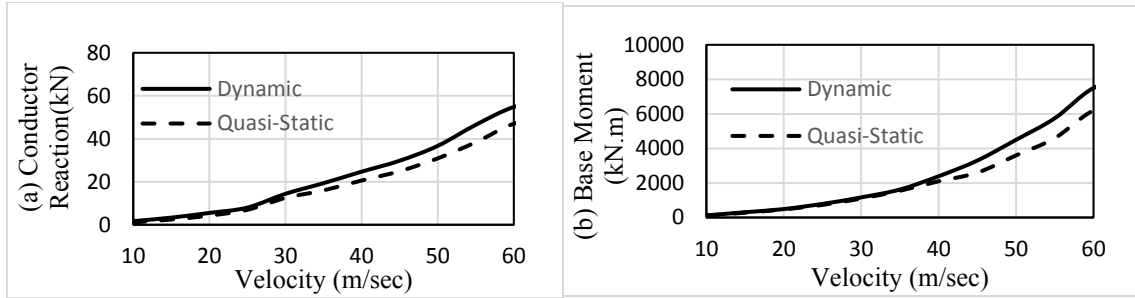
Fig. 3-6. (a-b) Peak responses for the conductors and the pre-stressed concrete pole

3.5. <u>DAF and GRF variations with wind speeds</u>

In this section, the variation of the dynamic amplification factor (DAF) and gust response factor (GRF) with different mean wind speeds for the three different pole systems is presented. GRF values are then compared with the values recommended by ASCE 74 (2010).

3.5.1 DAF variation for different responses with wind speed

The dynamic amplification factor (DAF) is defined as the ratio between the peak total response and the peak quasi-static response as expressed in Equation 3-6.

$$DAF = \frac{\hat{R}_T}{\hat{R}_{QS}} \tag{3-6}$$

Where: $\hat{R}_T$ is the peak total response and $\hat{R}_{QS}$ is the peak quasi-static response.

The variations in the DAF with the mean wind velocity for the conductor reaction and the pole base moment responses are shown in **Fig. 3-7** (a), (b) and (c) for the 100 m, 200 m and 300 m pole systems, respectively.
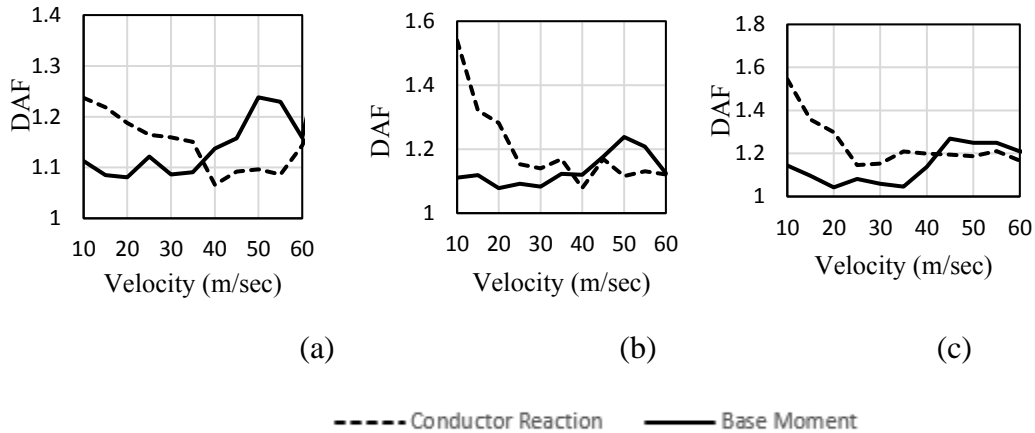
Fig. 3-7. (a-c) DAF for the three pre-stressed concrete pole systems

By investigating the values and the trend of the DAF, the following findings are obtained:

- The DAF of the conductor reactions has a decreasing trend with the increase of the mean wind speed. This trend results from the increase of the aerodynamic damping (see Equation 3-3) which attenuates the resonant component.

- The DAFs of the pole base moments have no specific trend for mean wind speeds between 10 to 40 m/sec. The poles are considered un-cracked under those mean wind speeds. The maximum DAFs are 13 %, 12 % and 14 % for the 100 m, 200 m and 300 m pole systems, respectively.

- The DAFs are found to be higher for mean velocities above 40 m/sec up to 60 m/sec as the poles crack and become more vulnerable to wind turbulent excitations. When the poles crack, their frequencies become close to the conductors' frequencies. This results in coupled pole- conductor mode shapes which is the main reason for the increase of the resonant component. The damping ratio for the cracked pole systems is assumed to be 5 % according to Newmark and Hall (1982). Hence, this damping ratio limits the maximum values of the DAF to be 24 %, 25 % and 27 % for the 100 m, 200 m and 300 m pole

systems, respectively. As such, the dynamic effect has to be considered while analyzing

the pre-stressed concrete pole systems under a normal wind speed higher than 40 m/sec.

3.5.2 GRF variation for different responses with wind speed

The gust response factors are evaluated for the poles' base moment as the ratio between the peak

total response, $\hat{R}_T$ and the mean response, M. This gust response factor is referred to as GF_T and

is plotted in **Fig. 3-8** a, b and c for the 100 m, 200 m and 300 m pole systems, respectively. Another

gust response factor is also evaluated which represents the ratio between the peak quasi-static

response, $\hat{R}_{Qs}$ and the mean response, M. It is referred to as GF_{QS} and is plotted in the same figure.

(a)   (b)   (c)

Fig. 3-8. (a-c) GRF for the base moment for the three pre-stressed concrete pole systems

It can be noted from **Fig. 3-8** that the values of GF_T are usually higher than the values of GF_{QS} due

to the inclusion of the resonant component.

Gust response factors are also evaluated using Davenport's (1979) expressions incorporated in the

ASCE 74 (2010) that account for the mean, background and resonant components. Gust response

factors resulting from Davenport's expression is referred to as GF_{T-ASCE}. The ASCE 74 (2010) simplifies Davenport's expressions by neglecting the contribution of the resonant component, which means it includes only the quasi-static response. The resulting gust response factor is referred to as $GF_{Qs-ASCE}$. Both GF_{T-ASCE} and $GF_{Qs-ASCE}$ are evaluated and also plotted in **Fig. 3-8** for comparison purpose with GF_T and GF_{Qs}, respectively. Pole base moments are chosen for comparing the gust response factors for the three considered pole systems.

By comparing the gust response factors obtained from the ASCE 74 (2010) with the gust response factors obtained from the dynamic analyses, the following findings can be stated.

- In most of the cases, the gust response factor obtained from the ASCE that includes the dynamic effect (Davenport 1979), GF_{T-ASCE}, is higher than the gust response factor obtained from the dynamic analyses, GF_T. This leads to the conclusion that the ASCE 74 (2010) overestimates the dynamic response.

- In some of the cases, $G_{FQS-ASCE}$ is found to be higher than the corresponding G_{FQS} values (over conservative). While in other cases, G_{FQS} is close to or slightly higher than the obtained $G_{FQS-ASCE}$ values which means that the ASCE 74 values are conservative in those cases.

- By comparing G_{FT} to $G_{QS-ASCE}$, it is found that G_{FT} is consistently higher than $G_{QS-ASCE}$. This comparison can be used to assess the importance of including the dynamic effects. The larger the discrepancy between G_{FT} and $G_{QS-ASCE}$, the more important is the dynamic effect. This discrepancy is found to be larger in the higher wind speed when the poles crack and coupled pole- conductor modes exist. This implies the importance of considering the dynamic effect while analyzing the poles under normal wind speeds above the cracking wind speed (i.e.40 m/sec).

3.6. <u>Conclusions</u>

A Numerical model capable of conducting dynamic analysis of pre-stressed concrete transmission lines is developed. The numerical model is employed to evaluate the dynamic behavior of three pre-stressed concrete pole systems with different spans. Peak total responses (i.e. including the dynamic effect) and peak quasi-static responses (i.e. neglecting the dynamic effect) are evaluated. Dynamic Amplification factor (DAF), defined as the ratio between peak total responses to the peak quasi-static responses, is evaluated. Total gust response factor, GRF_T, defined as the ratio between peak total response to the mean response is evaluated using the results from the dynamic analyses and is compared with the quasi-static gust response factor, GRF_{QS}, which is defined as the ratio between peak quasi-static response to the mean response. Total and quasi-static gust response factors, GRF_{T-ASCE} and $GRF_{QS-ASCE}$, based on Davenport's expressions included in the ASCE 74 (2010) are also evaluated. The following conclusions are obtained:

- Conductor reactions exhibit large Dynamic Amplification Factor (DAF) than the pole base moments especially at the low wind speeds. This trend results from the low conductor aerodynamic damping at lower wind speeds.

- DAF of the poles has no specific trend under mean wind speeds up to the cracking wind speed (40 m/sec). The maximum DAF do not exceed 13 %, 12 % and 14 % for the 100 m, 200 m and 300 m pole systems, respectively. This is mainly due to the discrepancy between the conductors' and poles' frequencies under mean wind speeds less than 40 m/sec.

- DAF exhibit higher values when the mean wind speeds exceed 40 m/sec. This is attributed to the fact that the poles crack when the mean wind speed is higher than 40 m/sec. The poles' cracking decreases the frequency of the whole transmission line system. As such, the poles' frequencies become close to the conductors' ones and coupled pole-conductor

mode appears. This results in increasing the resonant component and hence increasing the dynamic effect. For mean wind speeds greater than the cracking wind speed, the maximum values of the DAF are 24 %, 25 % and 27 % for the 100 m, 200 m and 300 m pole systems, respectively. As such, the dynamic effect is more important after the cracking of the poles.

- $GF_{T\text{-}ASCE}$, is over conservative and is usually higher than the gust response factor obtained from the dynamic analyses, GF_T.

- $G_{FQS\text{-}ASCE}$ is found to be considerably less than G_T for the three pole systems especially for the wind speeds above the cracking wind speed.

Based on the above findings, it is concluded that dynamic effect has to be accounted while evaluating conductor peak responses especially for low velocity magnitudes. It is also concluded that dynamic effect has to be considered for the cracked pole systems that exhibit coupled conductor-pole modes as the DAF reached 24 %, 25 % and 27 % for the 100 m, 200 m and 300 m pole systems, respectively.

3.7. <u>References</u>

Aboshosha, H., and El Damatty, A.A., (2014), "Effective technique for the reactions of transmission line conductors under high intensity winds", Wind and Structures. 18(3), 235-252.

Aboshosha, H., El Damatty, A. (2015), "Dynamic Effect for Transmission Line Conductors under Downburst and Synoptic Winds", Wind and Structures. 21(2),241-272.

Aboshosha, H., Ibrahim, A.M., El Damatty, A.A. and Hamada,A., (2016), "Dynamic Behaviour of Transmission Line Structures under Synoptic Wind Loads". Proceeding of CIGRE-IEC colloquim, Montreal, QC, Canada.

AIJ (2004), "RLB Recommendations for Loads on Buildings", Tokyo, Structural Standards Committee.

American Society of Civil Engineers (ASCE), (2010) "Guidelines for electrical transmission line structural loading", ASCE manuals and reports on engineering practice, No. 74, New York, NY, USA.

American Society of Civil Engineers (ASCE), (2012) "Prestressed Concrete Transmission Pole Structures", ASCE manuals and reports on engineering practice, No. 123, Reston, VA, USA.

Bachmann, H. et al. (1995), "Vibration problems in structures". Practical guidelines.

Bathe, K.J. 1996. Finite Element Procedures in Engineering Analysis, Prentice-Hall, Englewood Cliffs, New Jersey.

Chay, M. T., Albermani, F. and Wilson, R. (2006), "Numerical and analytical simulation of downburst wind loads", Engineering Structures 28(2), 240-254.

Chen, L. and Letchford, C.W. (2004a), "A deterministic–stochastic hybrid model of downbursts and its impact on a cantilevered structure", Engineering Structures 26(5), 619-629.

Chen, L. and Letchford, C.W. (2004b), "Parametric study on the along-wind response of the CAARC building to downbursts in the time domain", Journal of Wind Engineering and Industrial Aerodynamics, 92(9), 703-724.

Chen, S.E., Ong C. K. and Antonsson K., (2006), "Modal Behaviors of Spun-Cast Pre-Stressed Concrete Pole Structures", Proceeding of IMAC – XXIV.

Chen S.E., and Dai K., (2010), "Modal Characteristics of Two Operating Power Transmission Poles," Shock and Vibration, vol. 17, no. 4-5, 551-561.

Dai,K., (2009), "Dynamic Performance of Transmssion Pole stuructures under Blasting Induced Ground Vibration" A dissertation submitted to the faculty of The University of North Carolina at Charlotte, Charlotte, USA.

Dai,K. and Chen,S.E., (2008), "Vibration of spun-cast prestressed concrete poles", Proceedings IMAC – XXV, Orlando, Florida, USA.

Davenport, A.G., (1979). "Gust response factors for transmission line loading", Proceedings, 5th International Conference on Wind Engineering, Fort Collins, Colorado, 899-909, Pergamon Press.

Hamada,A., King,J.P.C., El Damatty,A.A., Bitsumlak,G. and Hamada,M.,(2017), "The response of a guyed transmission line system to boundary layer wind". Journal of Engineering Structures. vol. 139, 135–152 (2017).

Horr, A.M., Yibulayin, A., and Disney, P., (2004), "Nonlinear spectral dynamic analysis of guyed towers. Part II: Manitoba towers case study". Canada Journal of Civil Engineering, 31(6): 1061-1076.

Ibrahim, A.M., El Damatty, A. A. and Elansary A.M., (2017), "Finite element modelling of pre-stressed concrete poles under downbursts and tornadoes". Journal of Engineering Structures. 153, 370-382.

International Electrotechnical Commission (IEC), (2003), "Design Criteria of Overhead Transmission Lines", International Standard IEC-60826" Geneva, Switzerland.

Lantrip, T.B., (1995), "Identification of Structural Characteristics of Spun Prestressed Concrete Poles Using Modal Testing Methods", M.Sc. Thesis, Dept. of Civil and Environmental Engineering, University of Alabama at Birmingham.

Li, C.Q. (2000), "A stochastic model of severe thunderstorms for transmission line design". Probab. Eng. Mech., 15, 359-364.

Li, H. and Bai, H., (2006) "High-voltage transmission tower-line system subjected to disaster loads". Progress in Natural Science, vol. 16, no. 9, 899–911.

Loredo-Souza, A. and Davenport, A.G. (1998), "The effects of high winds on transmission lines". J. Wind Eng. Ind. Aerodyn., 74-76, 987-994.

Loredo-Souza, A. M. and Davenport, A. G., (2003), "The influence of the design methodology in the response of transmission towers to wind loading". Journal of wind engineering and industrial aerodynamics, 91(8): 995-1005.

Madugula, M. K. S., (2002), "Dynamic Response of Lattice Towers and Guyed Masts". American Society of Civil Engineers (ASCE), New York, NY, USA.

Momomura, Y., Marukawa, H., Okamura, T., Hongo, E. and Ohkuma, T., (1997). "Full-scale measurements of wind induced vibration of a transmission line system in a mountainous area". Journal of Wind Engineering and Industrial Aerodynamics, 72, 241-252.

Newmark, N. M. and Hall, W. J., (1982), "Earthquake spectra and design", Earth-quake Engineering Research Institute, Berekley, California, USA.

NRC "National Building Code of Canada", (2005), Associate Committee on the National Building Code, National Research Council, Ottawa.

Polyzois, D., Raftoyiannis, I.G. and Ibrahim, S., (1998), "Finite elements method for the dynamic analysis of tapered composite poles", Composite structures (43) 25-34.

Savory, E., Parke, G., Zeinoddini, M., Toy, N. and Disney, P. (2001), "Modeling of tornado and microburst induced wind loading and failure of a lattice transmission tower". Eng. Struct., 23, 365-375.

Simiu, E. and Scanlan, R. (1996). "Wind Effects on Structures", Third Edition, John Wiley and Sons.

Sparling, B. and Wegner, L. (2007), "Estimating peak wind load effects in guyed masts". Wind and Structures, 10(4), 347-366.

Von Karman T. (1948), "Progress in the Statistical Theory of Turbulence". Proceedings of the National Academy of Sciences of the United States of America, 34(11), 530-539.

CHAPTER 4

BEHAVIOUR, DESIGN AND NON-LINEAR FAILURE ANALYSIS OF

GUYED PRE-STRESSED CONCRETE POLES UNDER DOWNBURSTS

4.1.   <u>Introduction</u>

Transmission lines are one of the most critical infrastructural elements all over the globe. Any deficiency in such structures can seriously affect people`s lives and activities. High intensity wind (HIW) events in the form of downbursts represent a major threat on transmission line structures. A downburst is defined as a violent downdraft of moist and cold air that suddenly impinges the ground and spreads horizontally as per Fujita (1985). Li (2000) stated that downbursts are the reason for more than 90% of weather-related failures. In China, in 2005, 18 transmission towers carrying 500 kV lines and 60 towers carrying 110 kV lines collapsed due to strong wind events such as downbursts, tornadoes and typhoons (Zhang 2006). In Canada, many of transmission line structures failed in the past twenty years as a result of downbursts such as those reported by Manitoba Hydro (Mccarthy and Melsness, 1996) and Hydro One, Ontario in 2006. In 2016, 23 transmission towers failed during a series of downburst events in Australia (Australian Wind Alliance, 2016).

Many studies has been conducted to assess the response of transmission line structures under downburst loading. Shehata et al. (2005) developed and validated a finite element model to simulate the behavior of a guyed transmission line system under downburst. Shehata and El Damatty (2007) conducted a parametric study by varying the downburst size and location to obtain the critical downburst configurations acting on guyed transmission line structures. Yang and Zhang (2016) conducted two cases studies on the structural analysis of transmission towers under

downburst. Wang et al. (2009), Darwish et al. (2010), Darwish and el Damatty (2011) and Ladubec et al. (2012) also performed a number of studies on the effect of downburst forces on transmission lattice steel towers. Transmission line conductors' response under downburst was investigated by Aboshosha and El Damatty (2014). Aboshosha and El Damatty (2014) developed a numerical technique to investigate the behavior of transmission line conductors under downburst loading taking into account the non-linear behavior of the conductors including sagging, pre-tensioning forces and insulator's stiffness.

El Damatty et al. (2013) summarized the major findings of the attempts made in literature during the past decade to study the effect of downbursts on lattice steel transmission line structures. Despite the complexity of the downburst wind field and the fact that the downburst location with respect to the tower significantly affect the response, El Damatty et al. (2013) proposed three simplified critical downburst load cases to be considered in the design and analysis of lattice steel transmission line structures under downbursts. In each load case, the velocity profile along the towers' height and the conductors' spans are provided. Those simplified load cases provide the maximum responses of a number of lattice steel transmission towers under a huge number of possible downburst load configurations.

According to the supporting system, transmission line systems can be supported by lattice steel towers or pole-type structures. Few studies have assessed the behavior of pre-stressed concrete pole structures under downbursts. Ibrahim and El Damatty (2014) studied the behavior of a self-supported pre-stressed concrete pole under downbursts. Ibrahim et al. (2017) developed and validated a non-linear finite element model to assess the behavior of a pre-stressed concrete pole under downbursts and tornadoes. An extensive parametric study was conducted to obtain the downburst critical configurations which lead to the maximum straining actions on the pole. In

addition to that, a non-linear failure analysis was performed to determine the critical downburst jet velocity at which the pole experienced collapse. The concrete and pre-stressing strands' non-linear properties such as cracking, tension stiffening, creep, shrinkage and relaxation were taken into account in the analysis.

In the current study, the finite element model developed and validated by Ibrahim et al. (2017) is utilized to study the performance of guyed pre-stressed concrete poles under downbursts. Three guyed pre-stressed concrete pole systems with different spans are designed to remain un-cracked under normal synoptic wind speed of 40 m/sec based on the provisions of ASCE 74 (2010) and ASCE 123 (2012). A parametric study is conducted on the three guyed transmission line pre-stressed concrete pole systems taking into account the size and location variation of downburst wind events to identify the downburst critical load configurations which will lead to the maximum bending moments at the poles and the maximum tension forces at the guys. This is followed by a comparison that is made between the maximum responses obtained from the parametric study and the envelope of the critical downburst load cases proposed by El Damatty et al. (2013). The purpose of the comparison is to estimate if the proposed downburst load cases can be applied to the guyed pre-stressed concrete pole structures. Finally, a non-linear failure analysis is conducted to determine the downburst jet velocity (V_j) at which the guyed pole systems are expected to fail.

4.2. Numerical model

The localized nature of the downburst wind events in addition to the non-linear behavior of the transmission line conductors and guyed pre-stressed concrete poles makes the prediction of the response of the guyed pole systems quite challenging. As such, a sophisticated numerical model is developed to assess the behavior of guyed pre-stressed concrete pole structures under downbursts.

The numerical model consists of three components. Firstly, the three dimensional downburst wind field is simulated using Hangan et al. (2003) computational fluid dynamics (CFD) model. Secondly, the conductors' reactions are predicted using the computationally efficient semi-analytical technique developed and validated by Aboshosha and El Damatty (2014). Thirdly, the non-linear finite element model developed and validated by Ibrahim et al. (2017) is utilized to obtain the straining actions in the poles and the guys.

According to the study conducted in Chapter 3, the dynamic effect has to be considered in the analysis of self- supported pre-stressed concrete pole systems under synoptic wind loading of high synoptic wind speeds (i.e. > 40 m/sec). In this study, the dynamic amplification factor (DAF) - which is defined as the ratio between the total dynamic and quasi-static responses- was evaluated for the pole base moments of three pre-stressed concrete pole systems with different spans. The DAF was found to be 24%, 25% and 27 % for the 100 m, 200 m and 300 m, respectively. The synoptic wind turbulence intensity was assumed to be 14 % according to AS/NZS: 700 (2010).

In the current study, the analysis of guyed pre-stressed concrete poles under downbursts are performed considering the following facts:

1- Holmes et al. (2008) stated that the turbulence in a real downburst is 10 % which is less than the synoptic wind field turbulent intensity.

2- The frequency of the guyed concrete pole systems are greater than the frequency of the self-supported systems under a specific applied wind speed on both systems.

Based on these facts, the response of guyed pre-stressed concrete poles under downbursts are assumed to have a lower dynamic effect than the response of the self- supported pole systems

under normal wind. According to that assumption, the analysis of the guyed pre-stressed concrete pole structures under downburst wind loading is performed using a quasi-static approach.

4.2.1. Downburst forces

Wolfson et al. (1985), Fujita (1990), Gast and Schroeder (2003), Choi (2004) and Holmes et al. (2008) have made a few attempts to obtain the downburst field measurements. However, obtaining full scale data for such localized events is extremely hard. As such, numerical simulation of downbursts is considered a useful tool to estimate wind field velocities. A Computational Fluid Dynamics (CFD) model was developed by Hangan et al. (2003). The downburst outflow in this model consists of two velocity components: radial (horizontal) component (V_{RD}) and axial (vertical) component (V_{VL}). The factors affecting the values of the velocity components at a certain point are its location relative to the downburst center and its height above the ground. The wind field associated with the downburst is mainly affected by the parameters V_j, D_j, R and θ as shown in **Fig. 4-1**.
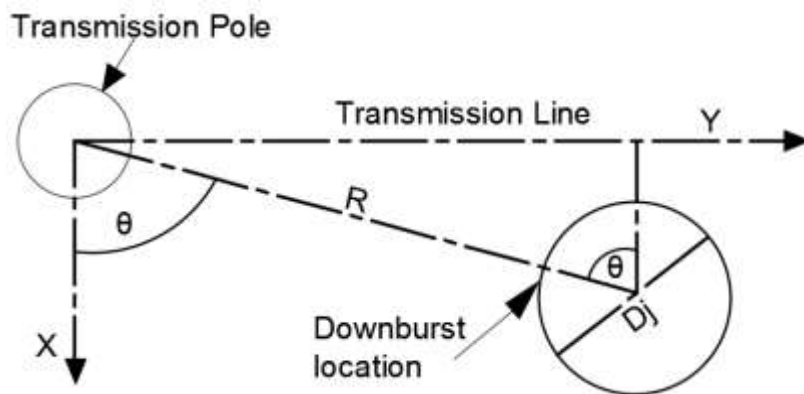
Fig. 4-1. Downburst Parameters

As shown in **Fig. 4-1**, the location of the center of the downburst with respect to the pole center is determined by the polar coordinates (distance (R) and the angle (θ)). The downburst intensity is defined by its jet diameter (Dj) and its jet velocity (Vj).

The downburst loads are obtained from the wind field. The velocity wind field is transformed into forces using the procedure provided in the ASCE-74 (2010) based on the following equation:

$$F_{wi} = \frac{1}{2}\rho_a \, GC_f \, A(Z_v \, V_i)^2 \qquad (4\text{-}1)$$

Where F_{wi} is the force developing in the i direction, ρ_a is the density of air = 1.225 (Kg/m^3), G is the gust factor , C_f is the drag force coefficient, A is the nodal projected area perpendicular to i direction, Z_v is the terrain factor and V_i is the downburst velocity in the i direction (units m/sec). For conductors and circular concrete poles, the value of the drag coefficient is taken equal to 1.0 according to ASCE-74 (2010) guidelines, and the same value is recommended for gust and terrain.

4.2.2. Modeling of conductors

Conductors' reactions are predicted using the analytical technique developed by Aboshosha and El Damatty (2014). This technique accounts for the variation of the loads along the conductor spans, insulators flexibility and the non-linear behaviour of the conductors including sagging and pre-tensioning forces.

4.2.3. Modeling of guyed pre-stressed concrete poles

4.2.3.1. Modeling of the pre-stressed concrete poles

The non-linear finite element model developed and validated by Ibrahim et al. (2017) is utilized to simulate the pre-stressed concrete poles behaviour. Frame elements are used to model the pre-stressed concrete poles. The finite element model accounts for the non-linear behavior of pre-

stressed concrete poles, the cracking and non-linear behavior of concrete, in addition to the long term effects such as creep, shrinkage and relaxation.

4.2.3.2.   Modeling of the guys

The guys are modelled using three non-linear dimensional frame elements with two nodes and six degrees of freedom per each node (three translational and three rotational). The stiffness of the guys depends on the applied pre-tensioning force. The guys can carry tension forces up to their rated breaking strength (RBS) as assigned by ASCE 91(1997). When the compression force in the guy exceeds the pre-tensioning force, the guys are assumed to slack.

4.3.   <u>Considered Guyed concrete pole properties</u>

The numerical model described earlier is employed to study the behaviour of three guyed pre-stressed concrete pole systems under downbursts. The following steps are conducted in this study:

1- Perform a parametric study by changing the downburst size and location in order to determine the critical downburst configurations leading to maximum effect on the guyed poles under a specific downburst jet velocity.

2- Compare the straining actions that developed in the guys and the poles under the critical downbursts configurations to the corresponding values obtained from applying the three load cases proposed by El Damatty et al. (2013).

3- Conduct a non-linear analysis for the guyed poles using this critical downburst configuration that considers post cracking behaviour in order to determine the downburst jet velocity that would lead to a full collapse of the pole or the guys. The failure of the guys in tension occurs when the tension forces reach the RBS of the guy. While the failure in

compression is due to slacking. In compression, a guy slacks if it is subjected to a compression force higher than the pre-tensioning force.

Three transmission guyed pole systems with different conductor spans are considered in this study. The three systems are designed to remain un-cracked under a synoptic wind speed of 40 m/sec based on the ASCE 123 (2012) and ASCE 74 (2010) guidelines. The three guyed pole systems have the following common geometric and material properties:

- Unsupported height of poles of 25.5 m.

- The outer diameters in the tip and the bottom are 281 and 459 mm, respectively.

- The inside diameters of the poles vary from 143 mm at the top to 321 mm at the bottom.

- Cross arms' length of 2.4 m supporting two conductors.

- Conductors having a projected area of 0.096 m^2, weight per unit length of 30 N/m and insulator length of 2.5 m and sag value of 2% relative to the span.

- Concrete with compressive strength of 75.8 MPa and pre-tensioned with 20M10 low relaxation pre-stressing strands.

- Two guys perpendicular to the conductors' line are used to support the pole.

-The guys' angle of inclination with the ground is 60^0.

-The guys' diameters are 12 mm.

-A single layer of 7-wire strands are used in the guys with a pre-tensioning force of 10 kN.

-The guys are of grade 1300 (CSA-G12).

-According to the ASCE-91 (1997), the guys' rated breaking strength (RBS) is 120 kN.

- The guys attachment points to the poles are at a height of 23m similar to the conductors' attachment points to the insulators.

The three systems differ in terms of conductor spans which are assumed to be 100 m, 200 m and 300 m, respectively. **Fig. 4-2** shows the layout of the guyed transmission pole systems.
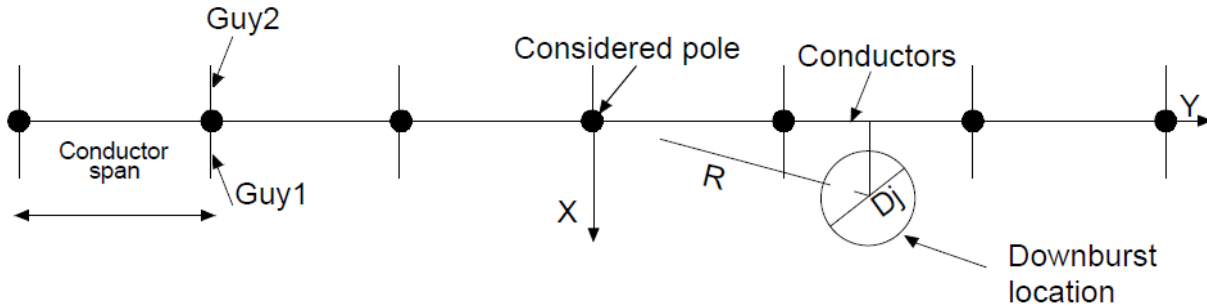
Fig. 4-2. Guyed pole systems (Plan View)

4.3.1. Response of guyed poles under downbursts

To understand the performance of the guyed poles under downbursts. **Fig. 4-3** is presented to help the reader to understand the behaviour of the guyed pre-stressed concrete pole systems under in-plane and out of plane downburst loads.
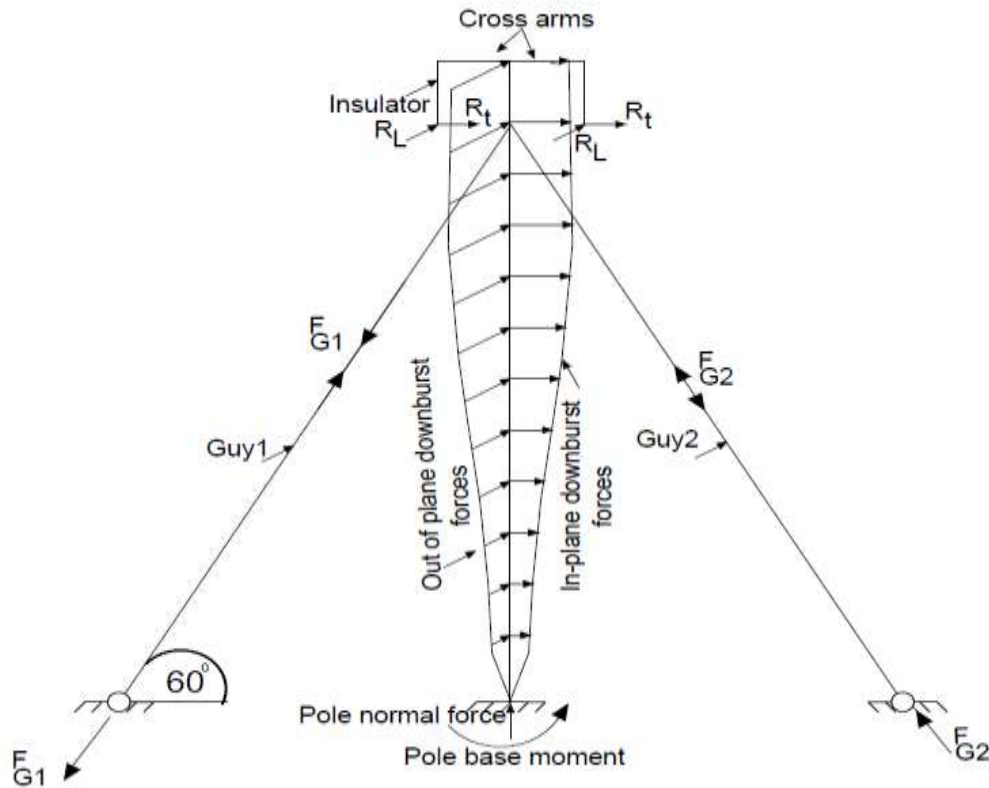
Fig. 4-3. Schematic diagram showing the guyed poles analysis under a downburst

Where:

R_t is the transverse conductor reaction, R_L is the longitudinal conductor reaction, F_{G1} is the force developing in guy1 and F_{G2} is the force developing in guy2.

The downburst loads acting on a guyed pre-stressed concrete transmission pole system can be divided into two main parts: (1) loads acting on the conductors and (2) loads acting on the pole.

As mentioned above, the guys' orientation is normal to the direction of the transmission line conductors. In addition to that, the guys of the three pole systems are attached to the poles at the same height where the conductors are attached to the insulators. As such, the guys act as the support of the conductors and the transverse conductors' reactions are fully transferred to the guys.

It should be noted that the guys only resist the component of the applied loads acting in a direction along its axes. Based on that, the conductors' longitudinal reactions are resisted only by the pole and the guys do not contribute in the resistance of those reactions.

The downburst loads acting on the pole are resolved into two components. The first component is in the direction perpendicular on the transmission lines (i.e. along with the guys' axes direction), while the second component is in the direction normal to the guys axes (i.e. along with the transmission lines direction). The first component is resisted by both the pole and the guys based on the relative stiffness between them. Meanwhile the second component is only resisted by the pole which acts as a cantilever pole in this case.

It should be noted that based on all the possible downburst configurations and the alignment of the guys with respect to the transmission lines of the three poles studied, guy1 is always subjected to tension forces while guy 2 is usually subjected to compression forces. If the compression force evaluated in guy2 due to the in-plane downburst forces acting on the poles in addition to the conductors' transverse reactions exceeds the value of the pre-tensioning force (i.e. 10 kN), guy2 will slack. In this case, only guy1 and the pole will support the guyed pole system while being subjected to the downburst. It is worth to mention that the value of the tension force that developed in guy1 in such cases exceeds 10 kN.

4.4. <u>Downburst parametric study</u>

The three guyed transmission poles designed to remain un-cracked under normal wind loads corresponding to reference wind speed of 40 m/sec are considered for the downburst analysis. In this section, a parametric study is conducted on three different guyed pre-stressed concrete pole systems. A total number of 924 downburst load configurations are applied to each of the three

systems. The objective is to determine the configurations that lead to maximum bending moment, tension and compression forces on each of the three poles and the guys.

The parametric study is conducted for a fixed value for the jet velocity Vj= 40m/sec. The downburst configuration is defined by the jet diameter Dj and the geometric parameters (R and θ) as shown in **Fig. 4-1**. In the parametric study, the downburst jet diameter is assumed to be varying from 500 m to 1500 m with an increment of 100 m. The ratio R/D_j is varied from 0 to 2 with an increment of 0.1, while the angle (θ) is varied between 0^0 and 90^0 with an increment of 30^0. The overturning moment (M_a) normalized by the pole ultimate capacity (M_r) at the pole base is determined for each configuration. The tension and compression forces in the guys are identified as well. In addition to that, the downburst velocities distributions across the conductors' spans and the poles' height are presented for the critical load cases.

4.4.1   Results of the Guyed pole system with conductor span 100m

4.4.1.1   *Pole base moment*

The results of the parametric study are presented in **Fig. 4-4** (a-d). Each figure corresponds to a specific value of "θ" and shows the variation of the ratio (M_a/M_r) with D_j and (R/D_j).

(a)   (b)
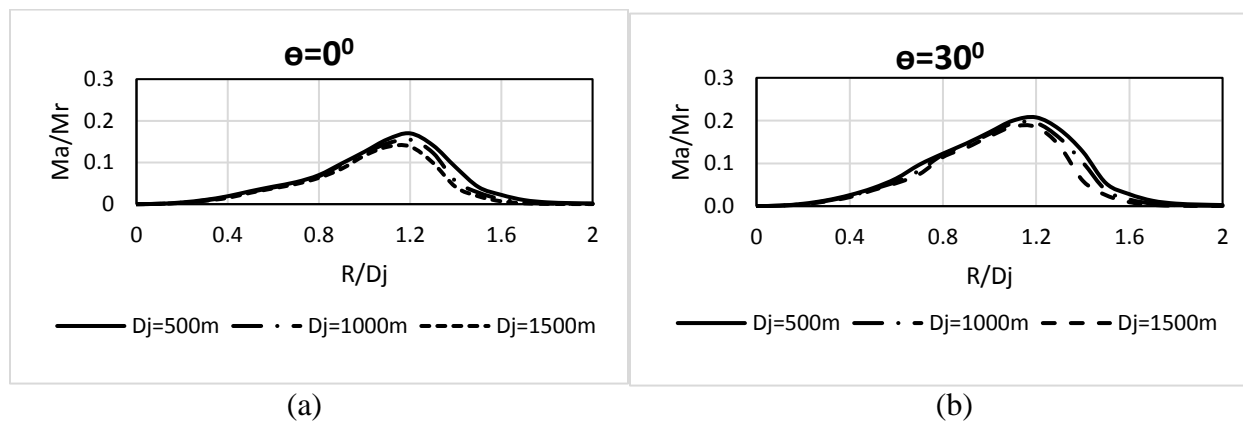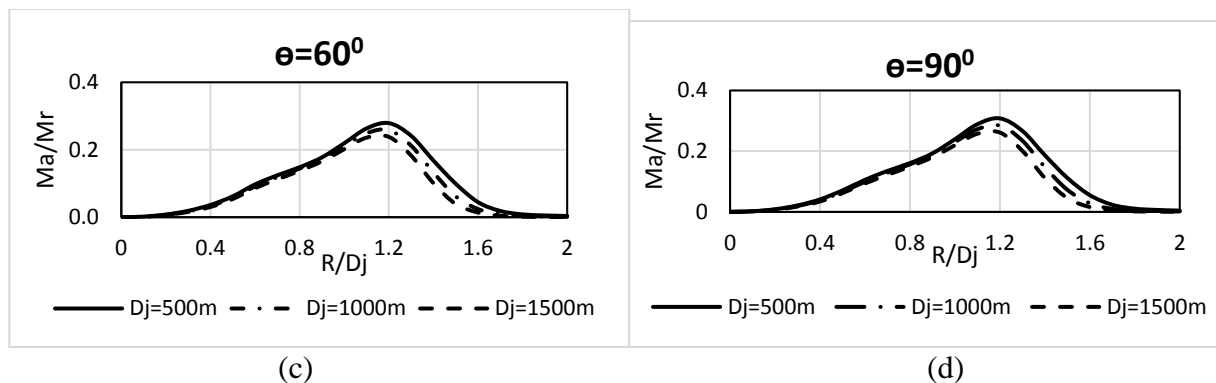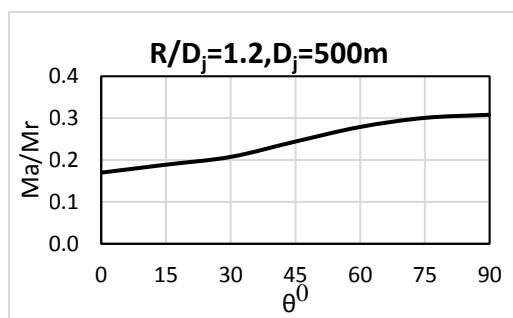
Fig. 4-4. (a-d) Variation of (M_a/M_r) with R/D_j

The figures indicate that the maximum (M_a/M_r) ratio occurs consistently at R/D_j=1.2. As such, the processing of the results is then focused on this ratio. **Fig. 4-5** shows the variation of (M_a/M_r) with D_j and θ for R/D_j =1.2, while **Fig. 4-6** shows the variation of the same ratio with θ for R/D_j =1.2 and D_j=500m.
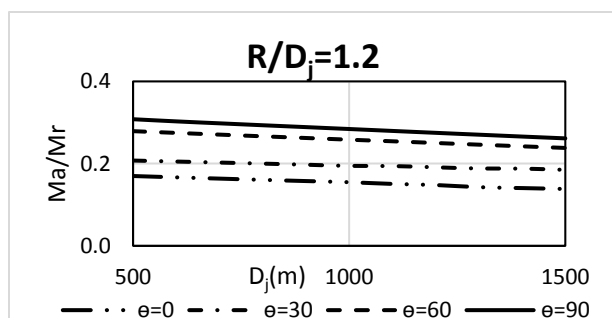
Fig. 4-5. Variation of (M_a/M_r) with D_j **Fig. 4-6.** Variation of (M_a/M_r) with θ

The figures indicate that the absolute maximum value for the ratio (M_a/M_r) occurs at the configuration D_j=500m, R/D_j =1.2 and θ =90^0, which can be considered the critical downburst configuration. This configuration leads to maximizing the bending moments acting on the pole base.

At θ=0^0, the conductors' reactions are only transversal. As such, the conductors' reactions are totally transferred to the guys. The downburst load on the pole is shared between the pole and the

guys. It is worth to mention that the contribution of the guys in resisting the downburst load on the pole in this case is the highest among all the other downburst configurations. This is attributed to the fact that at $\theta=0^0$ the entire downburst load component is in the direction of the guys and no downburst loads are acting on the pole out of plane.

By increasing θ, the transverse conductors' reactions decrease. As a result, the guys carry less load. Longitudinal conductors' reactions as well as the downburst load component which acts normal to the guys' axes are resisted by the poles. As mentioned before, the guys are not able to resist the loads perpendicular to its axes and the pole acts as a cantilever in resisting the out of plane loads.

At $\theta=90^0$, the conductors are unloaded. In this case the pole acts as a cantilever while resisting the out of plane downburst wind load acting on it without any support from the guys. This explains why the configuration of $\theta=90^0$ is considered as the most critical configuration which lead to maximum bending moments on the guyed pole systems.

4.4.1.2 *Forces in guy1 (FG1)*

The effect of changing downburst configurations on the forces developing in guy1 are presented in **Fig.4-7** (a-d). Each figure corresponds to a specific value of "θ" and shows the variation of the guy1 tension forces (F_{G1}) with D_j and (R/D_j).
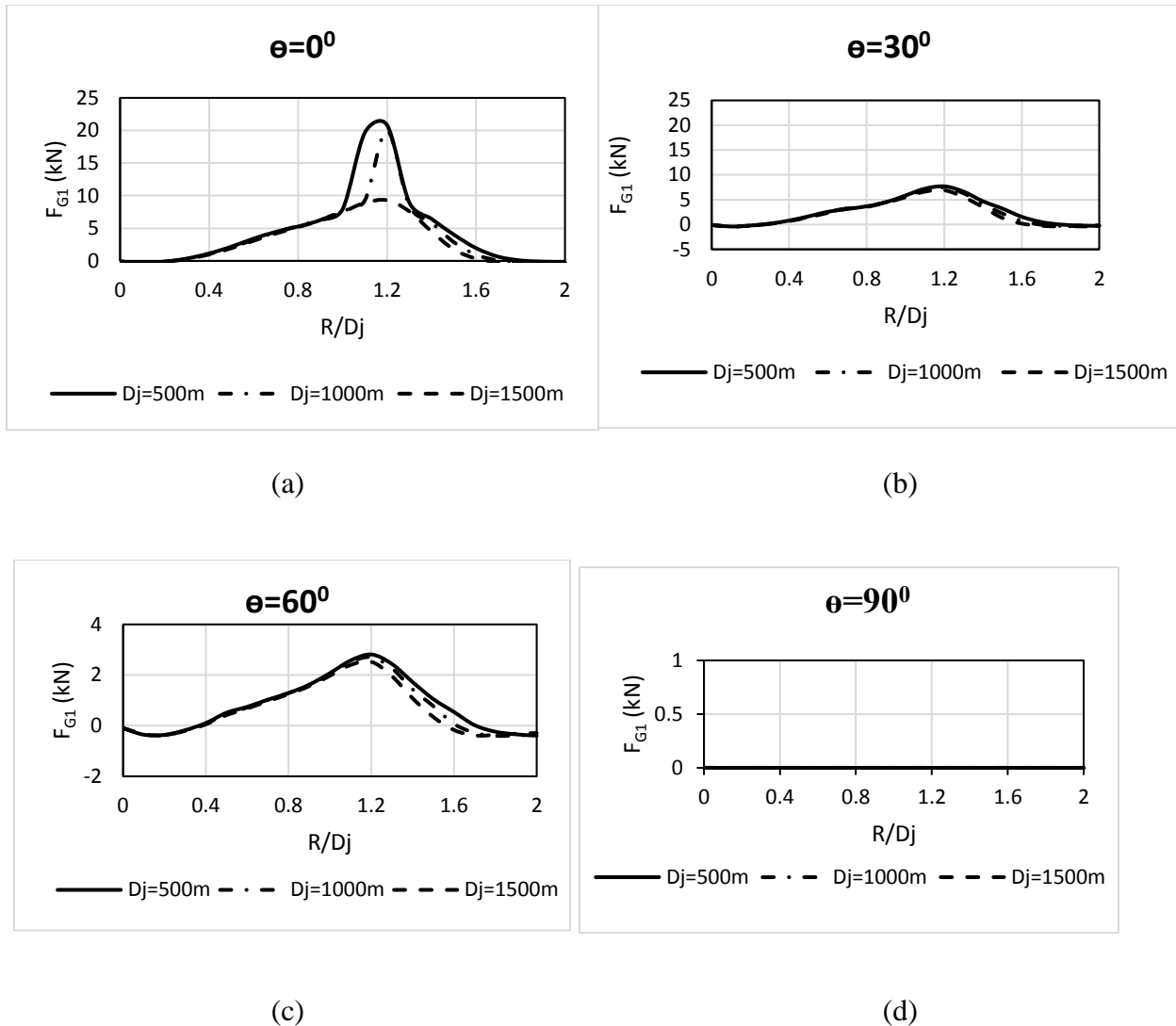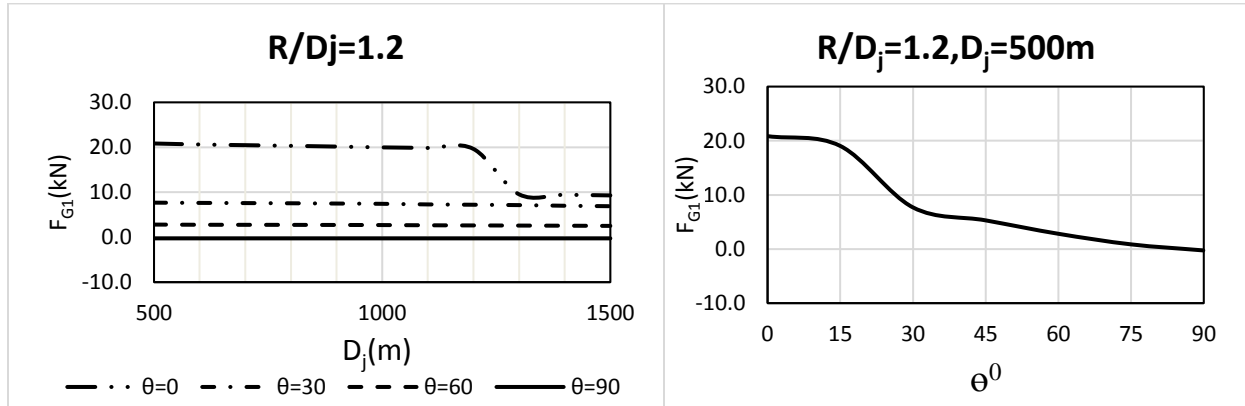
Fig. 4-7. (a-d) Variation of F_{G1} with R/D_j

As shown in the figures, the forces on guy1 are tension forces in all the downburst possible configurations. The critical case at which the tension of guy1 reaches the maximum value occurs when $R/D_j=1.2$. As mentioned before, the guys are not contributing in resisting the downburst load when $\theta=90^0$.

The magnitude of the forces in both guys are the same unless guy2 is subjected to a compression force greater than the guys' pre-tensioning force, which is 10 kN. Once the compression force in

guy2 exceeds 10 kN, guy2 slacks and the whole transverse conductor reaction is transferred to guy1. In such cases, the tension force in guy1 exceeds 10 kN. The following figures show the variation of guy1 forces with Dj and θ:


Fig. 4-8. Variation of F_{G1} with D_j **Fig. 4-9.** Variation of F_{G1} with θ

The variation of D_j does not significantly affect the value of the tension forces that developed in guy1. By investigating the variation of the tension forces values in guy1 with θ, it is found that θ=0^0 is the most critical configuration which leads to the maximum tension value for F_{G1}. For θ=0^0, D_j between 500m and 1200m and R/D_J=1.2, F_{G1} exceeds 10 kN which means that guy2 slacked in these downburst configurations. This finding is shown later in **Figs. 4-10** and **4-11.**

It can be noted from **Fig. 4-9** that with the increase of θ, the forces in guy1 decrease until its contribution becomes zero at θ=90^0. The higher values of the tension forces occurring in some cases at θ=0^0 and θ=15^0 is attributed to the slacking of guy2 in those cases. The critical downburst configuration which leads to the highest tension forces acting on guy1 occurs when θ=0^0, R/D_j=1.2 and Dj=500m.

4.4.1.3   Forces in guy2

The following figure shows the variation of the guy2 compression forces (F_{G2}) with R/D_j and D_j

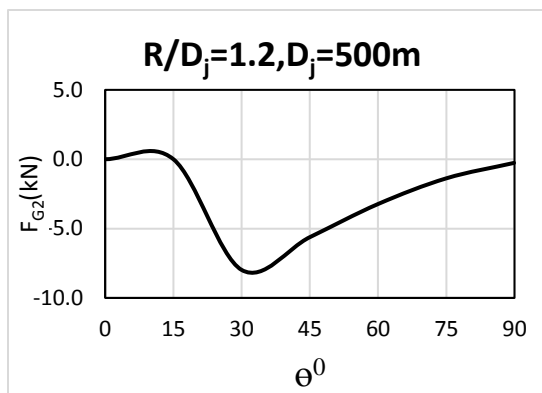that developed under each downburst case.
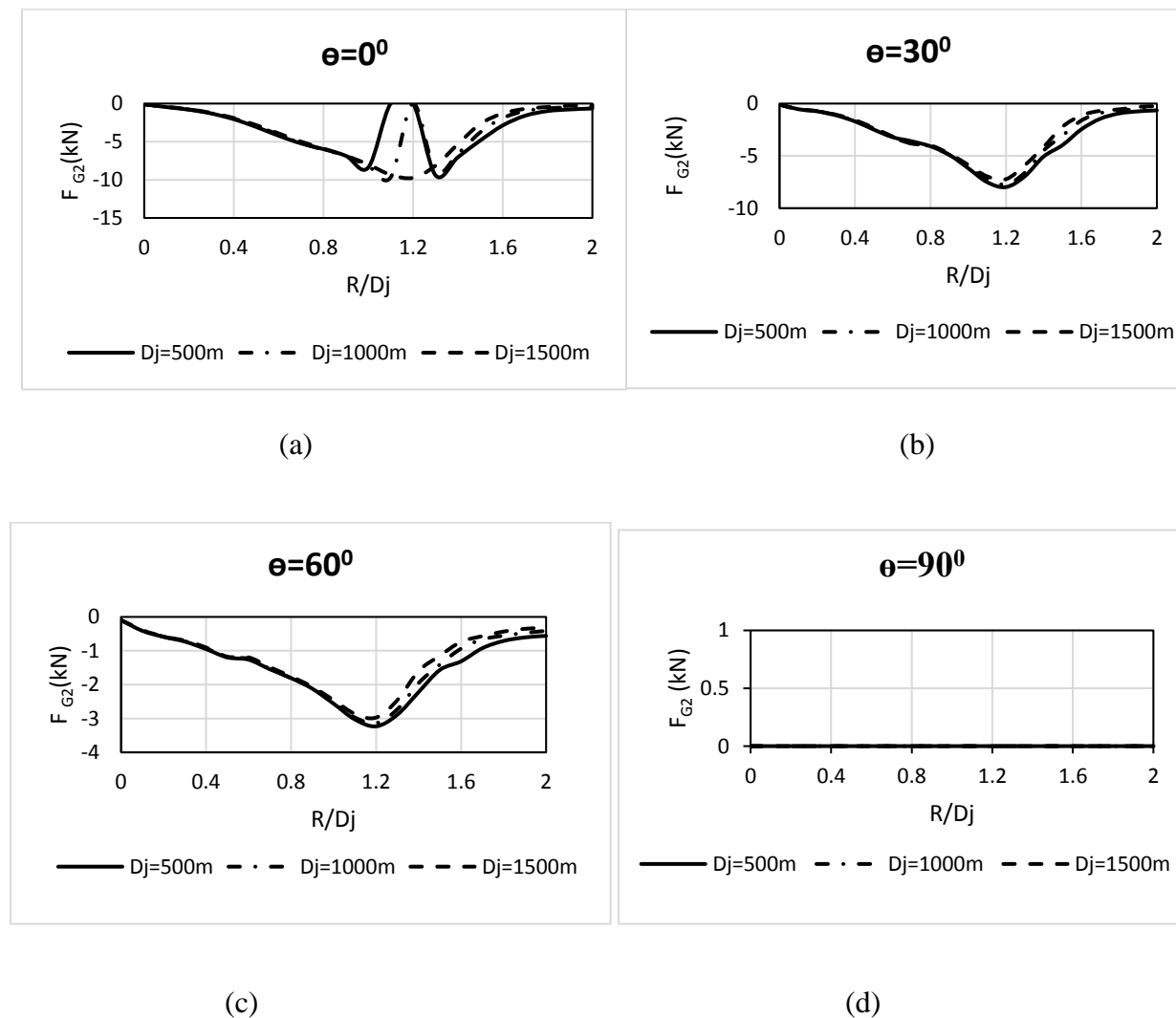
Fig. 4-10. (a-d) Variation of F_{G2} with R/D_j

The figure indicates that the compression force that developed in guy2 increases when the ratio

(R/D_j) approaches 1.2. However, when the compression force in the guy exceeds the pretension

force (10kN), the guy slacks and loses its stiffness. This case is shown in **Fig. 4-10**(a). The

following figures show the variation of the guy2 forces with D_j and θ:
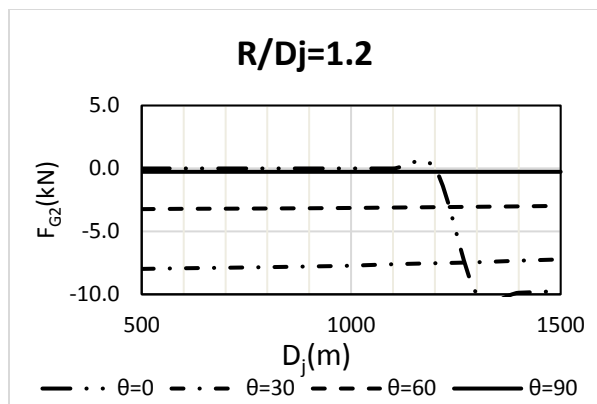
**Fig. 4-11.** Variation of F_{G2} with D_j **Fig. 4-12.** Variation of F_{G2} with θ

As shown in the figures, slacking occurs when the compression force in guy2 exceeds the pretension force (10kN). This occurs in the cases where $\theta=0^0$ and D_j is ranging between 500 and 1200 m. It should be mentioned that at $\theta=90^0$, the forces in guy2 are equal to zero.

As such, the critical downburst load case which cause the maximum tension force to occur in guy1 and the slacking of guy 2 is corresponding to $\theta=0^0$, $D_j=500m$ and $R/D_j=1.2$. At this critical load case, the distribution of the transverse forces on the conductors leads to the maximum conductor resultant horizontal reaction which is totally resisted by the guys. The variation of the conductors longitudinal and transverse reactions (R_c) normalized by the maximum resultant horizontal conductor reaction (R_{cmax}) with θ at $D_j=500m$ and $R/D_j=1.2$ is shown in **Fig. 4-13**.
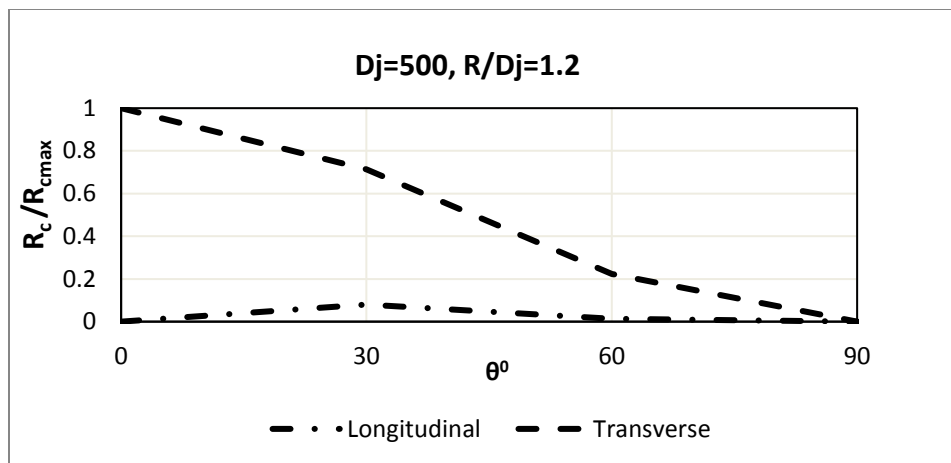
Fig. 4-13. Variation of conductor reactions with θ

The figure indicates that the highest transverse reactions occurs when $\theta=0^0$. It should be noted that the values of the longitudinal reactions are relatively low if compared with the transverse ones. At the case of $\theta=0^0$, $D_j=500m$ and $R/D_j=1.2$, the downburst wind field is fully loading the two spans adjacent to the guyed pole under consideration with an average velocity of $1.07V_j$. This is attributed to the fact that the jet diameter is greater than the sum of the two conductor spans (200 m) adjacent to the considered guyed pole. **Fig. 4-14** shows the distribution of the transverse downburst wind velocities ($V_{transverse}$) at the critical load case along the six conductor spans.
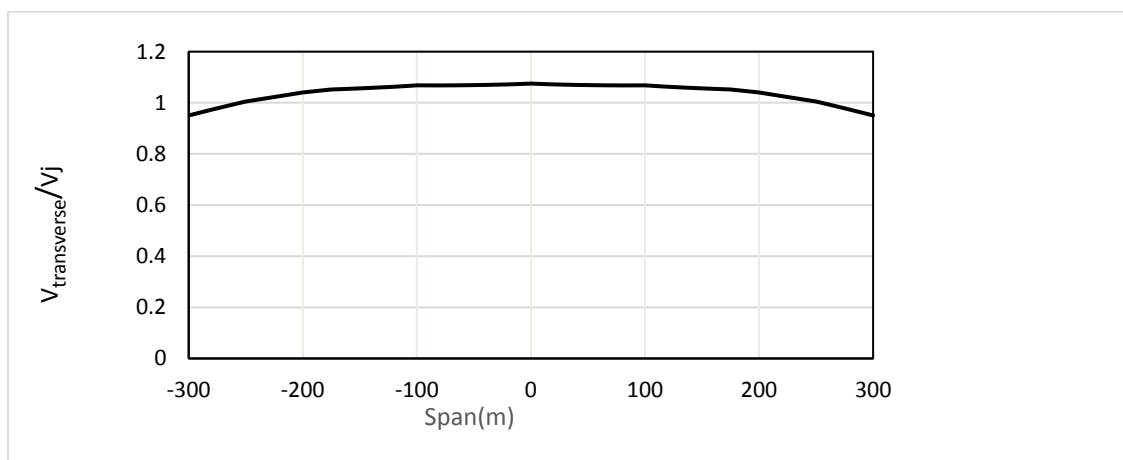
**Fig. 4-14.** Variation of $V_{transverse}$ along the conductor span

The distribution of the radial velocity along the pole height at the critical load case is shown in **Fig. 4-15**. The plots indicate that the downburst velocities along the pole height can reach up to 1.06 V_j.
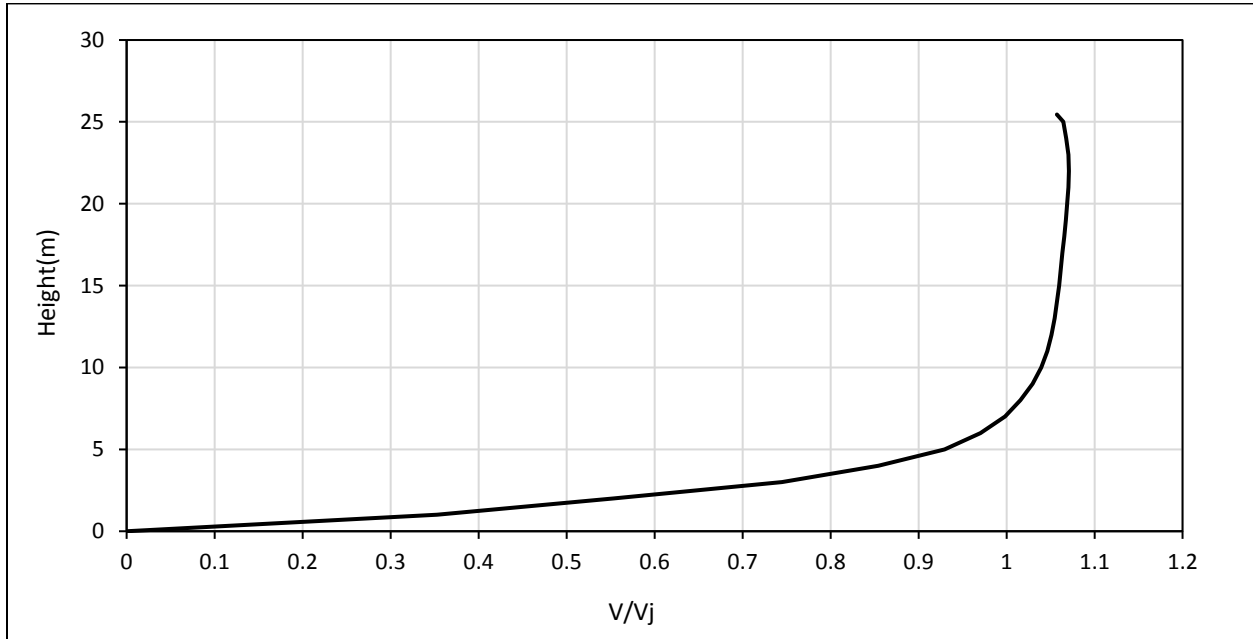
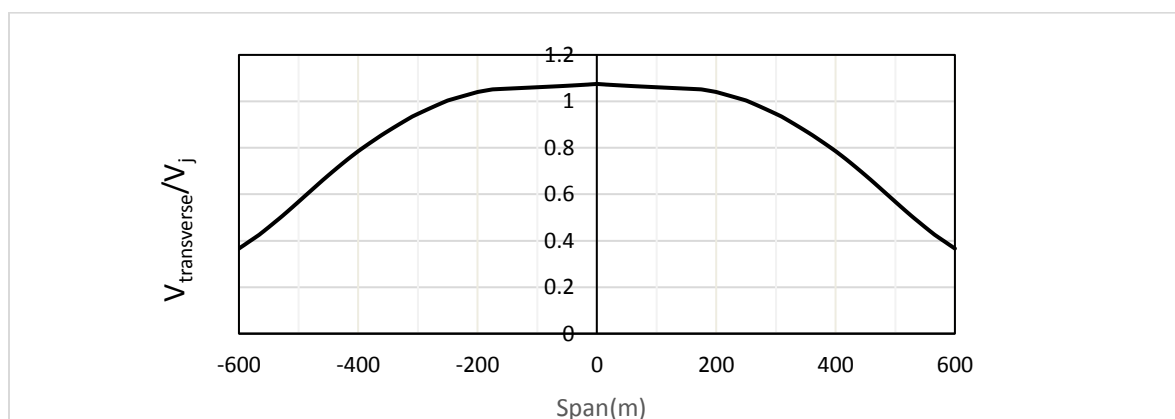**Fig. 4-15.** Downburst velocity distribution along the pole height

4.4.2   Results of the Guyed pole system with conductor span 200m

The figures showing the variation of the concrete pole base moments and guys' forces with the D_j, R/D_j and θ for conductor span of 200m are provided in Appendix A. The critical case which gives the highest base moment on the pole is found to happen at $R/D_j=1.2$, $\theta=90^0$ and $D_j=500$m, while the case which causes maximum tension forces on guy1 corresponds to $R/D_j=1.2$, $\theta=0^0$ and $D_j=500$m. The variation of the conductors longitudinal and transverse reactions (R_c) normalized by the maximum resultant horizontal conductor reaction (R_{cmax}) with θ at $D_j=500$m and $R/D_j=1.2$ is shown in **Fig. 4-16**.

Dj=500, R/Dj=1.2
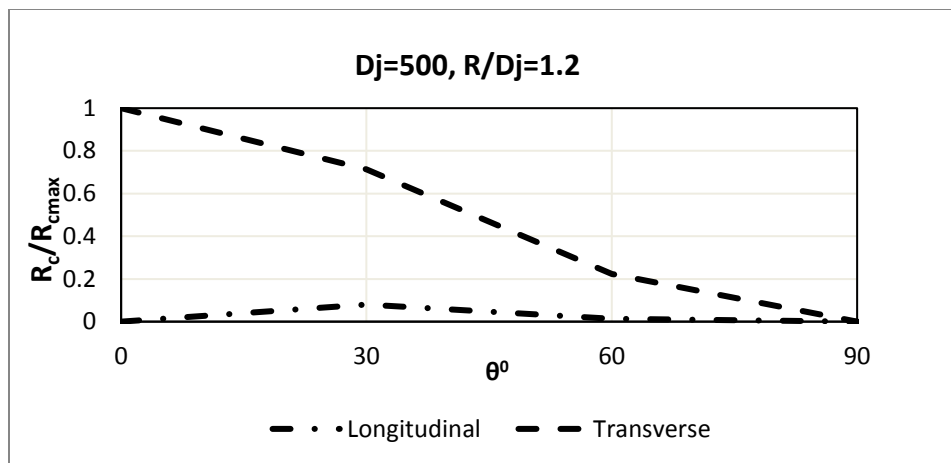
Fig. 4-16. Variation of conductor reactions with θ

In the case of θ=0⁰, D_j=500m and R/D_j=1.2, the downburst wind field is fully loading the two spans adjacent to the guyed pole under consideration with velocity that reaches up to 1.06 V_j. That is attributed to the fact that the jet diameter is greater than the sum of the two conductor spans (400 m) adjacent to the considered guyed pole. **Fig. 4-17** shows the distribution of the transverse downburst wind velocities ($V_{transverse}$) at the critical load case along the six conductor spans.
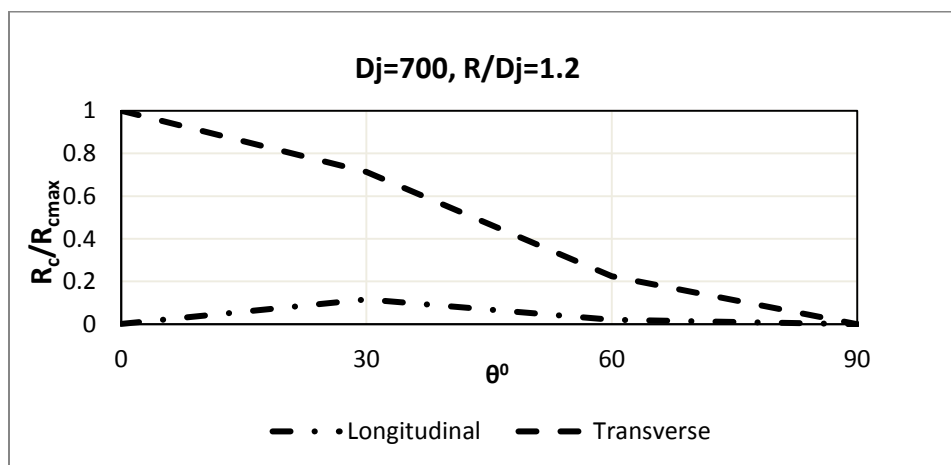

Fig. 4-17. Variation of $V_{transverse}$ along the conductor span

4.4.3   Results of the Guyed pole system with conductor span 300m

The figures illustrating the variation of the concrete pole base moments and guys' forces with the change of D_j, R/D_j and θ for conductor span of 300m are provided in Appendix B.

The critical case which gives the maximum base moment on the pole of a 300 m conductor span is found to be the same as the 100 m and 200 m spans. (i.e. $R/D_j=1.2$, $\theta =90^0$ and $D_j=500$m). As such, it can be concluded that the maximum pole base moments are independent of conductor spans.

For the guys of the 300 m pole system, the case which causes maximum tension forces on guy1 is when $R/D_j=1.2$, $\theta =0^0$ and $D_j=700$m. The variation of the conductors' longitudinal and transverse reactions (R_c) normalized by the maximum resultant horizontal conductor reaction (R_{cmax}) with θ at $D_j=700$m and $R/D_j=1.2$ is shown in the following figure.

Fig. 4-18. Variation of conductor reactions with θ

To explain why the case $D_j=700$ m is more critical that the $D_j=500$ m case for the 300 m span, the transverse velocity distribution of the downburst load case of $D_j=700$m is plotted along the span

of the conductors and compared to the cases D_j=500 m, 600 m, 700 m, 800 m and 900 m, respectively.
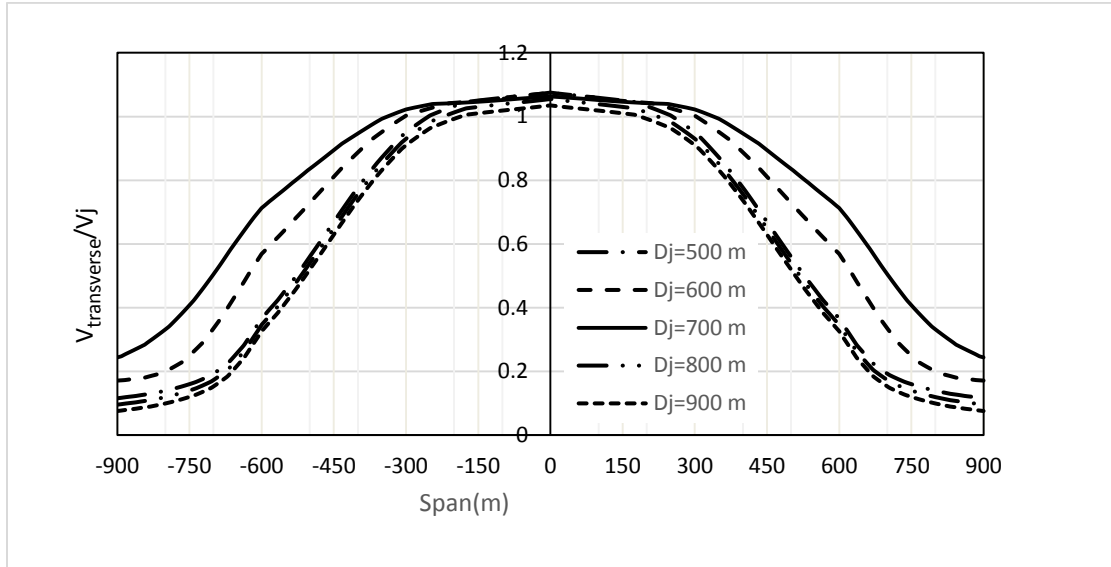
Fig. 4-19. Variation of $V_{transverse}$ along the conductor span

It is obvious from the plots that for the case D_j=700 m, the velocities' magnitudes along the conductor spans is higher than the other cases. This leads to higher conductor reactions and consequently greater guys' forces.

4.5. <u>Comparison between the parametric study results and proposed critical load cases</u>

El Damatty et al. (2013) proposed three critical load cases to simulate the effect of downbursts on transmission line structures. In this section, the three load cases are applied on the three different guyed pre-stressed concrete pole systems. The maximum bending moment ratios (M_a/M_r) and maximum tension forces F_{G1} under the proposed load cases are obtained. Those values are then compared to the corresponding values obtained from the parametric study conducted earlier in this

study. The purpose is to check if the proposed load cases by El Damatty et al. (2013) can be applied while simulating the behaviour of guyed pre-stressed pole structures under downbursts.

The three load cases proposed by El Damatty et al. (2013) are as follows:

Load case 1: ($\theta=0^0$)

In this load case, the pole is loaded with a vertical wind velocity profile of a value of 1.1 V_j in a direction normal to the transmission line, while the two conductors adjacent to the pole of interest are loaded with 0.92 V_j.

Load case 2: ($\theta=90^0$)

In this load case, the pole is loaded with a vertical wind velocity profile of a value of 1.1 V_j in a direction along with the transmission line. The conductors in this load case are unloaded.

Load case 3: ($\theta=30^0$)

In this load case, the pole is loaded with two vertical wind velocity profiles of values of $0.75V_j$ and $0.43V_j$ in directions normal and parallel to the transmission line, respectively, while the conductors are loaded with an unequal and a non-uniform velocity distribution on the spans adjacent to the tower of interest. This unequal loading is used to obtain the transverse conductor reaction. It should be noted that this load case lead to a longitudinal conductor reaction. The estimation of the conductor reactions under this load case is provided in El Damatty et al. (2013).

El Damatty et al. (2013) load cases are applied on the three pole systems and the maximum (M_a/M_r) and F_{G1} values are obtained and compared to the parametric study results in **Figs. 4-20 and 4-21**.
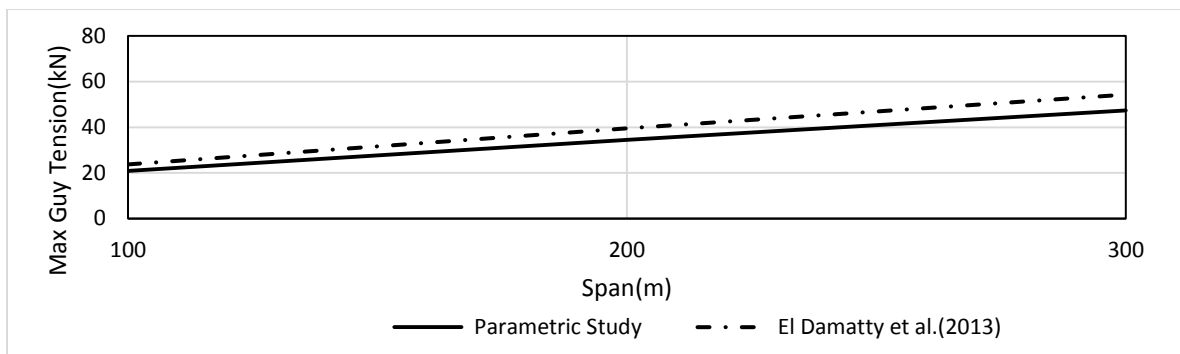
Fig. 4-20. Maximum Guy tension using parametric study and El Damatty et al. (2013) load
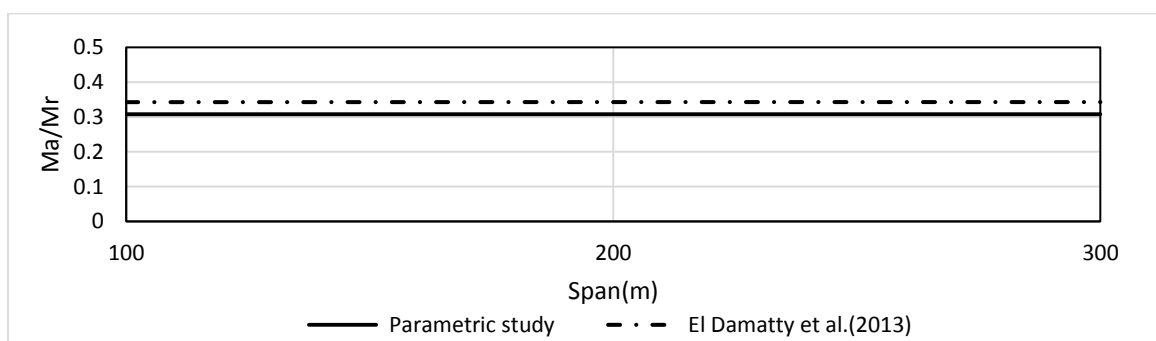
cases

Fig. 4-21. Maximum pole base moment using parametric study and El Damatty et al. (2013)

load cases

The comparison between the parametric study results and the proposed critical load cases shows a

very good agreement. The difference between the maximum bending moments obtained from the

current study and the corresponding ones proposed by El Damatty et al. (2013) is 3%, while the

difference in the peak forces that developed in the guys is ranging between 4 to 6 % based on the

conductor span.   El Damatty et al. (2013) load cases are found to be more conservative in the

estimation of the maximum straining actions on the guyed pole systems. Based on that, the

proposed load cases recommended by El Damatty et al. (2013) can be considered while simulating

the guyed pre-stressed concrete pole systems under downbursts. Instead of performing 924

downburst cases, the peak responses of the guyed pre-stressed concrete transmission poles under downbursts can be evaluated by applying the simple load cases proposed by El Damatty et al. (2013). This will result in a huge saving in the computational time.

4.6. <u>Failure analysis</u>

After determining the critical downbursts configuration, a failure analysis is performed on the considered transmission pre-stressed pole to identify the downburst jet velocity at which the pole and the guys collapses.

Regarding the poles failure analysis, it was mentioned earlier that the critical downburst configuration that affects the maximum bending moments developed in the guyed pole systems is independent of the spans. As such, only the 100 m pole system is considered in the failure analysis of its supporting pre-stressed concrete pole. The ratio (M_a/M_r) under downburst jet velocities varying between 40 and 70 (m/sec) with an increment of 5 (m/sec) is calculated and plotted in **Fig. 4-22**.
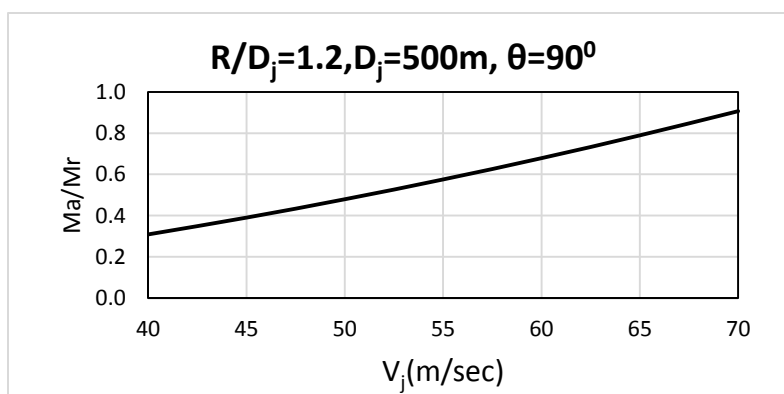

Fig. 4-22. Variation of maximum pole moment with V_j for different conductor spans

It can be noted from the figure that the maximum base moment at the pole does not reach to the ultimate pole capacity. This indicates that the guyed pre-stressed concrete poles which are

designed to remain un-cracked under normal wind speed of 40 m/sec will not fail under downburst jet velocity of 70 m/sec.

The variation of maximum guy tension of the pole with different jet velocities is then plotted for each span in **Fig. 4-23**. The configuration $(R/D_j=1.2, \theta=0^0)$ is used to obtain the maximum guys' forces. D_j for the 100 and 200 m spans is assumed to be 500m while $D_j=700$m for the 300 m span.
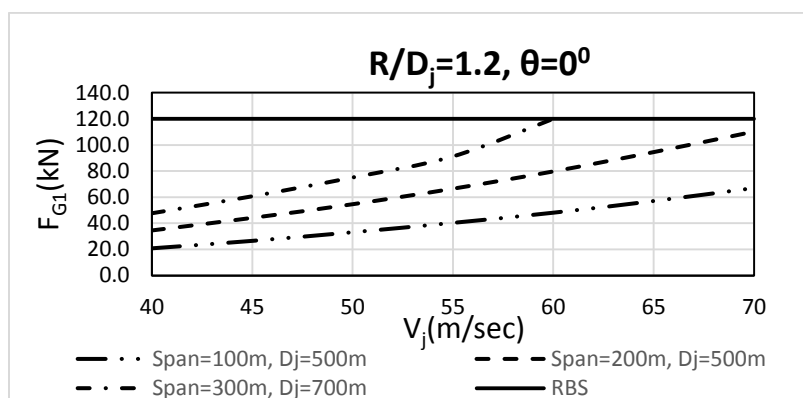
Fig. 4-23. Variation of maximum guy1 force with V_j for different conductor spans

It is found that guy1 reaches the rated breaking strength (120 kN) when the downburst jet velocity V_j exceeds 60 (m/sec) for span 300m. However, in spans 100 m and 200 m, guy1 does not reach the rated breaking strength.

4.7. Conclusions

In the current study, a numerical technique is utilized combining the following: 1) CFD model to simulate downbursts wind fields, 2) a semi-closed form solution that is capable of determining the conductor reactions under such localized high intensity wind events, and 3) a non-linear finite element model for the guyed pre-stressed concrete pole structures that can predict the internal forces of such types of poles under downbursts. The main conclusions drawn from this study can be summarized in the following points:

1- The critical downburst configuration which leads to the maximum pole base moment is $\theta=90^0$, $D_j=500$m and R/$D_j=1.2$.

2- The critical downburst configuration which leads to the maximum pole base moment is independent of the conductor spans.

3- The critical downburst configuration which leads to the maximum guys forces is when $\theta=0^0$, $D_j=500$m and R/$D_j=1.2$ for spans ranging from 100 to 200 m and when $\theta=0^0$, $D_j=700$m and R/$D_j=1.2$ for a span of 300m.

4- The guyed pre-stressed concrete pole systems designed to remain un-cracked under normal wind speed of 40 m/sec do not collapse when their spans are ranging between 100 m and 200 m. However, the guys reach the rated breaking strength in the guyed concrete pole system that carries 300 m conductor spans when the jet speed exceeds 60 m/sec.

5- The previously developed load cases are found to be conservative and can be used in the design and analysis of guyed pre-stressed concrete pole transmission lines under downbursts.

4.8.   <u>References</u>

Aboshosha, H., and El Damatty, A.A., (2014), "Effective technique for the reactions of transmission line conductors under high intensity winds", Wind and Structures. 18(3), 235-252.

American Society of Civil Engineers (ASCE), (2010) "Guidelines for electrical transmission line structural loading", ASCE manuals and reports on engineering practice, No. 74, New York, NY, USA.

American Society of Civil Engineers (ASCE), (1997) "Design of guyed electrical transmission structures", ASCE Manuals and Reports on Engineering Practice, vol. 91, New York, NY, USA.

American Society of Civil Engineers (ASCE), (2012) "Prestressed Concrete Transmission Pole Structures", ASCE manuals and reports on engineering practice, No. 123, Reston, VA, USA.

Australian Standard/New Zealand Standard (AS/NZS) 7000, (2010) "Overhead line design detailed procedures", Standards Australia Limited/Standards New Zealand, North Sydney, Australia.

Australian Wind Alliance, (2016): http://www.windalliance.org.au/

Choi E.C.C., (2004), "Field measurement and experimental study of wind speed profile during thunderstorms", J. Wind Eng. Ind. Aerodyn., 92, 275-290.

Darwish, M., El Damatty A.A., and Hangan, H., (2010), "Dynamic characteristics of transmission line conductors and behaviour under turbulent downburst loading", Wind and Structures 13(4), 327-346.

Darwish, M., and El Damatty, A.A., (2011), "Behavior of self-supported transmission line towers under stationary downburst loading", Wind and Structures 14(5), 481-4.

El Damatty, A.A., Hamada, A., Elawady, A. (2013), "Development of Critical Load Cases Simulating the Effect of Downbursts and Tornados on Transmission Line Structures", proceedings of the Eighth Asia-Pacific Conference on Wind Engineering, Chennai, India.

Fujita, T., (1985), "The downburst: microburst and macroburst", SMRP Research Paper 210, University of Chicago, USA.

Fujita, T., (1990), "Downbursts: meteorological features and wind field characteristics", Journal of Wind Engineering and Industrial Aerodynamics 36, 75–86.

Gast, K.D., Schroeder, J.L., (2003). "Supercell rear-flank downdraft as sampled in the 2002 thunderstorm outflow experiment", Proceedings of the 11th International Conference on Wind Engineering. ICWEIA, 2233–2240.

Hangan, H., Roberts, D., Xu, Z., and Kim, J., (2003), "Downburst simulation. Experimental and numerical challenges", Proceedings of the 11th International Conference on Wind Engineering, Lubbock, TX, USA.

Holmes, J., Hangan, H., Schroeder, J., Letchford, C., Orwig, K., (2008), "A forensic study of the Lubbock-Reese downdraft of 2002", Wind Structures 11 (2), 137–152.

Ibrahim, A.M. and El Damatty, A.A., (2014), "Behaviour of Prestressed Concrete Poles under Downburst Loading", Proceeding of ASCE conference, Hamilton, ON, Canada.

Ibrahim, A.M., El Damatty, A. A. and Elansary A.M., (2017), "Finite element modelling of pre-stressed concrete poles under downbursts and tornadoes". Journal of Engineering Structures. 153, 370-382.

Ladubec, C., El Damatty, A.A., and El Ansary, A., (2012), "Effect of geometric nonlinear behaviour of a guyed transmission tower under downburst loading", Proceedings of the International Conference on Vibration, Structural Engineering and Measurement, Shanghai, China, Trans. Tech. Publications, 1240-1249.

Li C. Q. (2000), "A stochastic model of severe thunderstorms for transmission line design", Probab. Eng. Mech. 15, 359-364.

McCarthy, P., and Melsness, M., (1996), "Severe weather elements associated with September 5, 1996 hydro tower failures near Grosse".

Shehata, A., El Damatty, A.A., and Savory, E., (2005), "Finite element modeling of transmission line under downburst wind loading", Finite Elements in Analysis and Design 42(1), 71-89.

Shehata, A., and El Damatty, A.A., (2007), "Behaviour of guyed transmission line structures under downburst wind loading", Wind and Structures International Journal 10(3), 249-268

Wang, X., Lou, W., Li, H., and Chen, Y., (2009), "Wind-induced dynamic response of high-rise transmission tower under downburst wind load", Journal of Zhejiang University 43(8), 1520-1525.

Wolfson, M., DiStefano, J., Fujita, T., (1985), "Low-altitude wind shear characteristics in the Memphis, TN area", Proceedings of the 14th conference on severe local storms, American Meteorological Society, Indianapolis, IN, USA., 322–7.

Yang F., and Zhang H., (2016), "Two case studies on structural analysis of transmission towers under downburst", Wind and Structures, Vol. 22, No. 6, 685-701.

Zhang, Y., (2006), "Status quo of wind hazard prevention for transmission lines and countermeasures", East China Electric Power 34(3), 28-31.

4.9. <u>Appendix A</u>

Results of the guyed pole with conductor spans of 200m

4.9.1 Pole bending moment

(a)

(b)

(c)

(d)
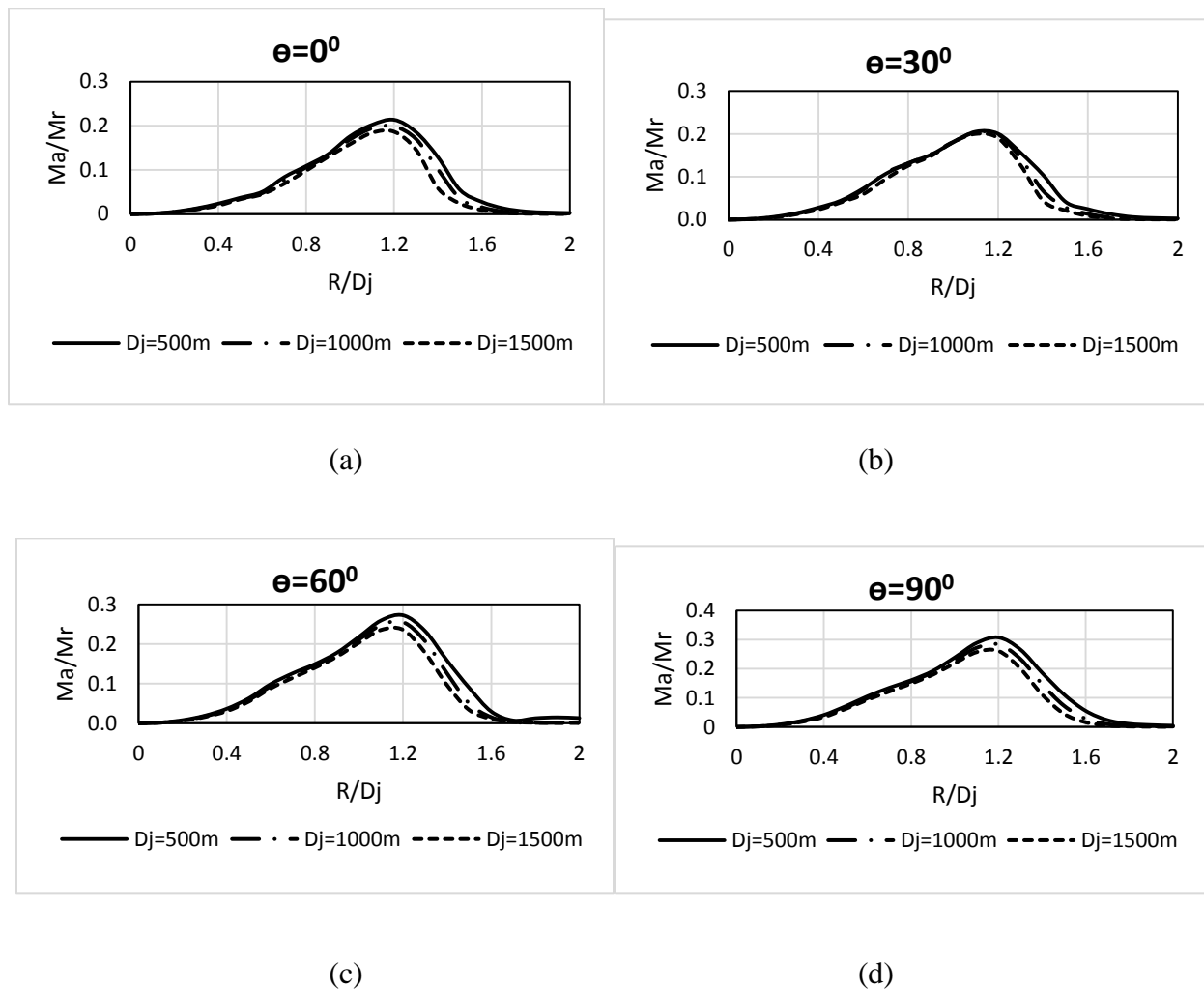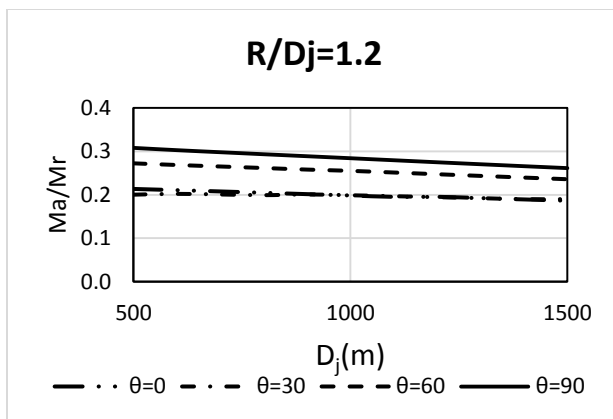
Fig. 4-24. (a-d) Variation of (M_a/M_r) with R/D_j

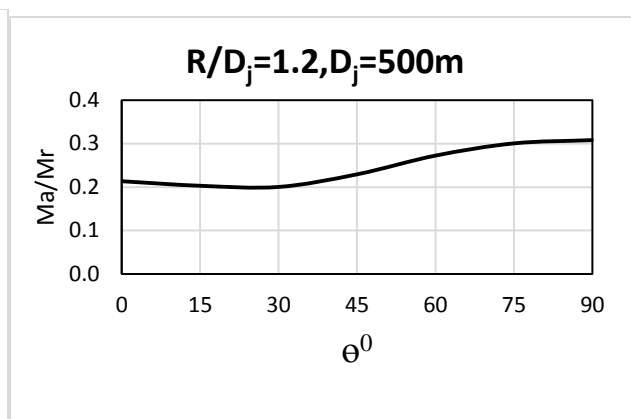**Fig. 4-25.** Variation of (M_a/M_r) with Dj   **Fig. 4-26.** Variation of (M_a/M_r) with θ

4.9.2 Guy1 forces

(a)

(b)

(c)

(d)

Fig. 4-27. (a-d) Variation of F_{G1} with R/D_j
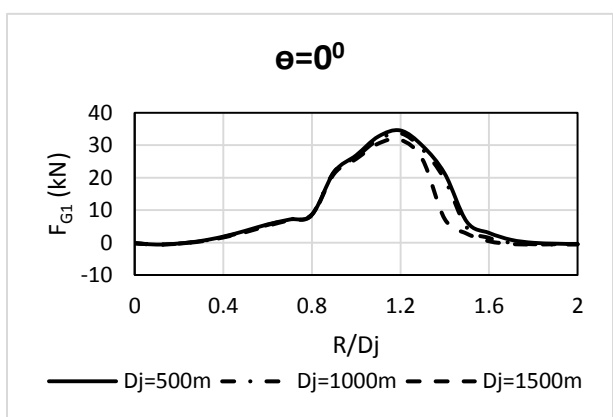
Fig. 4-28. Variation of F_{G1} with D_j

Fig. 4-29. Variation of F_{G1} with θ

4.9.3 Guy2 forces

(a)

(b)

(c)

(d)

Fig. 4-30. (a-d) Variation of F_{G2} with R/D_j

Fig. 4-31. Variation of F_{G2} with D_j **Fig. 4-32.** Variation of F_{G2} with θ

4.10. <u>Appendix B</u>

<u>Results of the guyed pole with conductor spans of 300m</u>

4.10.1 Pole bending moment

(a)   (b)

(c)   (d)
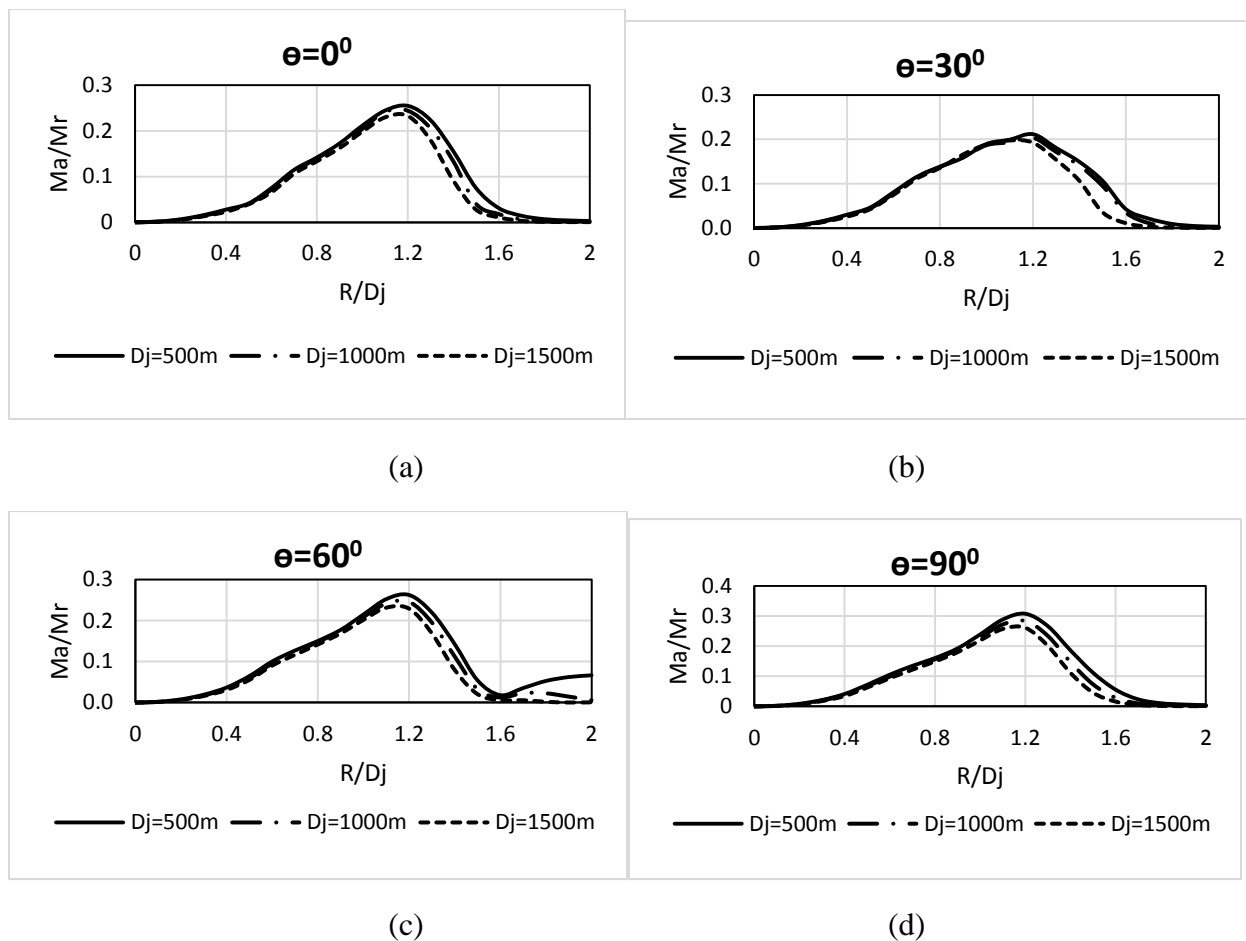
Fig. 4-33. (a-d) Variation of (M_a/M_r) with R/D
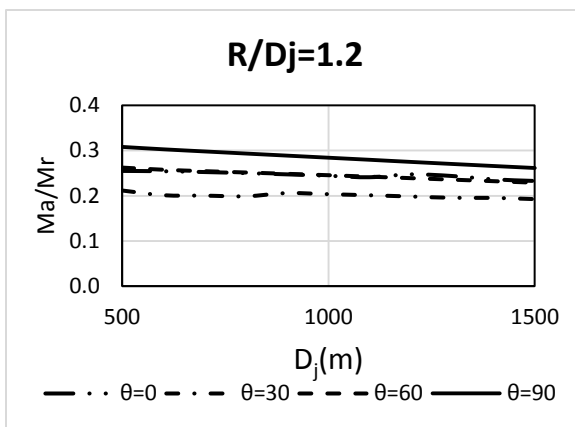
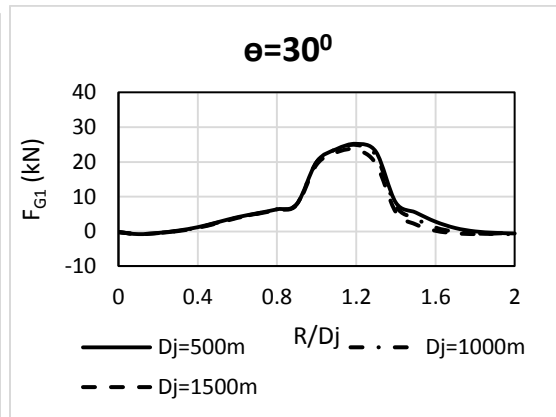**Fig. 4-34.** Variation of (M_a/M_r) with Dj
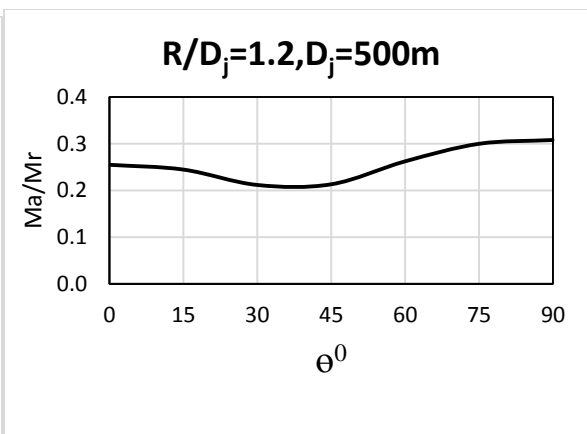
Fig. 4-35. Variation of (M_a/M_r) with θ
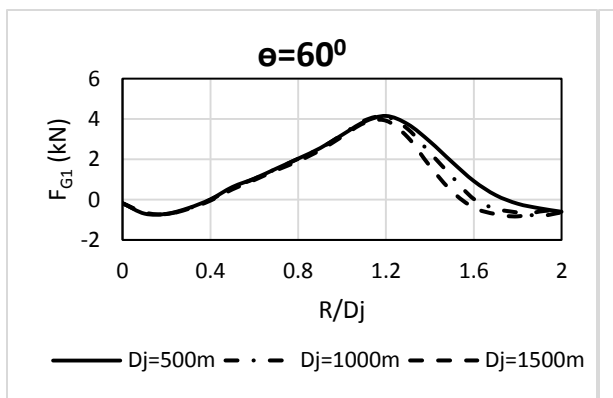
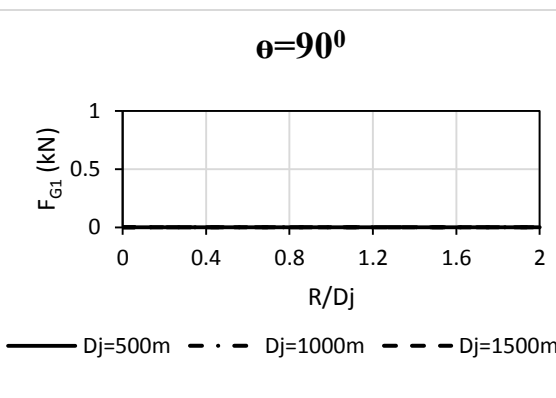### 4.10.2 Guy1 forces
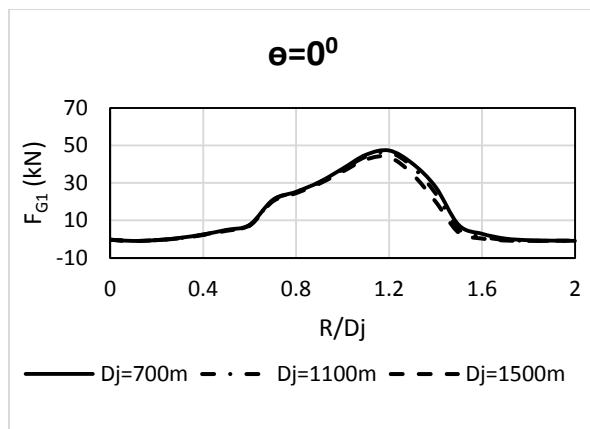
(a)
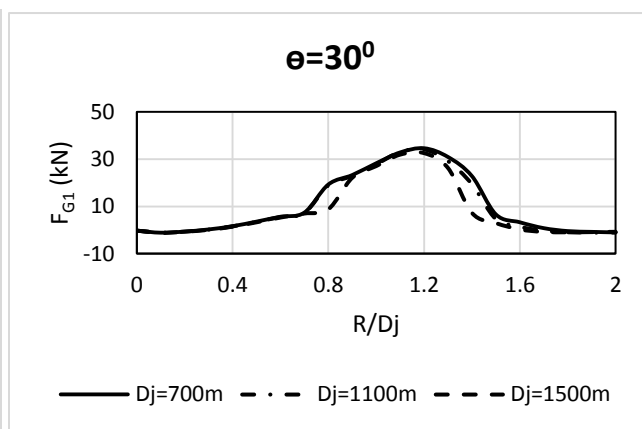
(b)

(c)
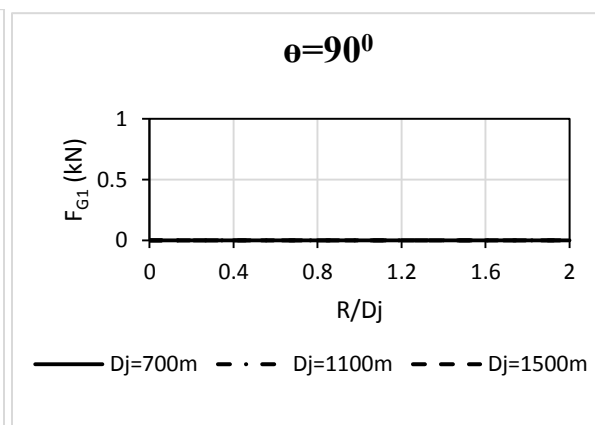
(d)

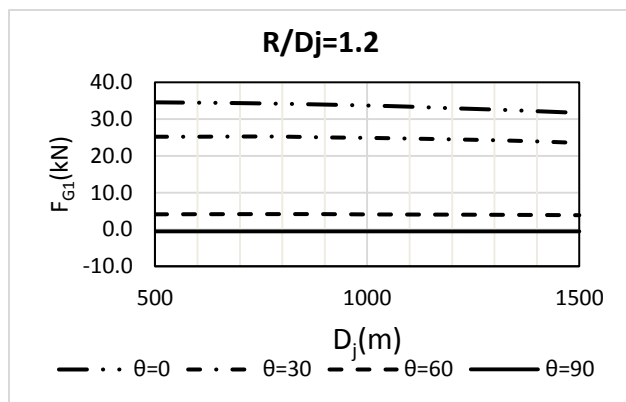**Fig. 4-36.** (a-d) Variation of F_{G1} with R/D_j
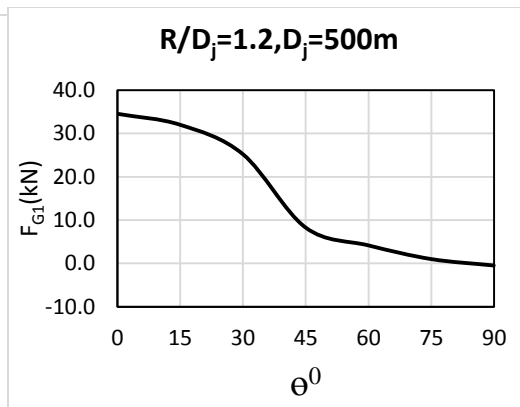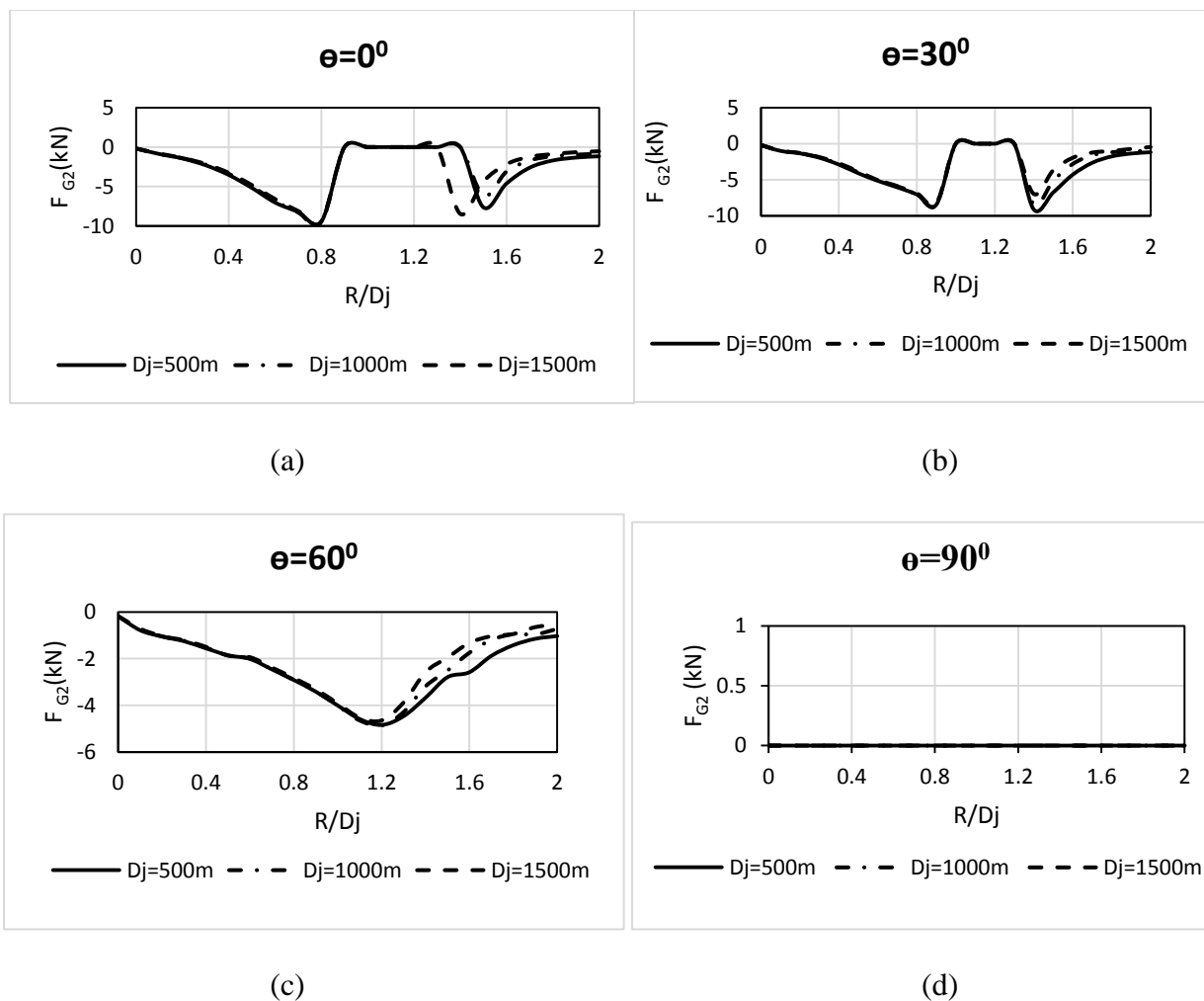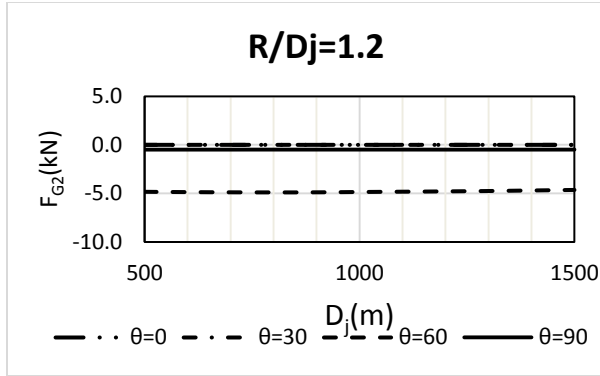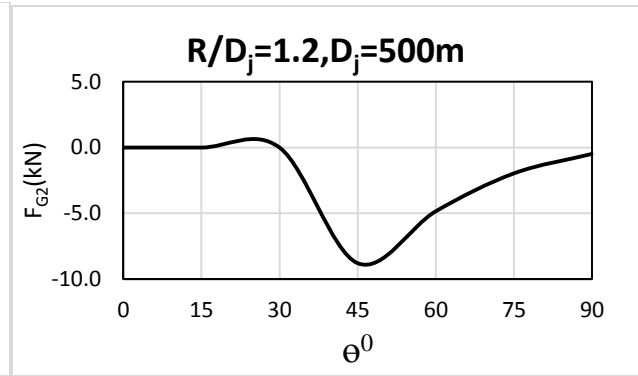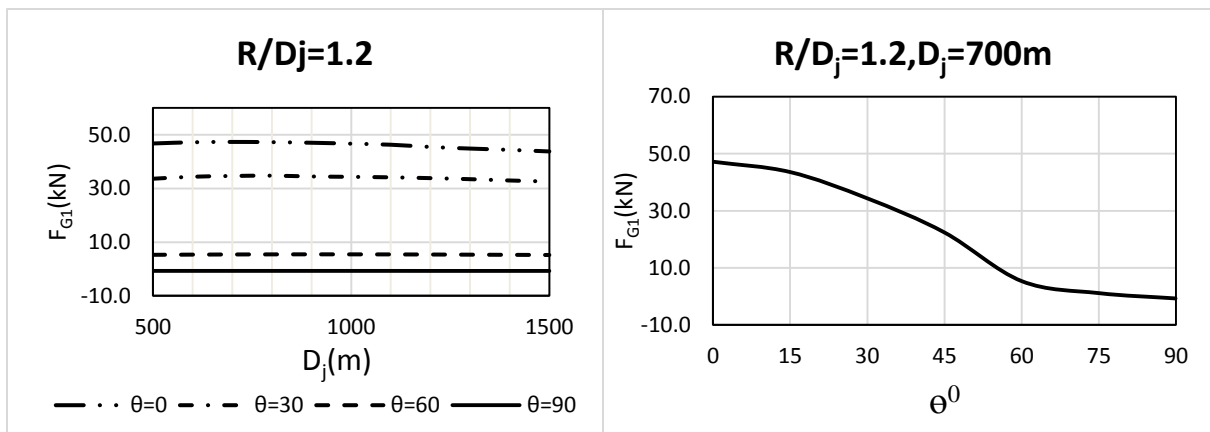
Fig. 4-37. Variation of F_{G1} with D_j

Fig. 4-38. Variation of F_{G1} with θ

4.10.3 Guy2 forces

(a)

(b)

(c)

(d)
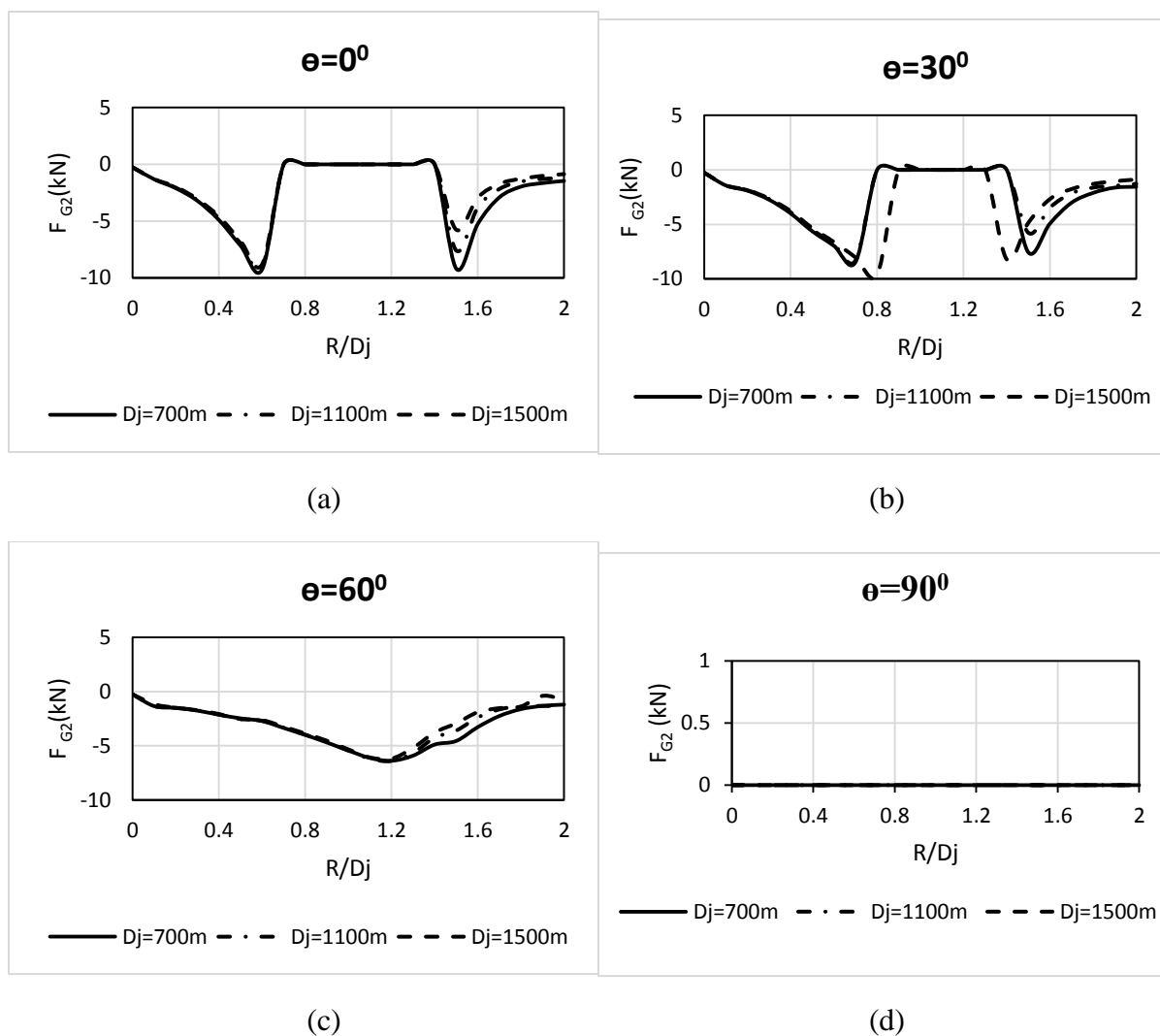
Fig. 4-39. (a-d) Variation of F_{G2} with R/D_j
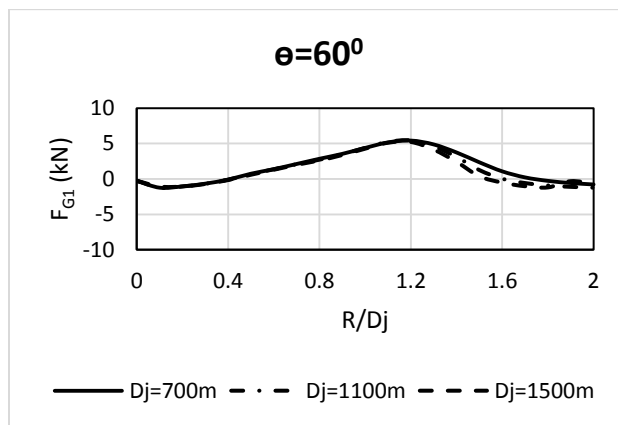
R/Dj=1.2

R/D$_j$=1.2,D$_j$=700m
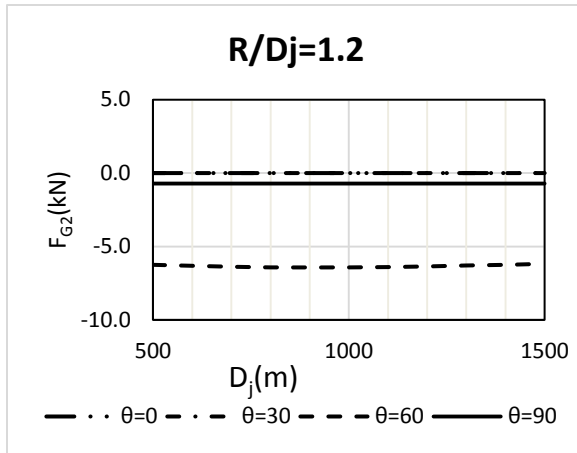
Fig. 4-40. Variation of F$_{G2}$ with D$_j$
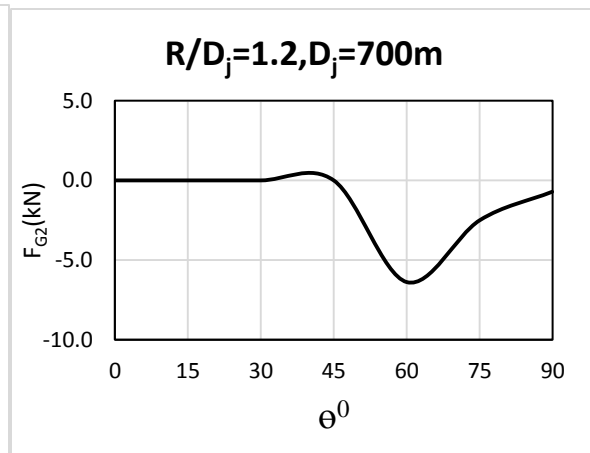
Fig. 4-41. Variation of F$_{G2}$ with θ

CHAPTER 5

BEHAVIOUR, DESIGN AND NON-LINEAR FAILURE ANALYSIS OF GUYED PRE-STRESSED CONCRETE POLES UNDER TORNADOES

5.1. <u>Introduction</u>

Tornado wind events represent a major threat on the continuous supply of electricity around the globe. In 2011, NOAA (National Climatic Data Center) reported that 1718 tornadoes were the cause of a total loss of $25 billion in the United States. A large number of failures of transmission line structures (TLs) were reported in the past few decades. Those failures were attributed to high intensity wind (HIW) events which could be in the form of tornadoes or downbursts.

Tornadoes are defined by Fujita (1981) as rotating wind vortices with high wind speeds affecting relatively narrow paths. Fujita and Pearson (1973) classified tornadoes according to their intensity and size. The major specific characteristic of tornadoes is its local high intensity wind speed. The complexity of identifying the tornado loads on a transmission line system comes from the fact that the forces acting on the conductors, ground wires and the supporting tower vary according to the relative location of the tornado event with respect to the system.

As reported by Ishac and White (1994), South Western Ontario exhibits the highest rates of tornadoes among all the populated areas in Canada. Those tornadoes were the reason of most of transmission line failures in this area. Five out of six weather related failures of transmission towers that belong to Ontario Hydro company were due to tornadoes as reported by Behncke and White (2006). CIGRE (2006) mentioned that 65 % of weather-related transmission lines' failures were due to tornadoes. In 2007, a number of pre-stressed concrete transmission poles failed during a high wind storm in Kitchener, Canada, (Kuebler, 2008). The failures were attributed to the

excessive forces acting on the conductors. Li (2000) reported that 90 % of transmission line structures' failures were caused by HIW events. In China, in 2005, 18 transmission towers carrying 500 kV lines and another 60 towers carrying 110 kV lines collapsed due to strong wind events such as tornadoes, downbursts and typhoons (Zhang 2006). Despite the previously mentioned failures, the design codes and practices such as ASCE 74 (2010) and CIGRE (2009) have provided limited information on considering the tornado loads in designing transmission line structures.

The previously reported failures in addition to the lack of design provisions triggered a research group at Western University, Canada to study the effect of tornado wind events on transmission line structures. Savory et al. (2001) investigated the failure of self-supported transmission line structures under tornadoes. Shehata et al. (2005) developed and validated the first finite element model to simulate the behavior of a guyed transmission line system under downburst loadings. This model was extended by Hamada et al. (2010) to be capable of investigating the behavior of transmission line structures under tornadoes. The behavior of guyed transmission lines under tornadoes was studied by Hamada and El Damatty (2011) and (2013). Altalmas et. al (2012) studied the progressive failure of a self-supported and a guyed transmission line structures under tornadoes. Transmission line conductors' response under HIW including downbursts and tornadoes was investigated by Aboshosha and El Damatty (2014). Aboshosha and El Damatty (2014) developed a numerical technique to investigate the behavior of transmission line conductors under tornado and downburst loading taking into account the non-linear behavior of the conductors including sagging, pre-tensioning forces and insulator's stiffness.

El Damatty et al. (2013) summarized the major findings of the attempts made in literature during the past decade to study the effect of tornadoes on lattice steel transmission line structures. Hamada and El Damatty (2016) proposed a number of simplified critical tornado load cases to be

considered in the design and analysis of lattice steel transmission line structures under tornadoes. In each load case, the velocity profile along the towers' height and the conductors' spans were provided. Those simplified load cases managed to obtain the maximum responses of a number of lattice steel transmission towers under a large number of possible tornado load configurations.

It should be noted that transmission line systems can be supported by lattice towers or pole-type structures. Only few studies have assessed the behavior of self-supported pre-stressed concrete pole structures under tornadoes. Ibrahim and El Damatty (2016) performed a sensitivity analysis on a self-supported pre-stressed concrete pole under a number of F2 tornado load cases. Ibrahim et al. (2017) developed and validated a non-linear finite element model to assess the behavior of pre-stressed concrete pole systems under downbursts and tornadoes.

An extensive parametric study was performed by Ibrahim et al. (2017) by changing the tornado locations with respect to a self-supported pre-stressed concrete pole system. This led to identifying the critical tornado configurations which maximize the bending moments developed in the pole. In addition to that, a failure analysis is conducted to identify the maximum tornado wind speed which the pole can sustain. The same procedures were done for downburst loadings and a comparison between the tornado and downburst critical load cases was made. It was found that the self-supported pre-stressed concrete pole system -that was designed based on ASCE 74 (2010) and ASCE 123 (2012) provisions to remain un-cracked under normal wind loading of 40 m/sec- will fail if subjected to a critical downburst configuration of a jet speed up higher than 65 m/sec. However, this self-supported system can withstand F2 tornado wind loads without experiencing collapse.

According to their structural system, pre-stressed concrete poles can be in the form of self-supported, guyed or H-framed poles. The forces that develop in the guys decrease the overturning bending moments in the pole systems. In the current study, the non-linear finite element model developed by Ibrahim et al. (2017) is utilized to analyze a number of guyed pre-stressed concrete poles under tornadoes. Based on the fact that, the majority of tornadoes' intensities are equal to or less than F2 (ASCE 2010 and CIGRE 2009), the current study only considers the effect of F2 tornadoes on pre-stressed concrete transmission poles.

In this study, three guyed pre-stressed concrete pole systems with different spans are designed to remain un-cracked under normal synoptic wind loading of 40 m/sec based on the provisions of ASCE 74 (2010) and ASCE 123 (2012). A parametric study is conducted on the three systems to identify the critical F2 tornado configurations which will lead to the maximum bending moments on the poles and forces on the guys. After identifying the critical load cases, a failure analysis is then conducted to identify the maximum F2 tornado wind speed (V_{f2max}) that the pole systems can sustain without collapse. Finally, a comparison is made between the tornado load cases that was developed by Hamada and El Damatty (2016) and the critical tornado load configurations obtained from this study. The main purpose of the comparison is to check whether if the load cases proposed by Hamada and El Damatty (2016) can be applied on the pre-stressed pole systems or they are limited to the application to lattice steel tower systems.

The work conducted in this study is presented as follows. In the next section, the formulation of the numerical model is described including the simulated tornado wind field, the conductors' anaylsis under tornadoes and the finite element model for guyed pre-stressed concrete poles. Section 5.3, provides details on the guyed pre-stressed concrete transmission poles considered in the study. This is followed by conducting an extensive parametric study in section 5.4 to determine

the critical tornado configurations which lead to the maximum straining actions on the three guyed pole systems. In section 5.5, non-linear analyses are conducted to determine the F2 tornado velocities that the three guyed pole systems are able to sustain before full collapse. In section 5.6, a description of the critical tornado load cases proposed by Hamada and El Damatty (2016) is presented. The envelope of the proposed load cases is compared to the maximum straining actions obtained in the current study. The conclusions drawn from the current study are presented in section 5.7.

5.2. Numerical model

A numerical model is developed to study the behavior of guyed pre-stressed concrete poles under tornadoes. This model consists of three main components. Firstly, the tornado wind field is simulated using Hangan and Kim (2008) computational fluid dynamics (CFD) model. Secondly, the non-linear behavior of the conductors is predicted using the model developed by Aboshosha and El Damatty (2014). This model is a semi-analytical model which accounts for the effects of the conductors' pretension forces, sagging and insulator's stiffness. Finally, the non-linear behavior of the pre-stressed concrete pole systems are simulated using the finite element model that was developed by Ibrahim et al. (2017). The following figure illustrates the components of the numerical model incorporated in this study.

(1) Tornado CFD model Hangan and Kim (2008)	→	(2) Conductors' reactions Aboshosha and El Damatty (2014)	→	(3) Pre-stressed concrete poles model Ibrahim et al. (2017)
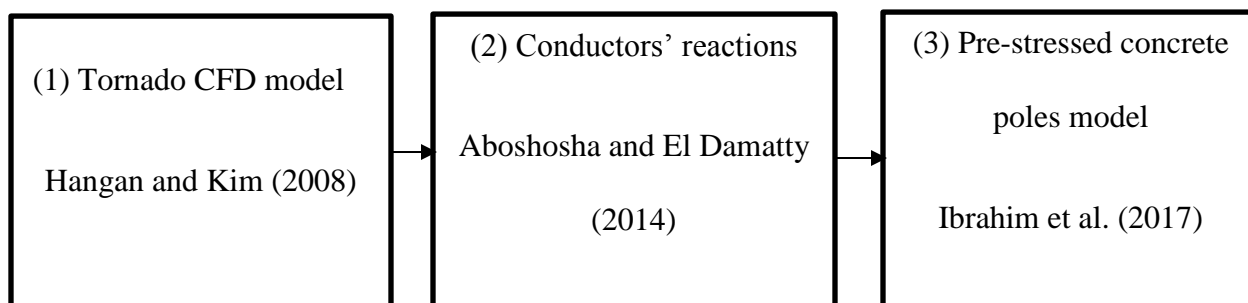
Fig. 5-1. Numerical model components

5.2.1. Tornado wind field

Field measurements of tornadoes are hard to be performed. The intensity and scale of tornadoes cannot be measured by traditional recording stations in the field. Therefore, the simulation of tornado events relies mainly on numerical modeling.

Hangan and Kim (2008) conducted a three dimensional computational fluid dynamics (CFD) simulation for the wind field associated with tornadoes. The velocity field was conducted at a steady state manner. Therefore, the velocity profile does not vary with time. Hangan and kim (2008) validated their CFD model by comparing the velocity field results with Baker (1981), Wurman (1998) and Sarkar et al. (2005).

Tornado wind field consists mainly of three mean velocity components; radial V_{mr}, tangential V_{mt} and vertical V_{mv} velocities. The location of the tornado wind field with respect to a transmission tower has a great influence on the tornado loading experienced by the tower and is defined by the two polar parameters (R) and (θ), as shown in **Fig. 5-2**.
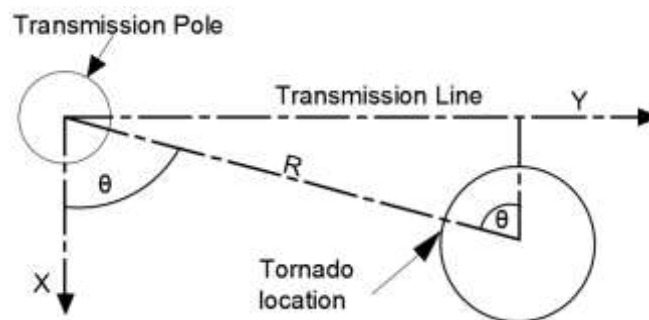
Fig. 5-2. Tornado Parameters

According to ASCE No.74 guidelines (2010), the wind forces acting on a nodal point are given by the following equation:

$$F_{wi} = \frac{1}{2}\rho_a \, G C_f \, A(Z_v \, V_i)^2 \qquad\qquad \text{Equation (5-1)}$$

Where F_{wi} is the force developed in i direction, ρ_a is the density of air = 1.225 (Kg/m³), G is the gust factor and C_f is the drag force coefficient, A is the nodal projected area perpendicular to i direction, Z_v is the terrain factor and V_i is the tornado velocity in i direction (units m/sec).

For conductors and circular concrete poles, the value of the drag coefficient is taken equal to 1.0 according to ASCE No. 74 guidelines (2010), and the same value is recommended for gust and terrain factors.

To show the variation of the pre-stressed pole base moment with the location of the tornado wind event with respect to the pole system, five F2 tornado configurations with V_{f2max} of 50 m/sec are applied to a pre-stressed concrete system with a pole height of 25.5 m and a conductor span of 100 m. The conductor is attached at an elevation of 23m. The pole base moment is calculated in each tornado case. **Table 5-1** shows the values of the pole base moments corresponding to each tornado configuration.

Table 5-1 Variation of pole base moment with tornado locations

Tornado configuration	R (m)	θ^0	Pole base moment (kN.m)
1	216	0	89.72
2	108	15	170.56
3	132	45	173.16
4	72	75	227.65
5	120	90	271.60

It can be concluded from the table that the location of the tornado wind event with respect to the transmission line system can seriously affect the values of straining actions that develop in the system.

5.2.2. Modeling of conductors

Conductors' reactions are predicted using the analytical technique developed by Aboshosha and El Damatty (2014). This technique accounts for the variation of the loads along the conductor spans, insulators flexibility and the non-linear behaviour of the conductors including sagging and pre-tensioning forces. This technique is based on applying compatibility of displacements and equilibrium of forces on the conductors using a semi-closed form solution that determines the displacement and reactions of the conductor under HIW events. Aboshosha and El Damatty (2014) has proven that this semi-closed form numerical technique is more efficient compared to finite element method in terms of computational time.

5.2.3. Modeling of guyed pre-stressed concrete poles

5.2.3.1. Modeling of the pre-stressed concrete poles

The non-linear finite element model developed and validated by Ibrahim et al. (2017) is utilized to simulate the pre-stressed concrete poles behaviour. Frame elements are used to model the pre-stressed concrete poles. The finite element model accounts for the non-linear behavior of pre-stressed concrete poles, the cracking and non-linear behavior of concrete, tension stiffening, in addition to the long term effects such as creep, shrinkage and relaxation.

5.2.3.2. Modeling of the guys

The guys are modelled using three non-linear dimensional frame elements with two nodes and six degrees of freedom per each node (three translational and three rotational). The stiffness of the

guys depend on the applied pre-tensioning force. The guys can carry tension forces up to their rated breaking strength (RBS) as assigned by ASCE 91(1997). While in compression, if the guys force exceeds the pre-tensioning force, they are assumed to slack.

5.3. <u>Description of the considered guyed pre-stressed concrete pole systems</u>

Three transmission guyed pole systems with different conductor spans are considered in this study. The three systems are designed to remain un-cracked under a synoptic wind speed of 40 m/sec based on the ASCE 123 (2012) and ASCE 74 (2010) guidelines. The three guyed pole systems have the following common geometric and material properties:

<u>Poles' properties:</u>

- Unsupported height of poles of 25.5 m.

- The outer diameters in the tip and the bottom are 281 and 459 mm, respectively.

- The inside diameters of the poles vary from 143 mm at the top to 321 mm at the bottom.

- Cross arms' length of 2.4 m supporting two conductors.

- Concrete with compressive strength of 75.8 MPa

<u>Pre-stressing strands' properties:</u>

- Pre-tensioned with 20M10 low relaxation pre-stressing strands.

<u>Conductors' properties:</u>

- Conductors having a projected area of 0.096 m^2, weight per unit length of 30 N/m, sag value of 2% relative to the span while the insulators' length is 2.5 m.

 Guys' properties:

- Two guys perpendicular to the conductors' line are used to support the pole.

-The guys' angle of inclination with the ground is 60^0.

-The guys' diameters are 12 mm.

-A single layer of 7-wire strands are used in the guys with a pre-tensioning force of 10 kN.

-The guys are of grade 1300 (CSA-G12).

-According to the ASCE-91 (1997), the guys' rated breaking strength (RBS) is 120 kN.

- The guys attachment points to the poles are at a height of 23m similar to the conductors'

attachment points to the insulators.

The three systems differ in terms of conductor spans. The conductor spans used are 100 m, 200 m

and 300 m, respectively. **Fig. 5-3** shows the layout of the guyed transmission pole systems.
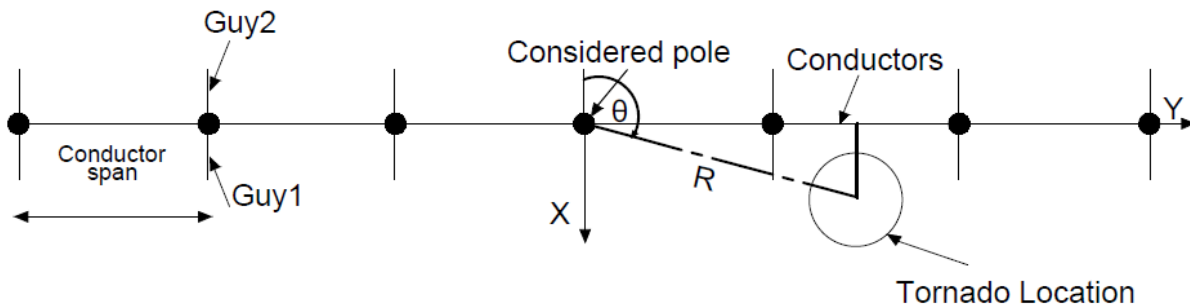
Fig. 5-3. Guyed pole systems (Plan View)

5.3.1. Response of guyed poles to tornadoes

To understand the behaviour of the guyed poles under tornadoes, **Fig. 5-4** is presented to help the

reader to understand this behaviour under in-plane and out of plane tornado loads.
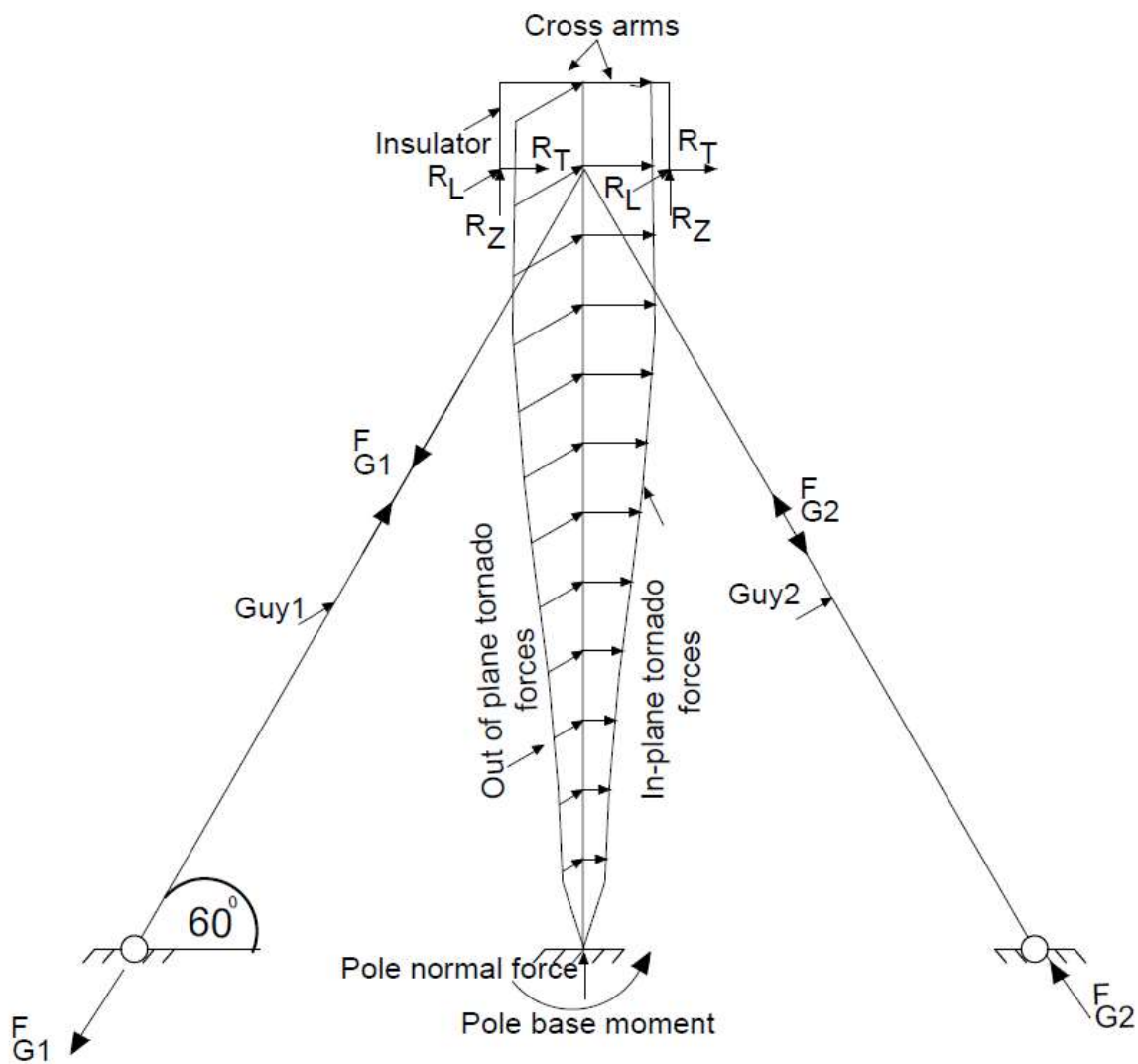
Fig. 5-4. Schematic diagram showing the guyed poles analysis under a tornado

In this figure, R_T is the transverse conductor reaction, R_L is the longitudinal conductor reaction, R_Z is the vertical conductor reaction, F_{G1} is the force developing in guy1 and F_{G2} is the force developing in guy2.

The tornado loads acting on a guyed pre-stressed concrete transmission pole system due to radial, tangential and vertical velocity wind fields are resolved into: (1) horizontal and vertical loads acting on the conductors and (2) horizontal and vertical loads acting on the pole.

As mentioned above, the guys' orientation is perpendicular to the direction of the transmission line conductors. In addition to that, the guys of the three pole systems are attached to the poles at the same height where the conductors are attached to the insulators. As such, the guys act as the support of the conductors and the transverse conductors' reactions are fully transferred to the guys.

It should be noted that the guys only resist the component of the applied loads acting in the direction along their axes. Based on that, the conductors' longitudinal reactions are only resisted by the pole. The guys do not contribute in the resistance of these reactions.

The tornado loads acting on the pole are resolved into two horizontal components and one vertical component. The first horizontal component is in the direction perpendicular on the transmission line conductors (i.e. along with the guys' axes direction), while the second horizontal component is in a direction along with the transmission lines direction (i.e. normal to the guys' axes direction) and the vertical component is in the direction of the pole axis. The first horizontal component is resisted by the pole and the guys based on the relative stiffness between them. Meanwhile the second horizontal component is only resisted by the pole which acts as a cantilever structure in this case. The third component develops a normal force (tension or compression) on the pole.

It should be noted that if the compression force evaluated in guy1 or guy2 due to the in-plane tornado forces on the poles in addition to the conductors' transverse reactions exceeds the value of the pre-tensioning force (i.e. 10 kN), the guy will slack. In this case, only the other guy which is subjected to tension together with the pole will support the guyed pole system.

5.4. <u>Tornado parametric study</u>

The three guyed transmission poles designed to remain un-cracked under normal wind loads corresponding to the cracking wind speed of 40 m/sec are considered for the tornado analysis. In this section, a parametric study is conducted on three different guyed pre-stressed concrete pole systems. A total number of 312 F2 tornado load configurations with a maximum tornado speed (V_{f2max}) of 50 m/sec are applied to the three systems. The objective is to determine the configurations that lead to maximum bending moment, tension and compression forces on each of the three poles and the guys, respectively.

The tornado configuration is defined by the geometric parameters (R and θ) as shown in **Fig. 5-2**. In the parametric study, the radial distance R is assumed to be varying from 12 m to 288 m with an increment of 12 m, while the angle (θ) is varied between 0^0 and 180^0 with an increment of 15^0. The overturning moment (M_a) normalized by the pole ultimate capacity (M_r) at the pole base is determined for each configuration. The tension and compression forces in the guys are identified as well. In addition to that, the tornado velocities distributions across the conductors' spans and the poles' height are presented for the critical load cases.

5.4.1. Results of the Guyed pole with conductor span 100m

5.4.1.1.   *Pole base moment*

The results of the parametric study are presented in **Fig. 5-5** (a-c). Each figure corresponds to a specific values of "θ" and shows the variation of the ratio (M_a/M_r) with R.

(a)   (b)   (c)
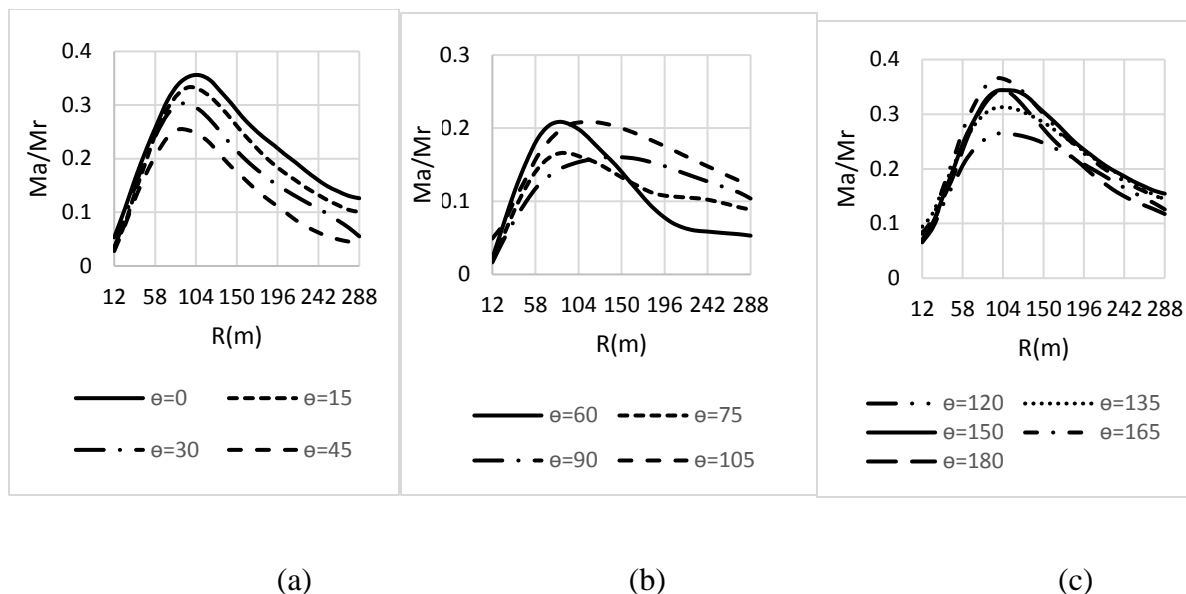
Fig. 5-5. (a-c) Variation of Ma/Mr with R

All the plots show a similar trend involving an increase of (M_a/M_r) with R up to a certain value of R and then a decrease beyond this value. The critical values of (R) which gives the highest (M_a/M_r) values vary between 70 m and 120 m depending on the angle (θ). The results indicate that the absolute maximum value for the ratio (M_a/M_r) occurs at R=96 m and $\theta=165^0$. As such, the variation of (M_a/M_r) with (θ) at R= 96 m is plotted in **Fig. 5-6**, which indicates that the maximum value occurs at $\theta=165^0$.
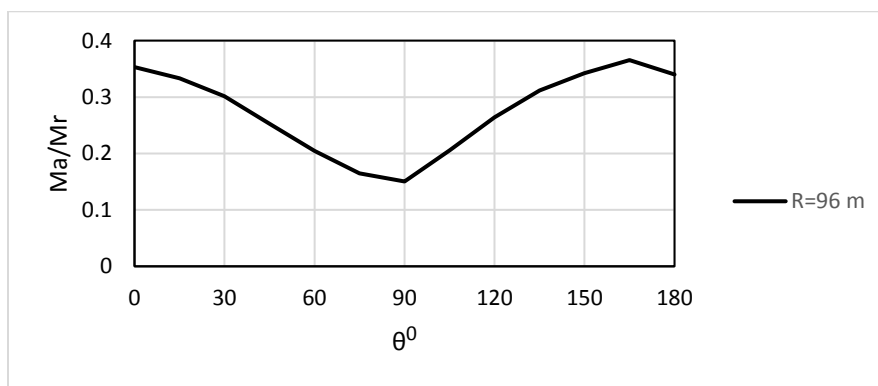
Fig. 5-6. Variation of Ma/Mr with θ

It can be noticed from the previous figures that the bending moment at the pole base in most of the cases decreases with the increase of θ until θ reaches 90^0 and then it increases.

The large variations in the responses of the guyed pole system to F2 tornado configurations is attributed to the complexity and interference of many parameters such as the loading transferred to the pole and the conductors as well as the highly non-linear behavior of pre-stressed concrete poles, guys and conductors.

5.4.1.2. Forces in guy1

The following figure show the distribution of guy1 tension and compression forces (F_{G1}) that develops under each tornado case.

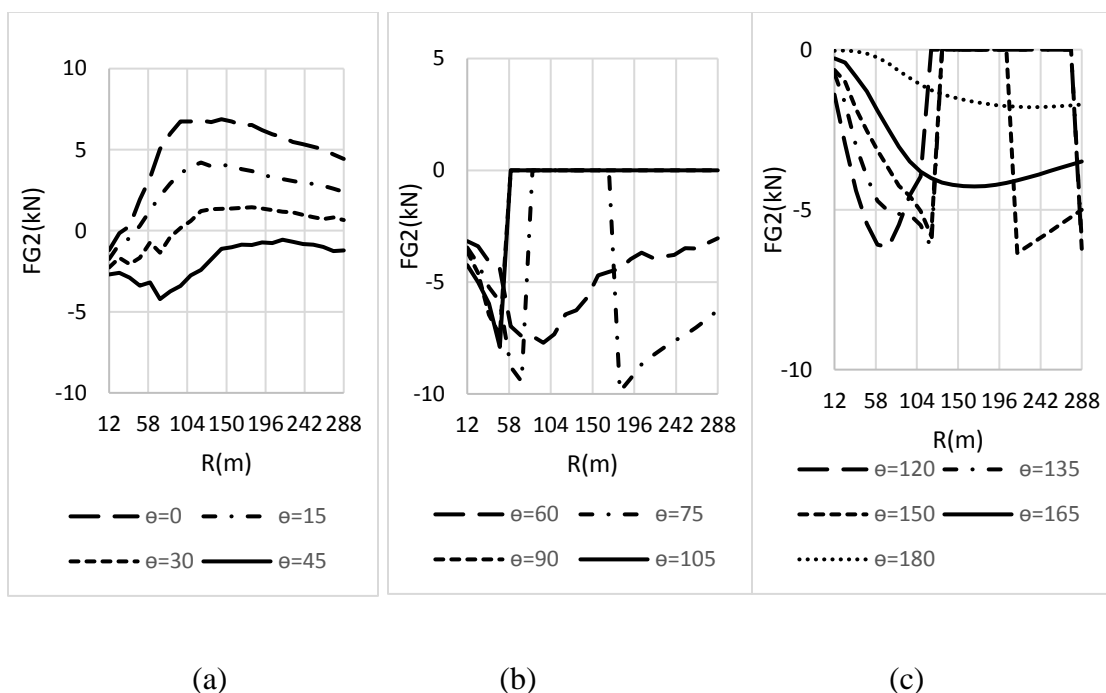(a)   (b)   (c)
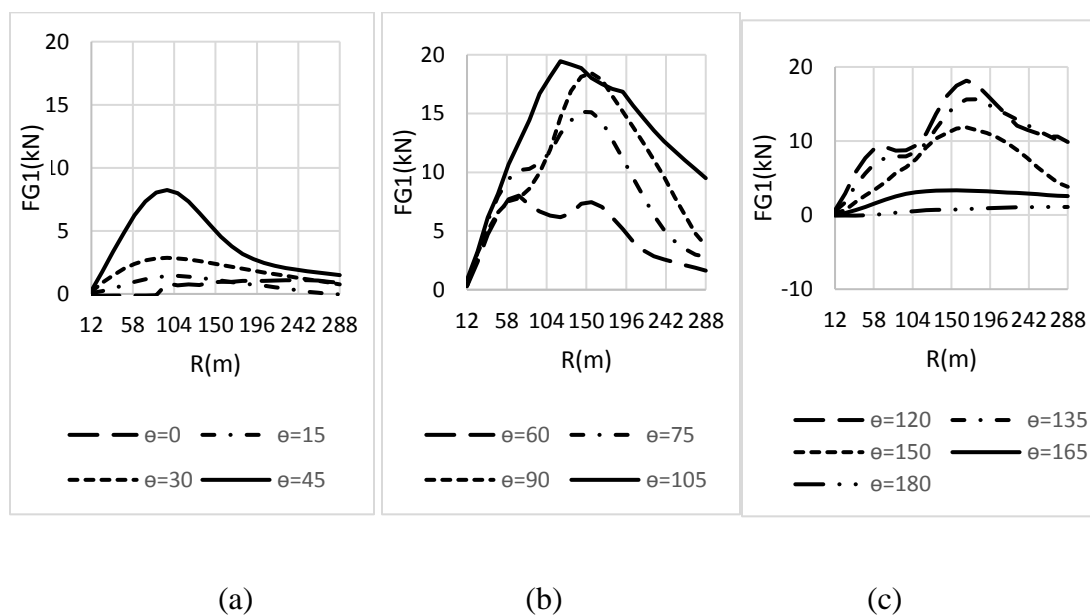
Fig. 5-7. (a-c) Variation of Guy 1 forces with R

As shown in the previous figures, the forces on guy1 are tension forces in most of the cases. The critical case which gives the maximum tension forces occurs when R=120 m and θ =105 ^{0}. The sudden increase in the tension forces in some cases is attributed to the slacking of guy2. When

guy2 slacks, it loses its axial stiffness and the forces are resisted by the pole and guy1 instead of being shared by guy1, guy2 and the pole. This results in a slight increase in the bending moment acting on the pole base in those cases.

5.4.1.3.   Forces in guy2

Fig. 5-8Figs. 5-8 (a-c) show the distribution of the guy2 tension and compression forces (F_{G2}) developed under each tornado case.

(a)   (b)   (c)

Fig. 5-8. (a-c) Variation of Guy 2 forces with R

As shown in the previous figures, the forces on guy2 are compression forces in all of the cases. The slacking occurs when the compression force in guy2 exceeds the pretension force (10kN).

By applying 312 F2 tornado cases on a 100 m guyed pre-stressed transmission concrete pole structure, it can be concluded that the critical case which gives the maximum base moment on the pole corresponds to R=96m and $\theta=165^0$. Also the case at which guy1 is subjected to maximum

tension forces occurs when R=120 m and θ=105 ^{0}. **Figs. 5-9 and 5-10 (a-b)** illustrate the distribution of the transverse and vertical tornado velocity components along the conductor spans as well as the resolved velocity components in X and Y directions along the pole height (normalized by 50 m/sec which is the F2 tornado speed included in the parametric study) in the two main critical cases.
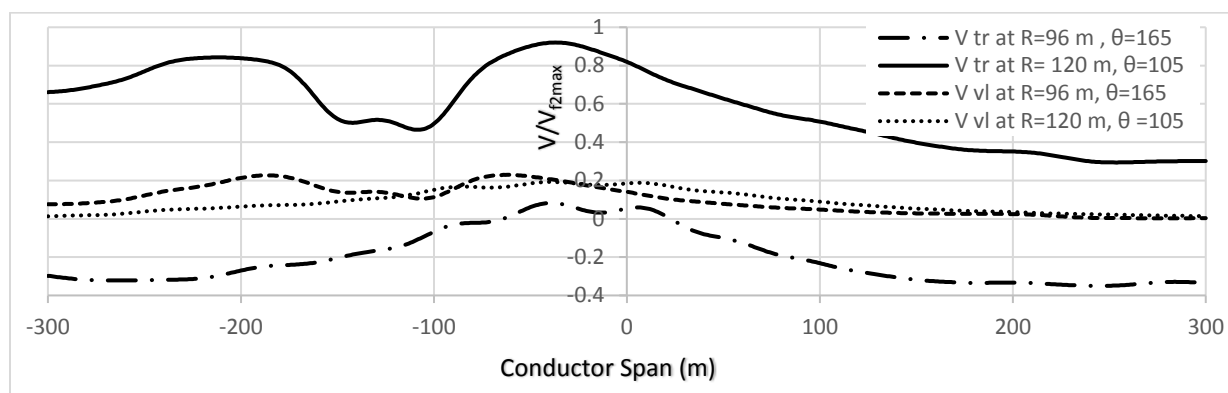
Fig. 5-9. Tornado velocity distribution on the conductors
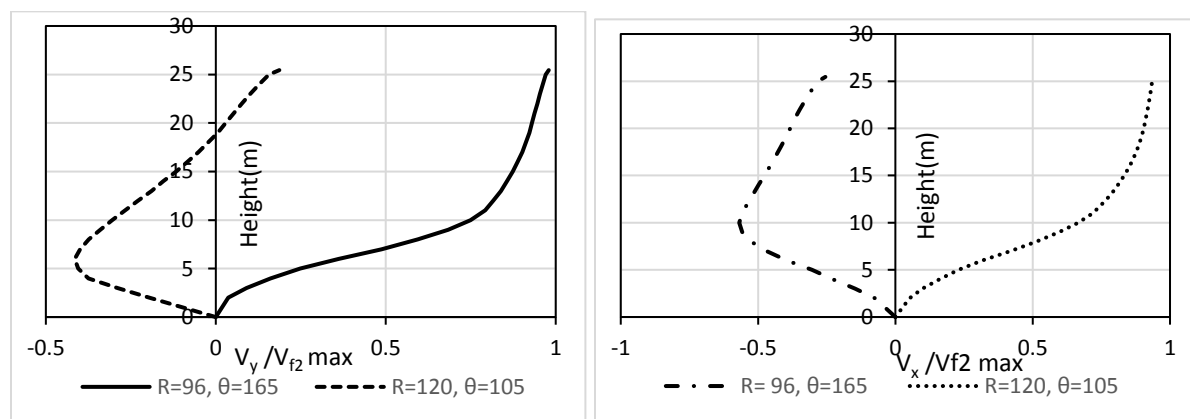
(a)   (b)

Fig. 5-10. (a, b) Tornado velocity distribution on the pole

As shown from **Fig. 5-9**, the distribution of the transverse velocity -along the two conductor spans adjacent to the considered pole- in the case of R= 120m and θ=105 ^{0} results in the largest transverse conductors' reactions. As such, the guys are subjected to the maximum tension forces in this case.

Given that, the pole acts as a cantilever in resisting V_y while the guy and the pole act together to resist V_x, the case of R= 96 m and θ=165^0 with the velocity distribution in Y-direction shown in **Fig. 5-10** (a) leads to the maximum bending moments on the pole.

5.4.2. Results of the Guyed pole with conductor span 200m

The figures illustrating the variation of the concrete pole base moments and guys' forces with the change of R and θ for conductor span of 200 m are provided in Appendix A.

It is found that the critical case which gives the highest base moment on the pole occurs when R=96m and θ=165^0 while the case which causes maximum tension forces on guy1 corresponds to R=120m and θ=105^0. The critical velocity field distribution along the pole height is the same as **Fig. 5-10** while the transverse and vertical velocities' distributions along the conductor spans for both cases are illustrated in **Fig. 5-11**.
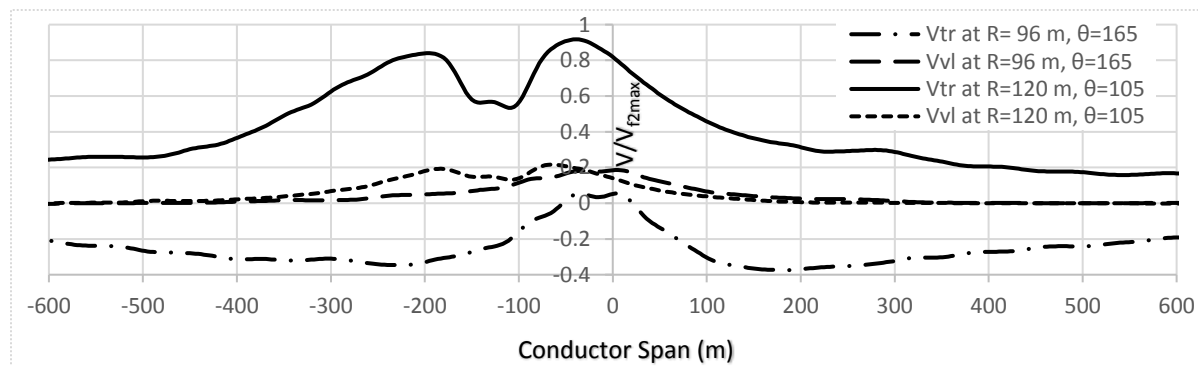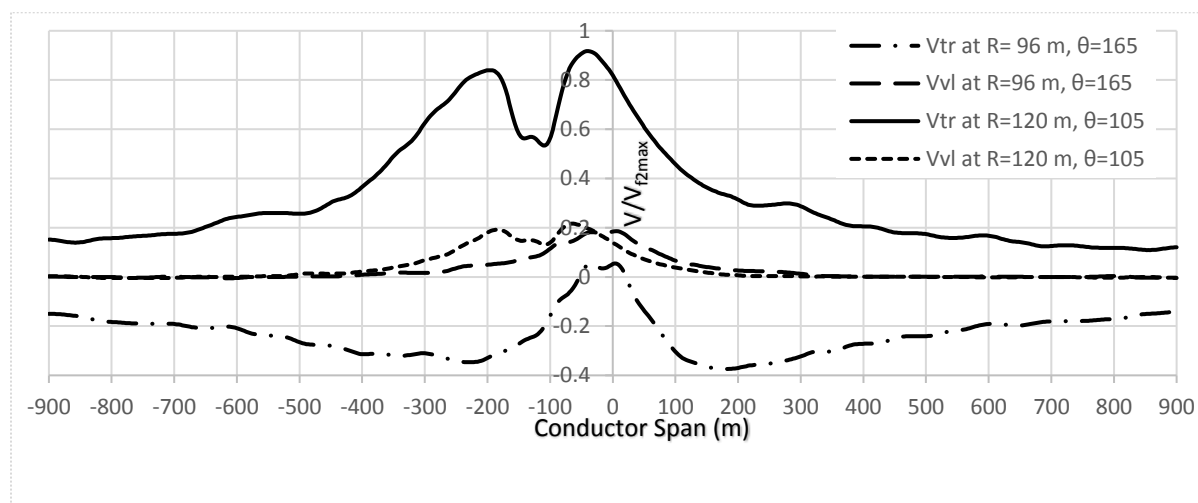

Fig. 5-11. Tornado velocity distribution on the conductors

It can be noted from **Fig. 5-11** that the conductors exhibit larger transverse velocity component due to the tornado configuration R=120 m and θ=105^0 compared to the case R=96 m and θ=165^0. This results in larger conductor reactions and consequently larger guy forces at R=120 m and θ=105^0. As such, this configuration is considered the critical tornado load configuration which leads to the largest tension forces in the guys.

5.4.3. Results of the Guyed pole with conductor span 300m

The figures illustrating the variation of the concrete pole base moments and guys' forces with the change of R and θ for conductor span of 300m are provided in Appendix B.

The critical case which gives the highest base moment on the pole is found to be corresponding to R=96 m, and θ=165^0, while the case which causes maximum tension forces on guy1 happens when R=120 m and θ=105^0. The critical velocity field distribution along the pole height is the same as **Fig. 5-10** . Similar to the 100 m and the 200 m guyed pole systems, the values of velocity field distribution along the conductor spans for the guys' critical load configuration are found to be the largest among all the possible tornado configurations. This is illustrated in **Fig. 5-12**.

Fig. 5-12. Tornado velocity distribution on the conductors

It should be noted that the critical load cases obtained from the parametric studies are the same for the three pole systems with the different conductor spans. The following figures illustrate the critical tornado configuration on the three pole systems:
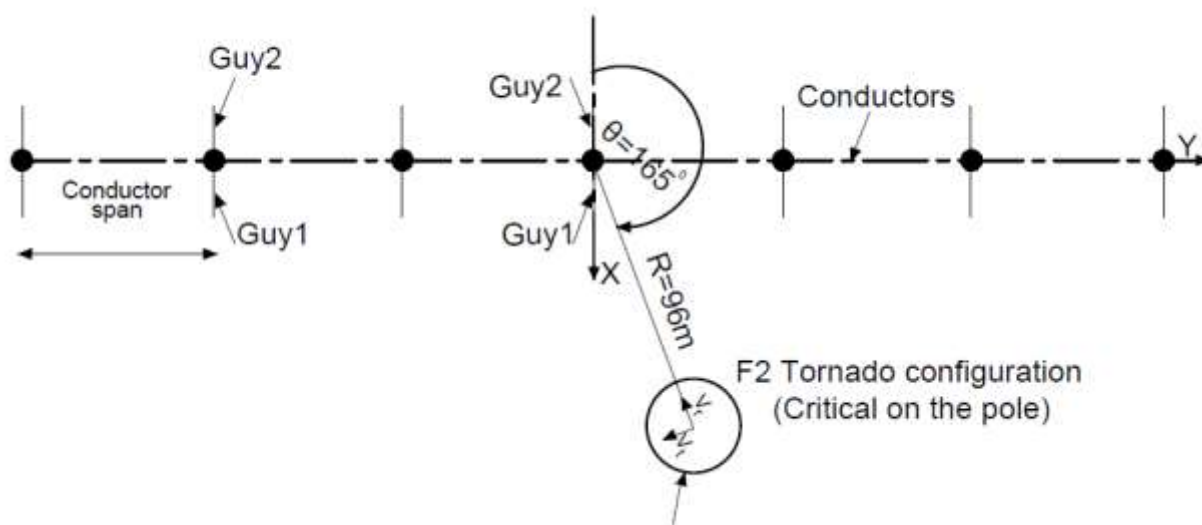
Fig. 5-13. Critical tornado configuration on the poles
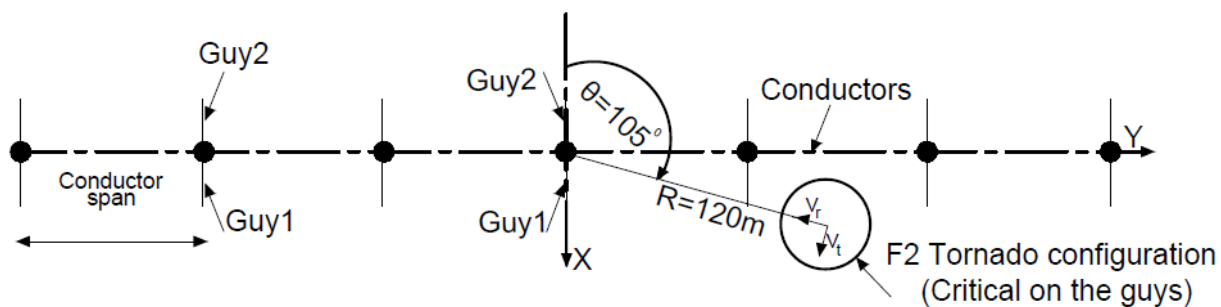
Fig. 5-14. Critical tornado configuration on the guys

5.5.   Failure analysis

After determining the two critical F2 tornado configurations which lead to the maximum bending moments and tension forces on the poles and the guys, respectively, a failure analysis is performed on the considered transmission pre-stressed pole to identify the F2 tornado velocity at which the pole and the guys collapse.

 The three pole systems are considered in the failure analysis. The ratio (M_a/M_r) under maximum F2 tornado velocities (V_{f2max}) varying between 50 and 72 (m/sec) with an increment of 5.5 (m/sec) is calculated for the critical tornado case (R=96 m and θ=165^0) and is plotted in **Fig. 5-15**.
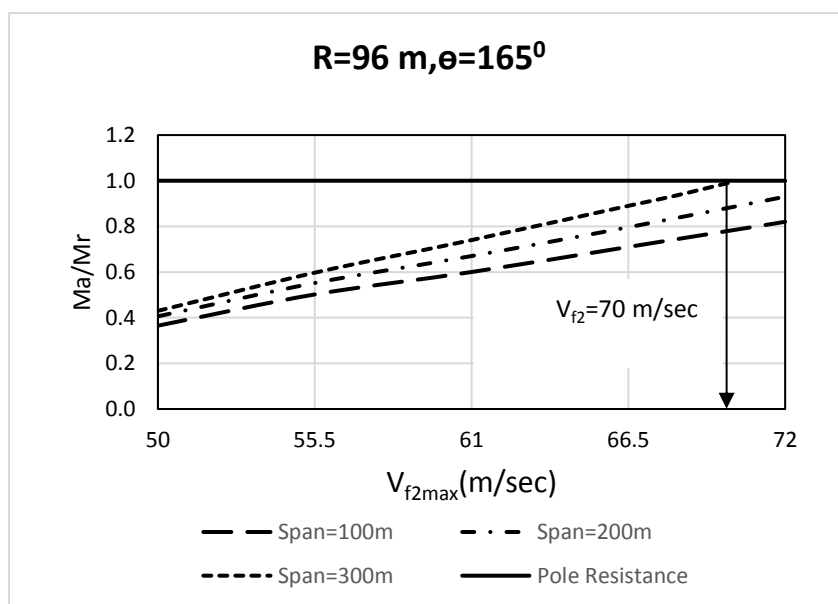
Fig. 5-15. Variation of maximum pole moment with V_{f2max} for different conductor spans

It can be noted from the figure that the maximum base moment at the pole does not reach to the ultimate pole capacity for spans 100 m and 200 m. However, the 300 m pole system reaches its ultimate bending capacity when the F2 tornado velocity is equal to 70 m/sec. This indicates that the guyed pre-stressed concrete pole systems of 100 m and 200 m conductors' spans which are

designed to remain un-cracked under normal wind speed of 40 m/sec will not fail under an F2 tornado of speed 72 m/sec. However, the 300 m pole can sustain an F2 tornado velocity up to 70 m/sec.

The variation of maximum guy tension of the pole with different F2 tornado velocities is then plotted in for each span in **Fig. 5-16**. The configuration (R =120, θ =105^0) is applied to obtain the guys' maximum tension forces.
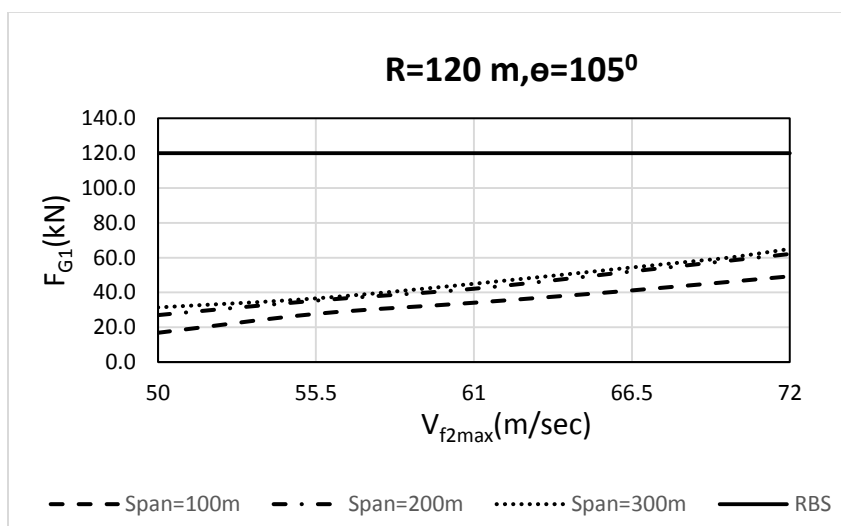
Fig. 5-16. Variation of maximum guy1 force with V_j for different conductor spans

It should be noted that the guys of the three pole systems are found not reaching their RBS under the critical F2 tornado configuration.

5.6. Comparison between the parametric study results and proposed critical load cases

Hamada and El Damatty (2016) proposed eight critical load cases to simulate the effect of F2 tornadoes on transmission line structures. In this section, the eight load cases are applied to the

three different guyed pre-stressed concrete pole systems. The maximum bending moment ratios (M_a/M_r) and maximum tension forces F_{G1} under the envelope of proposed load cases are obtained. Those values are then compared to the corresponding values obtained from the parametric study conducted earlier in this study. The purpose is to check if the proposed critical tornado load cases by Hamada and El Damatty (2016) can be applied on the guyed pre-stressed concrete pole structures under tornadoes.

Each load case of the eight proposed load cases consists of a combination between vertical and horizontal velocity profiles to be applied on the supporting tower and the conductors, respectively. In the next subsection, the proposed load cases are presented to explain how the loads proposed by Hamada and El Damatty (2016) are applied to the tower systems.

5.6.1.   Tornado load cases

In each load case, the vertical velocity components on the pole in the X and Y directions are given along the height as well as the transverse velocity component normal to the conductors. The following figures show the proposed wind velocity distributions along the conductors' span and the height of the pole, respectively.
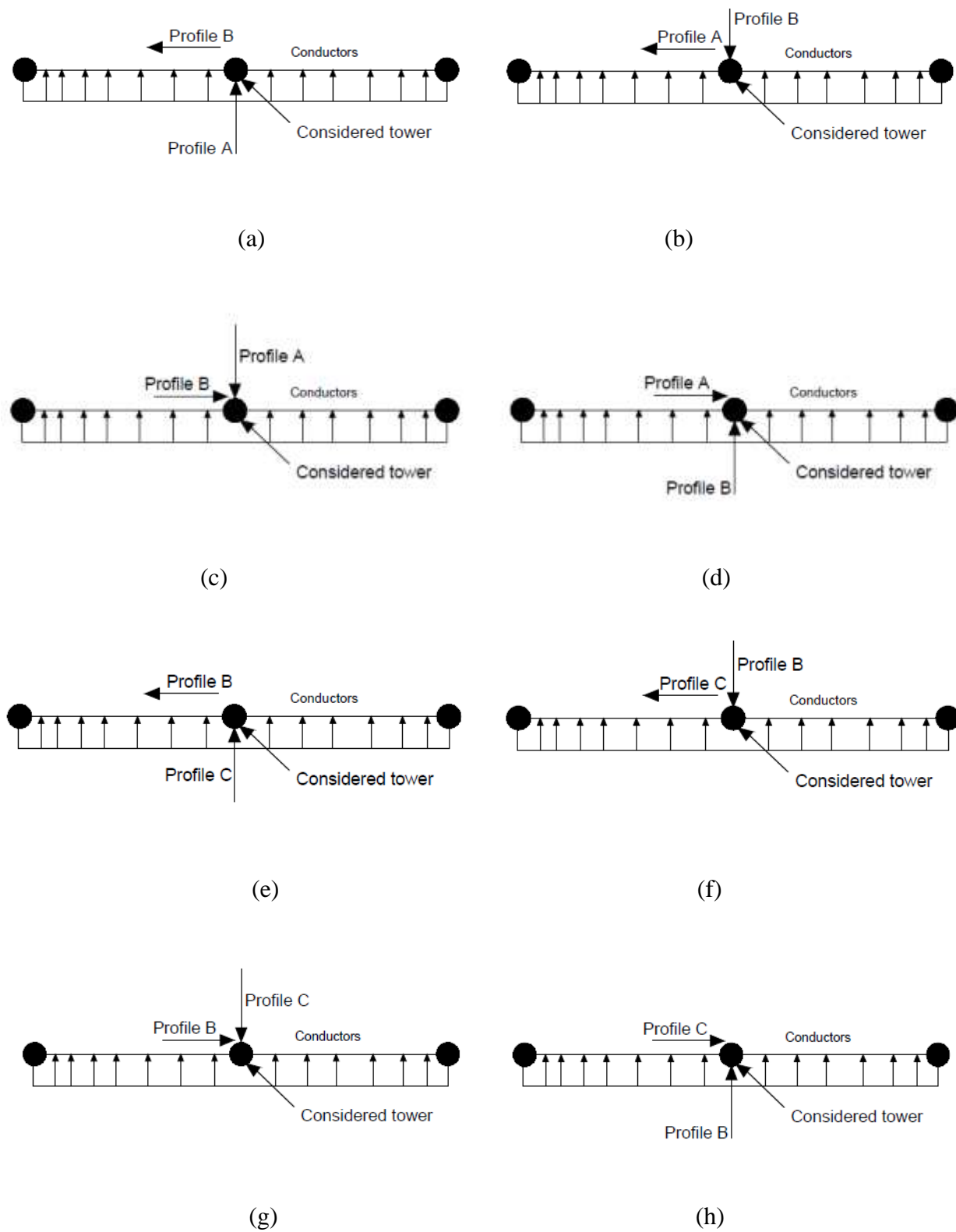
Fig. 5-17. (a-h) Tornado load cases (Hamada and El Damatty 2016)
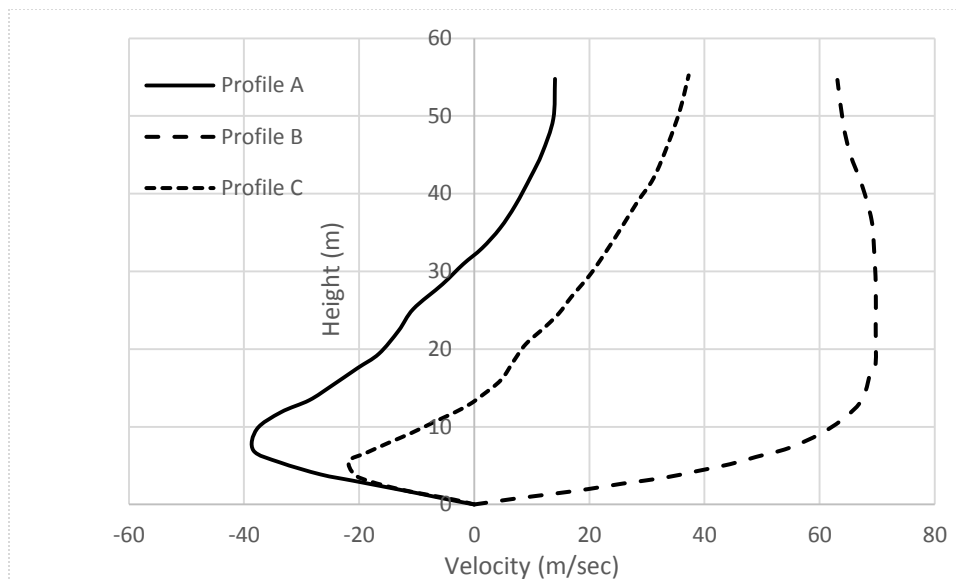
Fig. 5-18. Vertical critical tornado wind profiles (Hamada and El Damatty 2016)

For the eight load cases (a-h), the two conductors adjacent to the considered tower are loaded with a uniform wind speed of 72 m/sec. The span reduction factor (SRF) proposed by Behncke and Eric Ho (2009) is evaluated and multiplied by the loads that acting on the conductors.

$$SRF = W_G \left(1 - 0.25\, W_G / L\right)/L \qquad \text{Equation (5-2)}$$

Where, W_G is the tornado gust factor as is taken as 150 and L is the conductor span.

After calculating the conductors' reactions, the vertical profiles (A, B and C) are applied to the poles alternatively as shown in **Fig. 5-17** (a-h). The envelope of the eight load cases is then evaluated and the maximum poles' base moments as well as guys' reactions are obtained.

For example, in load case a, Profiles (A) and (B) are applied to the pole systems in (−X) and (-Y) directions, respectively. While in load case f, Profiles (B) and (C) are applied to the pole systems in (X) and (-Y), respectively.

5.6.2. Comparison

The envelope of the eight load cases proposed by Hamada and El Damatty (2016) is obtained and compared to the results of the parametric study conducted earlier in this study. The maximum bending moment ratios (M_a/M_r) and maximum tension forces F_{G1} are used for the comparison purpose. **Figs. 5-19 and 5-20** show the comparison results.
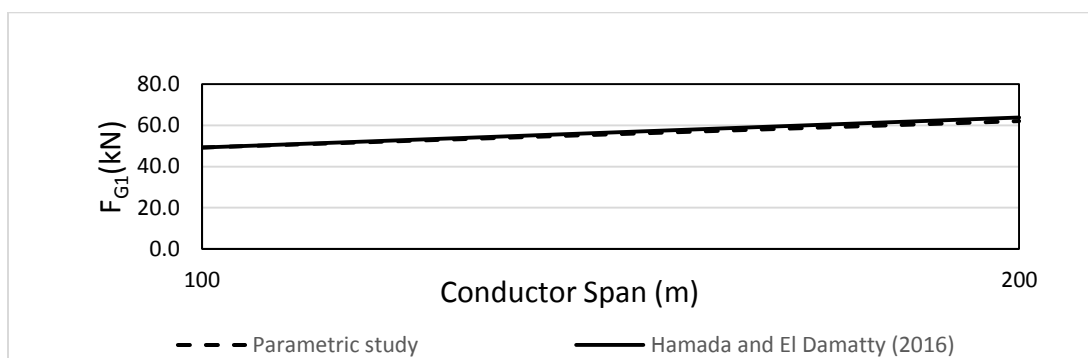
Fig. 5-19. Maximum Guy tension using parametric study and load cases proposed by Hamada
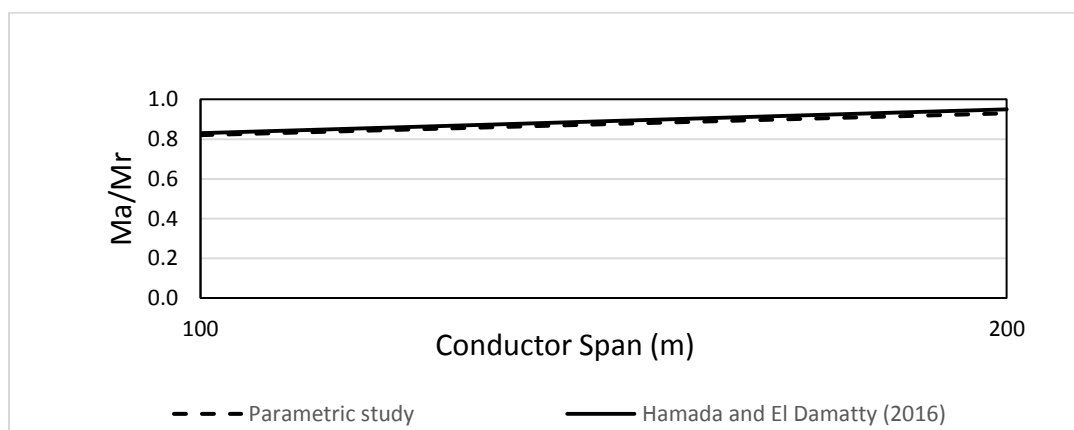
and El Damatty (2016)

Fig. 5-20. Maximum pole base moment using parametric study and load cases proposed by

Hamada and El Damatty (2016)

The comparison between the parametric study results obtained and the proposed critical load cases shows an excellent agreement. The difference between the maximum bending moments obtained from the current study and the corresponding ones proposed by Hamada and El Damatty (2016) is 2%. Meanwhile, the difference in the peak forces developed in the guys is 3 %. It should be mentioned that bending failure has occurred to the guyed pole system of 300 m conductors' span under the critical F2 tornado load case obtained from the parametric study as well as the envelope of the eight load cases recommended by Hamada and El Damatty (2016). Based on that, the proposed load cases recommended by Hamada and El Damatty (2016) can be considered while designing the guyed pre-stressed concrete pole systems to resist tornadoes. Instead of performing 312 tornado cases, the peak responses of the guyed pre-stressed concrete transmission poles under tornadoes can be predicted by applying the eight load cases proposed by Hamada and El Damatty (2016).This will result in a significant saving in the computational time.

It should be mentioned that the F2 tornado load cases develop bending moments in the pre-stressed concrete poles that can reach up to 83% and 95 % of the capacity of the 100 m and 200 m pole systems, respectively. However, the peak tension forces in the guys are considered quite small compared to the rated breaking strength (RBS), which is 120 kN.

5.7. <u>Conclusions</u>

In the current study, a numerical technique is utilized combining the following: 1) CFD models to simulate tornado wind fields. 2) A semi-closed form solution that is capable of determining the conductor reactions under such localized high intensity wind events. 3) A non-linear finite element model for the guyed pre-stressed concrete pole structures that can predict the internal forces of

such types of poles under tornadoes. The main conclusions drawn from this study can be summarized in the following points:

1- The critical tornado configuration which will lead to the maximum pole base moment is independent on the conductor spans and occurs when R=96 m, $\theta = 165^0$.

2- The critical tornado configuration which will lead to the maximum guys forces is independent on the conductor spans and occurs when R=120 m, $\theta = 105^0$.

3- Slacking of guys due to high compression forces occurs under a number of critical F2 tornado cases.

4- The guyed pole systems of spans 100 m and 200 m which are designed to remain un-cracked under normal wind loading of 40 m/sec do not fail under the critical tornado configurations. However, the 300 m conductor span guyed pole system will be subjected to bending failure in the supporting pole if the maximum F2 tornado speed exceeds 70 m/sec.

5- The previously developed load cases are conservative and can be used in the design and analysis of guyed pre-stressed concrete transmission pole structures under F2 tornadoes, this will lead to a significant saving in the computational time when analyzing pre-stressed concrete pole structures under tornado loading.

5.8.   <u>References</u>

Aboshosha, H., and El Damatty, A.A., (2014), "Effective technique for the reactions of transmission line conductors under high intensity winds", Wind and Structures. 18(3), 235-252.

Altalmas, A., El Damatty, A. A., and Hamada, A. (2012). "Progressive failure of transmission towers under tornado loading". Annual Conference of the Canadian Society 21 for Civil Engineering 2012: Leadership in Sustainable Infrastructure, CSCE 2012, June 6, 2012 - June 9, Canadian Society for Civil Engineering, Edmonton, AB, Canada, 2220- 2229.

American Society of Civil Engineers (ASCE), (2010). "Guidelines for electrical transmission line structural loading", ASCE manuals and reports on engineering practice, No. 74, New York, NY, USA.

American Society of Civil Engineers (ASCE), (2012). "Pre-stressed Concrete Transmission Pole Structures", ASCE manuals and reports on engineering practice, No. 123, Reston, VA, USA.

American Society of Civil Engineers (ASCE), (1997). "Design of guyed electrical transmission structures", ASCE Manuals and Reports on Engineering Practice, vol. 91, New York, 1997.

Baker, D. E. (1981). "Boundary layers in laminar vortex flows". Ph.D. thesis. Purdue University, USA.

Behncke, R. and Eric Ho, T. (2009). "Review of Span and Gust Factors for Transmission Line Design" Electrical Transmission and Substation Structures Conference 2009-ASCE.

Behncke, R.H., and White, H. B. (2006). "Applying Gust Loadings to Your Lines" Proceedings of the 9th International Conference on Overhead Lines, American Society of Civil Engineers (ASCE), Fort Collins, Colorado.

CIGRÉ (Conseil International des Grands Réseaux Électriques/ International Council on Large Electrical Systems) SC-22 WG22-06 (2006). "Review of IEC 826: Loading and Strength of Overhead Lines. Part 3: Analysis of Recent Transmission Line Failures". Scientific Committee B2 on Overhead Lines.

CIGRÉ (Conseil International des Grands Réseaux Électriques/ International Council on Large Electrical Systems) (2009). "Overhead line design guidelines for mitigation of severe wind storm damage." Scientific Committee B2 on Overhead Lines, B2. 06.09.

El Damatty, A.A., Hamada, A., Elawady, A. (2013), "Development of Critical Load Cases Simulating the Effect of Downbursts and Tornados on Transmission Line Structures", proceedings of the Eighth Asia-Pacific Conference on Wind Engineering, Chennai, India.

Fujita, T. T., and Pearson, A. D. (1973). "Results of FPP classification of 1971 and 1972 tornadoes." 8th Conference on Severe Local Storms (abstracts only), USA, 609.

Fujita, T. T. (1981). "Tornadoes and downbursts in the context of generalized planetary scales." J.Atmos.Sci., 38(8), 1511-34.

Hamada, A., Damatty, A.A.E., Hangan, H., and Shehata, A.Y. (2010). "Finite element modelling of transmission line structures under tornado wind loading". Wind and Structures, 13(5): 451-469.

Hamada, A., and El Damatty, A. A. (2011). "Behaviour of guyed transmission line structures under tornado wind loading". Computers and Structures, 89(11-12), 986-1003.

Hamada, A., and El Damatty, A. A. (2013). "Analysis and Behaviour of Guyed Transmission Lines under Tornado Wind Loads – Case Studies". Annual Conference of the Canadian Society for Civil Engineering 2013: General Conference, CSCE 2013, May 29, 2013 - June 1, Canadian Society for Civil Engineering, Montreal, QC, Canada.

Hamada M. and El Damatty A. (2016). "Load cases simulating tornadoes- Economic implications for transmission line structures design". Proceedings of CIGRE-IEC colloquim, Montreal, QC, Canada.

Hangan, H. and Kim, J. (2008). "Swirl ratio effects on tornado vortices in relation to the Fujita scale". Wind and Structures, An International Journal, 11(4), 291-302.

Ibrahim, A.M. and El Damatty, A.A., (2016). "Case Study to Assess the Sensitivity of Prestressed Concrete Poles to Tornadoes". Proceeding of the General Conference of the Canadian Society of Civil Engineering, London, ON, Canada.

Ibrahim, A.M., El Damatty, A. A. and Elansary A.M., (2017), "Finite element modelling of pre-stressed concrete poles under downbursts and tornadoes". Journal of Engineering Structures. 153, 370-382.

Ishac, M.F. and White, H.B. (1994). "Effect of tornado loads on transmission lines". In Proceedings of the 1994 IEEE Power Engineering Society Transmission and Distribution Conference, April 10, 1994 - April 15, 1994. Publ by IEEE, Chicago, IL, USA, 521- 527.

Kuebler,M., (2008). "Torsion in Helically Reinforced Prestressed Concrete Poles", M.Sc. thesis, University of Waterloo, Waterloo, Ontario, Canada.

Li, C.Q. (2000). "Stochastic model of severe thunderstorms for transmission line design". Probabilistic Engineering Mechanics, 15(4): 359-364.

Sarkar, P., Haan, F., Gallus, Jr., W., Le, K. and Wurman, J. (2005). "Velocity measurements in a laboratory tornado simulator and their comparison with numerical and full-scale data." 37th Joint Meeting Panel on Wind and Seismic Effects.

Savory, E., Parke, G. A. R., Zeinoddini, M., Toy, N., and Disney, P. (2001). "Modelling of tornado and microburst-induced wind loading and failure of a lattice transmission tower". Eng.Struct., 23(4), 365-375.

Shehata, A., El Damatty, A.A., and Savory, E., (2005). "Finite element modeling of transmission line under downburst wind loading". Finite Elements in Analysis and Design 42(1), 71-89.

Wurman, J. (1998). "Preliminary results from the ROTATE-98 tornado study". Preprints, 19th Conf. On severe local storms, Minneapolis, MN, 14-18 September.

Zhang, Y., (2006). "Status quo of wind hazard prevention for transmission lines and countermeasures". East China Electric Power 34(3), 28-31.

5.9.   Appendix A

Results of the guyed pole with conductor spans of 200m

5.9.1 Variation of pole base moment with R

(a)   (b)   (c)

Fig. 5-21. (a-c) Variation of Ma/Mr with R

5.9.2 Variation of pole base moment with θ

Fig. 5-22. Variation of Ma/Mr with θ

5.9.3 Guy1 forces

(a)   (b)   (c)

Fig. 5-23. (a-c) Variation of guy1 forces with R

5.9.4 Guy2 forces

(a)   (b)   (c)

Fig. 5-24. (a-c) Variation of guy1 forces with R

5.10. Appendix B

Results of the guyed pole with conductor spans of 300m

5.10.1 Variation of pole base moment with R

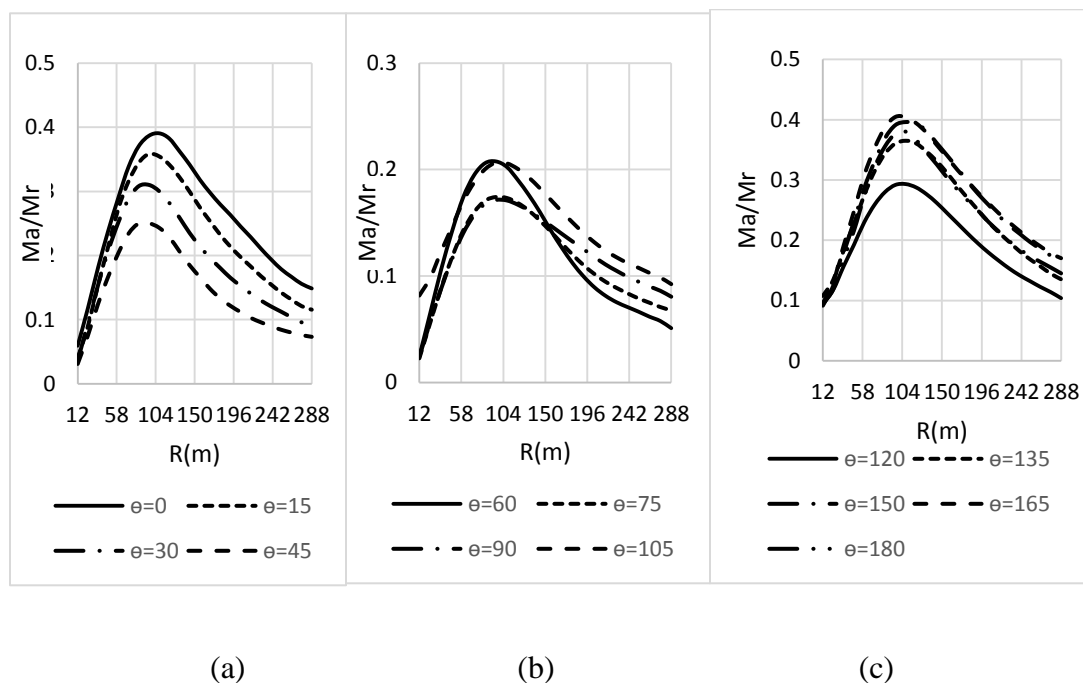(a)   (b)   (c)
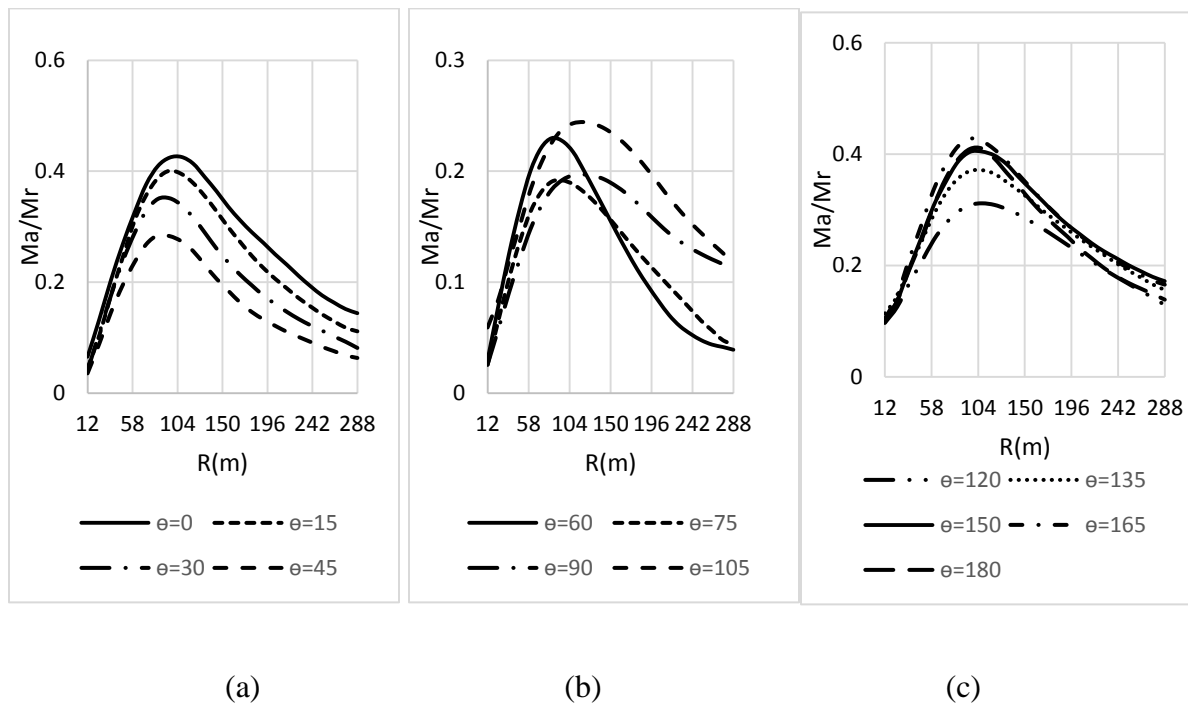
Fig. 5-25. (a-c) Variation of Ma/Mr with R

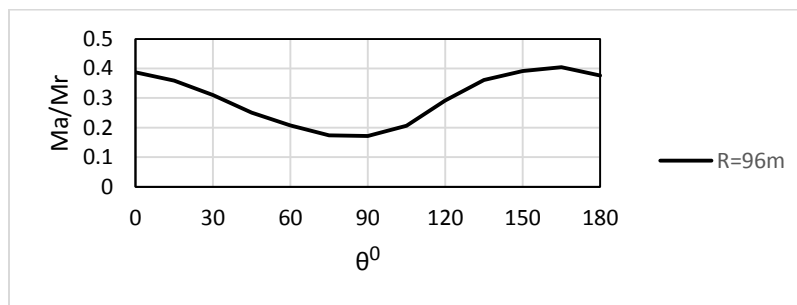#### 5.10.2 Variation of pole base moment with θ

Fig. 5-26. (a-c) Variation of Ma/Mr with θ

5.10.3 Guy1 forces

(a)   (b)   (c)
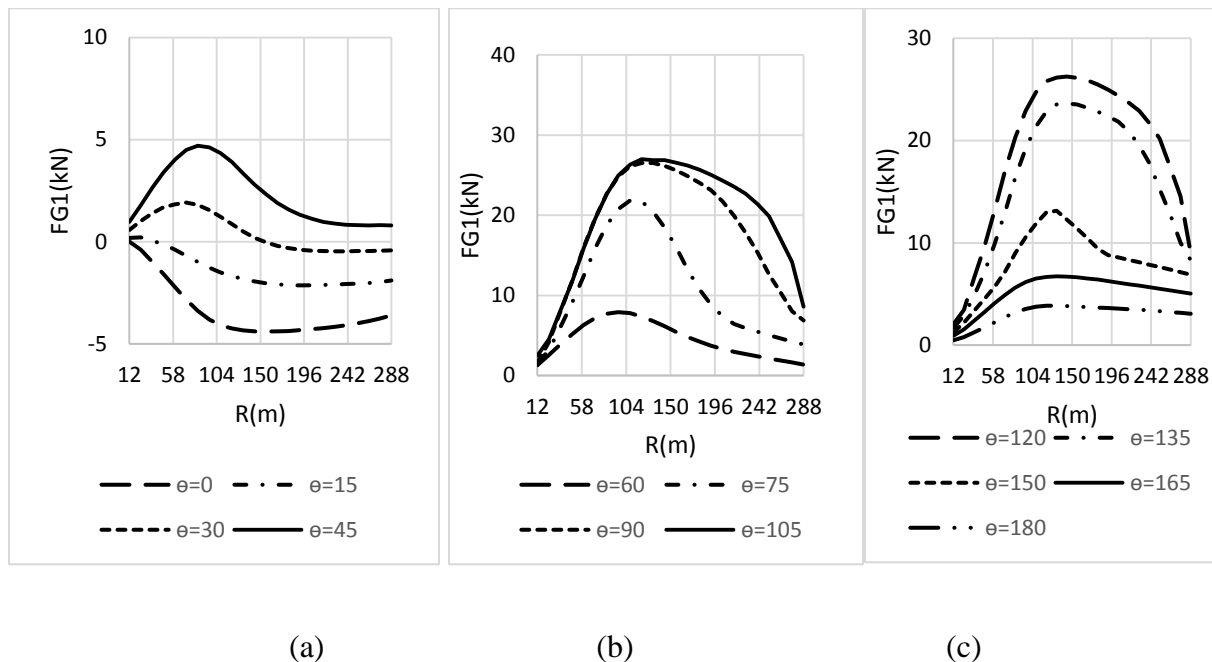
Fig. 5-27. (a-c) Variation of guy1 forces with R
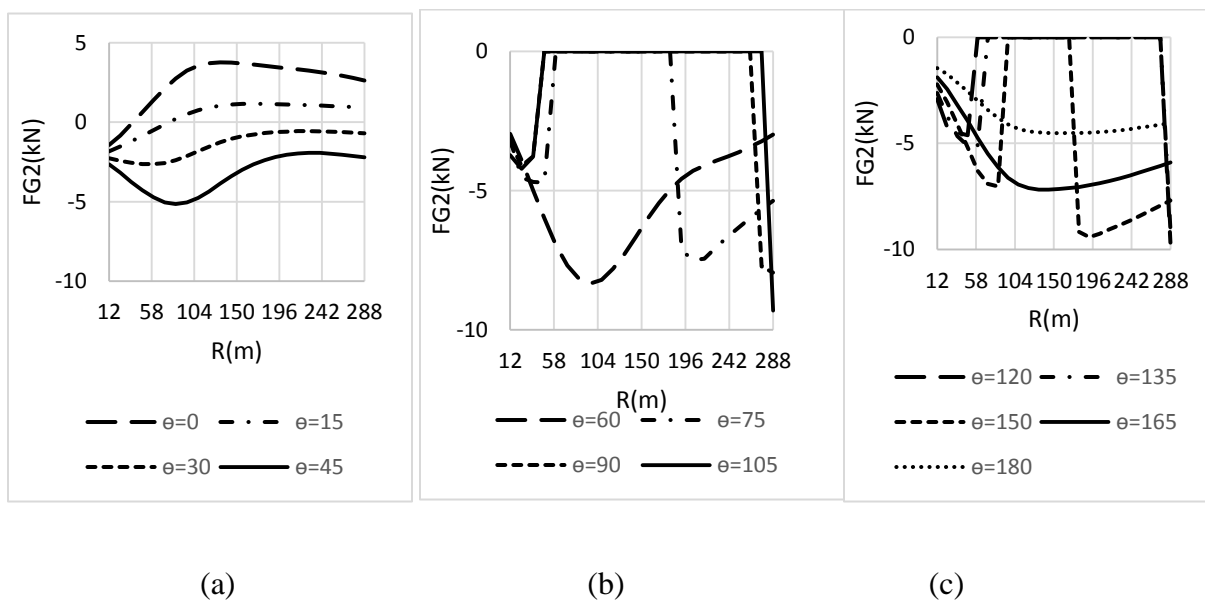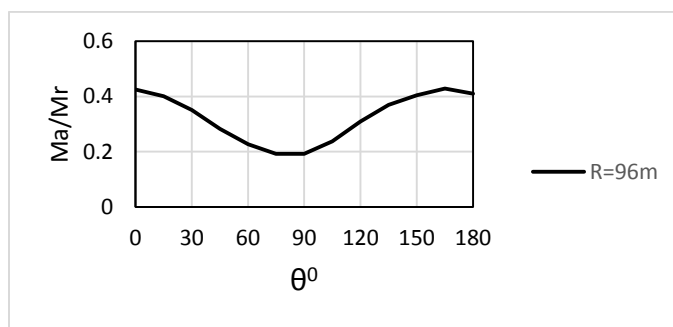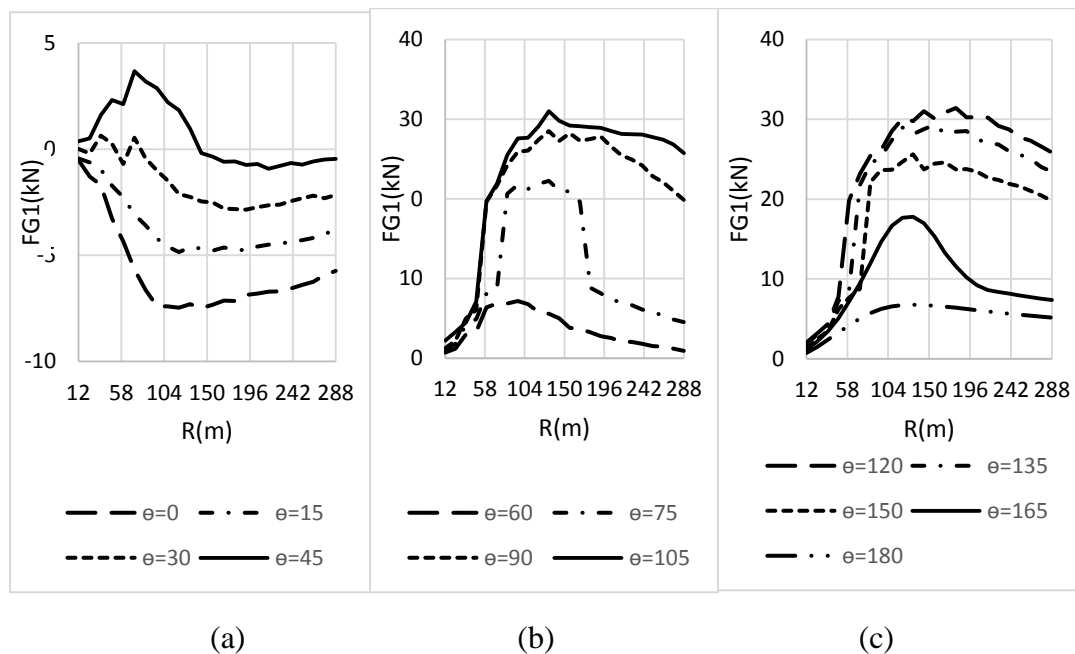
5.10.4 Guy2 forces

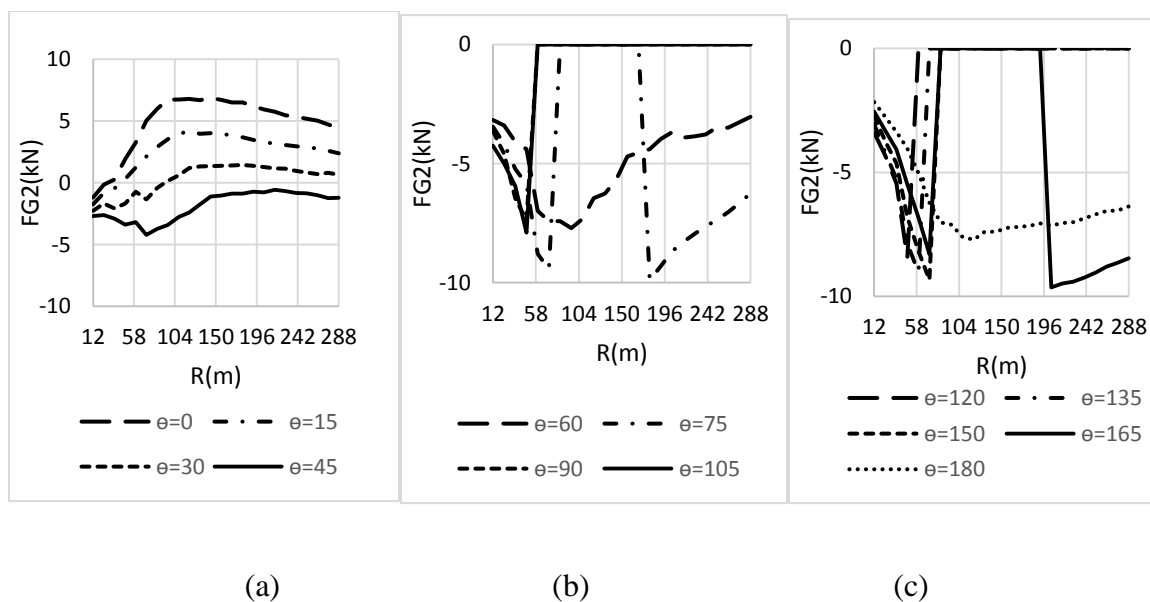(a)   (b)   (c)

Fig. 5-28. (a-c) Variation of guy2 forces with R

CHAPTER 6

SUMMARY AND CONCLUSIONS

6.1.   <u>Summary</u>

The research conducted in this thesis investigates the behavior of pre-stressed concrete transmission pole structures under high intensity wind (HIW) events. Firstly, a numerical model is developed and validated to study the behavior of pre-stressed concrete pole transmission line structures under downbursts and tornadoes using a quasi-static approach. The numerical technique is developed combining the following: 1) CFD models to simulate downbursts and tornadoes wind fields. 2) A semi-closed form solution that is capable of determining the conductor reactions under such localized high intensity wind events. 3) A non-linear finite element model for pre-stressed concrete pole structures that can predict the internal forces and deformations of such types of poles under HIW. The numerical model is validated using experimental results available in the literature. The numerical model is then utilized to study the behavior of a self-supported pre-stressed concrete pole supporting a 100 m span conductor. The pole is designed to remain un-cracked under a mean synoptic wind speed of 40 m/sec based on the current design codes. Extensive parametric studies are then conducted for the considered pole under 924 downburst cases and 312 F2-tornado cases. For downbursts, the parametric study involves varying the location and diameter of the downburst. For tornadoes, only the location is varied. The critical downburst and tornado configurations are obtained from those parametric studies. Incremental non-linear failure analyses are then conducted for the pole using the determined downburst and tornado critical configurations.

In order to obtain an upper bound for the dynamic effect of HIW on pre-stressed concrete poles, the numerical model is extended to be capable of conducting dynamic analysis of pre-stressed

concrete transmission lines under mean and turbulent synoptic wind loadings. The numerical model is employed to evaluate the dynamic behavior of three self-supported pre-stressed concrete pole systems with different spans (100 m, 200 m and 300 m). Peak total responses (i.e. including the dynamic effect) and peak quasi-static responses (i.e. neglecting the dynamic effect) are evaluated. The dynamic effect of the synoptic wind loads on the three systems is found to be negligible under low wind speeds and considerable under high normal wind speeds.

Given that the turbulence in high intensity wind events is less than the corresponding turbulence associated with synoptic wind and knowing that the frequencies of the guyed pre-stressed concrete poles are higher than the ones of the self- supported systems, the dynamic effect of HIW on guyed pre-stressed concrete pole structures is assumed to be negligible.

Finally, three guyed pre-stressed concrete transmission pole structures of different spans (100 m, 200 m, and 300 m) are analyzed under downbursts and tornadoes. Extensive parametric studies are conducted for the three pole systems under 924 downburst cases and 312 F2- tornado cases. The critical downbursts and tornadoes configurations which lead to the maximum straining actions in the poles and the guys are obtained. Failure analyses are then conducted to determine the maximum downburst and tornado velocities that the three pole systems can sustain without collapse. It should be noted that all the studied pre-stressed concrete pole systems in the current thesis are designed to remain un-cracked under a normal wind speed of 40 m/sec according to the current design codes.

6.2. <u>Conclusions</u>

The conclusions drawn from the study of the 100 m self-supported pre-stressed concrete pole system under HIW are:

1- Maximum downburst effect occurs at $\theta=0^0$, $D_j=500m$ and $R/D_j=1.2$.

2- A full collapse for the pole associated with concrete crushing occurs at a downburst jet velocity higher than 65 m/sec. The absolute maximum wind speed corresponding to this jet velocity is about 72 m/sec.

3- Maximum F2 tornado effect occurs for a tornado configuration of $R=144m$ and $\theta=105^0$.

4- The pole is able to sustain the maximum F2-tornado wind speed of 72 m/sec without experiencing full collapse.

5- For the same maximum wind speed, the critical downburst and tornado cases produce almost the same values for the velocities acting on the pole. In the meanwhile, higher velocity distribution is shown to occur for the downburst case. This is the main reason that downbursts turns to be more critical than tornadoes for the pre-stressed concrete transmission pole system.

The following conclusions are obtained after studying the dynamic behavior of three self-supported pre-stressed concrete pole systems with different spans (100 m, 200 m and 300 m) under mean and turbulent synoptic wind loadings:

1- Conductor reactions exhibit large Dynamic Amplification Factor (DAF) than the pole base moments especially at the low wind speeds. This trend results from the low conductor aerodynamic damping at lower wind speeds.

2- DAF of the poles has no specific trend under mean wind speeds up to the cracking wind speed (40 m/sec). The maximum DAF do not exceed 13 %, 12 % and 14 % for the 100 m, 200 m and 300 m pole systems, respectively. This is mainly due to the discrepancy

between the conductors' and poles' frequencies under mean wind speeds less than 40 m/sec.

3- DAF exhibit higher values when the mean wind speeds exceed 40 m/sec. This is attributed to the fact that the poles crack when the mean wind speed is higher than 40 m/sec. The poles' cracking decreases the frequency of the whole transmission line system. As such, the poles' frequencies become close to the conductors' ones and coupled pole-conductor mode appears. This results in increasing the resonant component and hence increasing the dynamic effect. For mean wind speeds greater than the cracking wind speed, the maximum values of the DAF are 24 %, 25 % and 27 % for the 100 m, 200 m and 300 m pole systems, respectively. As such, the dynamic effect is more important after the cracking of the poles.

4- $GF_{T\text{-ASCE}}$, is over conservative and is usually higher than the gust response factor obtained from the dynamic analyses, GF_T.

5- $G_{FQS\text{-ASCE}}$ is found to be considerably less than G_T for the three pole systems especially for the wind speeds above the cracking wind speed.

The main conclusions obtained from the analysis of three guyed pre-stressed concrete pole systems under downbursts and tornadoes are:

1- The critical downburst configuration which leads to the maximum pole base moment is $\theta=90^0$, $D_j=500m$ and $R/D_j=1.2$.

2- The critical downburst configuration which leads to the maximum pole base moment is independent of the conductor spans.

3- The critical downburst configuration which will lead to the maximum guys forces is when $\theta=0^0$, $D_j=500m$ and $R/D_j=1.2$ for spans ranging from 100 to 200 m and when $\theta=0^0$, $D_j=700m$ and $R/D_j=1.2$ for a span of 300m.

4- The guyed pre-stressed concrete pole systems do not collapse when their spans are ranging between 100 m and 200 m. However, the guys reach the rated breaking strength in the guyed concrete pole system that carries 300 m conductor spans when the jet speed exceeds 60 m/sec.

5- The critical tornado configuration which leads to the maximum pole base moment is independent on the conductor spans and occurs at R=96 m, $\theta =165^0$.

6- The critical tornado configuration which leads to the maximum guys forces is independent on the conductor spans and occurs at R=120 m, $\theta =105^0$.

7- The guyed pole systems of spans 100 m and 200 m do not fail under the critical tornado configurations. However, the 300 m conductor span guyed pole system will be subjected to bending failure in the supporting pole if the maximum F2 tornado speed exceeds 70 m/sec.

8- The previously developed critical downburst and tornado load cases are not just limited to lattice steel tower structures. They can be used to obtain the maximum straining actions on pre-stressed concrete pole systems.

6.3. <u>Recommendations for future work</u>

The current study investigated the behavior of pre-stressed concrete pole systems under downbursts, tornadoes and synoptic wind loadings. The following investigations are suggested for future research:

1- Studying the behavior of H-frame concrete pole systems under downbursts and tornadoes.

2- Assessing the dynamic response of guyed and H-framed pre-stressed concrete poles to fluctuating normal wind.

3- Extending the models that was developed in Chapters 2 and 3 to study the dynamic behavior of self-supported, guyed and H-framed pre-stressed concrete pole systems under both mean and turbulent downburst wind field components.

AHMED MANSOUR AHMED SADEK IBRAHIM

Education

- **Master of Science in Structural Engineering, Cairo University, Egypt** (2009-2012)
  Thesis Title *"Behaviour of Reinforced Concrete Barriers under the Effect of Blast Loads"*
  GPA: 3.88/4

- **Bachelor of Science in Civil Engineering, Cairo University, Egypt** (2004-2009)
  Rate of Appreciation: Distinction with Honor Degree.

Research Experience

Research Assistant, Western University, Canada (2012-2017)

- Developed a unique finite element model to assess the behaviour of pre-stressed concrete poles under tornadoes and downbursts.
- Developed an effective numerical model to assess the dynamic behaviour of lattice steel towers, steel poles and pre-stressed concrete poles under synoptic wind loading.
- Performed extensive parametric studies to assess the behaviour of pre-stressed poles under tornadoes, downbursts and synoptic wind loading.
- Participated in the technical report titled "*Dynamic Response of Transmission Lines under Wind-Volume2: Computer Simulation and Numerical Models*", this work is published by ***CEATI international***.
- Contributed in the development of critical downburst and tornado critical load cases which are in the final stage of implementation by the ***ASCE-74*** committee responsible for updating the loading guidelines for transmission line structures.

Research Assistant, Cairo University, Egypt (2009-2012)

- Evaluated the performance of reinforced concrete barriers under the effect of blast loads.

Teaching Experience

Teaching Assistant, Western University, Canada (2012-2017)

- Conducted lectures, tutorials and computer labs, marked assignments for the following courses:
    - Finite Element Analysis
    - Analysis of Buildings under Lateral Loads
    - Analysis of Indeterminate Structures
    - Reinforced and Pre-stressed concrete structures
    - Steel structures
    - Wooden and Masonary Structures

Teaching Assistant, Cairo University, Egypt (2010-2012)
- Conducted lectures, tutorials and computer labs, marked assignments for the following courses:
  - Structural Analysis
  - Reinforced and pre-stressed concrete structures
  - Reinforced Concrete Design Project

Professional Affiliations
- Member of Professional Engineers of Ontario (PEO), 2015-Current (EIT)
- Member of Canadian Society for Civil Engineering (CSCE), 2016-Current
- Member of American Society for Civil Engineering (ASCE), 2014-Current

Honors/Awards
- Dean's List of Honor, Cairo University (2005-2009)
- Precast/pre-stressed Concrete Institute award "Big Beam Competition" 2014.
- Precast/pre-stressed Concrete Institute award "Big Beam Competition" 2015.
- Nominated for the best TA award in Western University in 2016.

Publications

- Ibrahim, A.M., El Damatty, A. A. and Elansary A.M., (2017). "*Finite element modelling of pre-stressed concrete poles under do*wnbursts and tornadoes". Journal of Engineering Structures, 153, pp. 370-382.
- Technical Report, CEATI International Inc, (2017). "*Dynamic Response of Transmission Lines under Wind-Volume2: Computer Simulation and Numerical Models*".
- Ibrahim, A.M. and El Damatty, A.A., (2016), "*Case Study to Assess the Sensitivity of Prestressed Concrete Poles to Tornadoes*", Proceeding of the General Conference of the Canadian Society of Civil Engineering, London, ON, Canada.
- Ibrahim, A.M., Salem, H. and Farahat,A., (2016), "*Numerical Investigation of Reinforced Concrete Barriers Subjected to Blast Loading",* Proceeding of the General Conference of the Canadian Society of Civil Engineering, London, ON, Canada.
- Aboshosha, H., Ibrahim, A.M., El Damatty, A.A. and Hamada,A., (2016), "*Dynamic Behaviour of Transmission Line Structures under Synoptic Wind Loads",* Proceeding of CIGRE-IEC colloquim, Montreal, QC, Canada.
- Ibrahim, A.M. and El Damatty, A.A., (2014), "Behaviour of Prestressed Concrete Poles under Downburst Loading", Proceeding of ASCE conference, Hamilton, ON, Canada.